8-2018

Assessment of Melanocyte-Specific Primary and Memory Autoimmune Responses in Vitiligo-Prone Smyth and Vitiligo-Susceptible, Non-Expressing Brown Line Chickens

Daniel Morales Falcon
University of Arkansas, Fayetteville

Assessment of Melanocyte-Specific Primary and Memory Autoimmune Responses in Vitiligo-Prone Smyth and Vitiligo-Susceptible, Non-Expressing Brown Line Chickens

A dissertation submitted in partial fulfillment
of the requirements for the degree of
Doctor of Philosophy in Cell and Molecular Biology

by

Daniel Morales Falcon
University of California, Riverside
Bachelor of Science in Biology, 2003

August 2018
University of Arkansas

This dissertation is approved for recommendation to the Graduate Council.

_____
Gisela F. Erf, Ph.D.
Dissertation Director

_____
Yuchun Du, Ph.D.
Committee Member

_____
David McNabb, Ph.D.
Committee Member

_____
Suresh Thallapuranam, Ph.D.
Committee Member

Abstract

Vitiligo is an acquired de-pigmentation disorder characterized by the post-natal loss of epidermal melanocytes (pigment-producing cells) resulting in the appearance of white patches in the skin. The Smyth line of chicken is the only model for vitiligo that shares all the characteristics of the human condition including: spontaneous post-natal loss of melanocytes, interactions between genetic, environmental and immunological factors and associations with other autoimmune diseases. In addition, an avian model for vitiligo has the added benefit of an easily accessible target tissue (a growing feather) that allows for the repeated sampling of an individual and thus the continuous monitoring of local immune responses over time. Here, we sought to gain a comprehensive understanding of the initiating events leading to expression of vitiligo in growing feathers by monitoring the infiltration of leukocytes and concurrent immunological activities beginning prior-to visual onset and continuing throughout disease development. Furthermore, we examined the nature of the melanocyte-specific recall (i.e. memory) response by re-introducing the target cell (melanocyte) into the target tissue (growing feather) of completely depigmented Smyth chickens via intradermal injection. Lastly, we sought to gain insights into the role of melanocytes in provoking the autoimmune response by measuring the expression of co-stimulatory molecules in the presence of oxidative stress-inducing H_2O_2. During the primary response we observed characteristic rises in infiltrating B and αβ T cells as well as evidence of active recruitment and cell-mediated immune activities leading up to visual onset. Examination of growing feathers from vitiligo-susceptible Brown line chickens revealed novel anti-inflammatory immune activities which may be responsible for preventing vitiligo. We also observed characteristic memory-like increases in B and T cells as well as increases in recruitment and cell-mediated immune activities in response to injection of

melanocytes into growing feathers of completely depigmented Smyth chickens. Lastly, we observed increased expression of CD40 and B7-1 in melanocytes derived from growing feathers of Smyth chickens treated with H_2O_2. Collectively, these results further support the notion of cell-mediated immune destruction of melanocytes in growing feathers. Furthermore, these data open new avenues of study in the vitiligo-prone Smyth line and vitiligo-susceptible Brown line chickens.

Dedication

In loving memory of Don Marcos Falcón Ramírez.

Acknowledgements

First and foremost, I wish to express my deepest gratitude to my advisor and mentor Dr. Gisela Erf – for taking a chance on me and allowing me the space to grow as a researcher. Thank you for your patience, guidance and most of all your trust.

Thank you to my committee members Dr. Yuchun Du, Dr. David McNabb, Dr. Suresh Thallapuranam and Dr. David Zaharoff – for making this process so much easier through your responsiveness and honest criticisms. Your time and efforts are greatly appreciated.

Thank you to my lab mates past and present. Bob Dienglewicz, thank you for all you did in keeping the lab running efficiently – it made all of our jobs that much easier. To Dr. Marites Sales, thank you for stepping in and taking over so I could focus on wrapping things up. Thank you to my fellow graduate students, especially Dr. Kristen Byrne – for your comradery, friendship and for being such a pleasure to work with. Also to Chelsea Ellington, Kallie Sullivan, Huong Le, Lei Dong and Chris Lyle, thank you for your dedication to the team. Thank you to all the undergraduates who have helped with farm duties over the years, Guillermo Tellez, Jr., Eleni Solberg, Michael Kidd Jr. and Jared Sage.

Thank you to the Falcon, Celaya and Huerta families for their understanding and support. Mom and Dad, thank you for everything you have provided for me and Letty. Thank you for giving us the freedom to dream and for the means to pursue those dreams.

Finally, my wife Jessica. Thank you for your undying support and understanding throughout this whole process. We did it!

Table of Contents

A. Introduction 1

B. Literature review 10

a. Vitiligo Overview 11

b. Quality of Life Impact 11

c. Management of Vitiligo 12

d. Pathophysiology of Vitiligo 12

e. Findings from Mouse Models of Vitiligo 18

f. The Smyth Chicken Model for Autoimmune Vitiligo 20

C. Chapter I. Spontaneous immunological activities in the target tissue of vitiligo-prone Smyth and vitiligo-susceptible Brown lines of chicken 33

a. Introduction 34

b. Materials and Methods 38

c. Results 43

d. Discussion 51

e. References 58

D. Chapter II. Establishment of a method to assess and monitor melanocyte-specific autoimmune memory responses in the target tissue of completely de-pigmented vitiligo-prone Smyth chickens 90

a. Introduction 91

b. Materials and Methods 93

c. Results 98

d. Discussion 105

e. References 110

E. Chapter III. Assessment of immunological activities of primary feather-derived melanocytes in response to acute oxidative stress 135

a. Introduction 136

b. Materials and Methods 138

c. Results 143

d. Discussion 149

e. References 155

F. Conclusions 169

G. Appendices 171

List of Figures

Chapter I

Figure 1. Cell infiltration profiles for total leukocytes, macrophages, B cells and T cells in growing feathers of vitiligo-expressing Smyth 71

Figure 2. Cell infiltration profiles for total leukocytes, macrophages, B cells and T cells in growing feathers of parental control, non-expressing Brown line chickens 73

Figure 3. Cell infiltration profiles for T cell subsets in growing feathers of vitiligo-expressing Smyth and parental-control, non-expressing Brown line chickens 75

Figure 4. Quantification of changes in the T cell receptor repertoire 77

Figure 5. Alterations in the T cell receptor repertoire in growing feathers of vitiligo-expressing Smyth and non-expressing Brown line chickens 79

Figure 6. Gene expression profiles for potential early markers of immunological activities in growing feathers of vitiligo-expressing Smyth line chickens 81

Figure 7. Gene expression profiles for markers of pro-inflammatory and recruitment activities in growing feathers of vitiligo-expressing Smyth line chickens 82

Figure 8. Gene expression profiles for markers of cell-mediated immunity and anti-inflammatory activities in growing feathers of vitiligo-expressing Smyth line chickens 84

Figure 9. Expression profiles for genes significantly affected by age in growing feathers of parental-control, non-expressing Brown line chickens 86

Figure 10. Individual-specific T cell subset infiltration, gene expression and T cell receptor perturbation profiles in growing feathers of non-expressing Brown line chickens 88

Chapter 2

Figure 1. Lymphocyte infiltration profiles for feather-derived melanocyte- or vehicle-injected growing feathers from completely depigmented Smyth and fully pigmented parental-control Brown line chickens.....115

Figure 2. αβT cell subset infiltration profiles for feather-derived melanocyte- or vehicle-injected growing feathers from completely depigmented Smyth and fully pigmented parental-control Brown line chickens.....117

Figure 3. CD25+ T cell subset infiltration profiles for feather-derived melanocyte- or vehicle-injected growing feathers from completely depigmented Smyth and fully pigmented parental-control Brown line chickens 119

Figure 4. Alterations in the T cell receptor repertoire in growing feathers from completely depigmented Smyth and fully pigmented parental-control Brown line chickens injected with either feather-derived melanocytes or vehicle 121

Figure 5. Gene expression profiles of CCL19 and CCR7 in growing feathers of completely depigmented Smyth and fully pigmented Brown line chickens injected with either feather-derived melanocytes or vehicle.....123

Figure 6. Gene expression profiles of IL2 and IL2R in growing feathers of completely depigmented Smyth and fully pigmented Brown line chickens injected with either feather-derived melanocytes or vehicle.....125

Figure 7. Gene expression profiles of IL21 and IL21R in growing feathers of completely depigmented Smyth and fully pigmented Brown line chickens injected with either feather-derived melanocytes or vehicle.....127

Figure 8. Gene expression profiles of IFNG, FASLG and GZMA in growing feathers of completely depigmented Smyth and fully pigmented Brown line chickens injected with either feather-derived melanocytes or vehicle 129
Figure 9. Gene expression profiles of IL1B and IL18 in growing feathers of completely depigmented Smyth and fully pigmented Brown line chickens injected with either feather-derived melanocytes or vehicle.....131
Figure 10. Gene expression profiles of CTLA4, IL10 and TGFB1 in growing feathers of completely depigmented Smyth and fully pigmented Brown line chickens injected with either feather-derived melanocytes or vehicle 133
Chapter 3
Figure 1. Viability of primary melanocytes established from growing feathers of vitiligo-prone Smyth line (SL), vitiligo-susceptible parental-control Brown line (BL) and vitiligo-resistant distantly-related Light Brown Leghorn (LBL) chickens in the presence of varying concentrations of hydrogen peroxide 160
Figure 2. Expression of MHC-I and MHC-II in primary melanocytes established from growing feathers of vitiligo-prone Smyth line (SL), vitiligo-susceptible parental-control Brown line (BL) and vitiligo-resistant distantly-related Light Brown Leghorn (LBL) chickens in the presence of varying concentrations of hydrogen peroxide.....161
Figure 3. Relative expression of CAT, HMOX1 and HSP70 in primary melanocytes established from growing feathers of vitiligo-prone Smyth line (SL), vitiligo-susceptible parental-control Brown line (BL) and vitiligo-resistant distantly-related Light Brown Leghorn (LBL) chickens in the presence of varying concentrations of hydrogen peroxide 163

Figure 4. Relative expression of B7-1, CD40 and FAS in primary melanocytes established from growing feathers of vitiligo-prone Smyth line (SL), vitiligo-susceptible parental-control Brown line (BL) and vitiligo-resistant distantly-related Light Brown Leghorn (LBL) chickens in the presence of varying concentrations of hydrogen peroxide 165
Figure 5. Relative expression of IL6 and CXCL8 in primary melanocytes established from growing feathers of vitiligo-prone Smyth line (SL), vitiligo-susceptible parental-control Brown line (BL) and vitiligo-resistant distantly-related Light Brown Leghorn (LBL) chickens in the presence of varying concentrations of hydrogen peroxide 167
Figure 6. Relative expression of IL1B and IL18 in primary melanocytes established from growing feathers of vitiligo-prone Smyth line (SL), vitiligo-susceptible parental-control Brown line (BL) and vitiligo-resistant distantly-related Light Brown Leghorn (LBL) chickens in the presence of varying concentrations of hydrogen peroxide 168

List of Tables

Chapter I

Table 1. Target gene primer and probe sequences.....64

Table 2. Primers used for T cell receptor spectratyping.....66

Table 3. Spearman correlation coefficients relating perturbations in T cell repertoire (D-score) with infiltrating T cell and T cell subsets in growing feathers of vitiligo-expressing Smyth and non-expressing Brown line chickens.....67

Table 4. Spearman correlation coefficients relating perturbations in T cell repertoire (D-score) with T cell receptor allele group frequency in growing feathers of vitiligo-expressing Smyth and non-expressing Brown line chickens.....68

Table 5. Genes with no overall changes in expression relative to age in growing feathers of parental-control, non-expressing Brown line chickens.....70

Chapter 2

Table 1. Target gene primer and probe sequences.....113

Table 2. Primers used for T cell receptor spectratyping.....114

Chapter 3

Table 1. Target gene primer and probe sequences.....159

Introduction

Vitiligo is an acquired de-pigmentation disorder characterized by the loss of epidermal melanocytes resulting in the appearance of white patches in the skin. It is estimated to affect 0.5 – 1% of the population and has no preference for race, age or gender (Taïeb and Picardo, 2009; Ezzedine *et al.*, 2015; Picardo *et al.*, 2015). While not considered a life threatening disease, vitiligo has a strong negative impact on perceived quality of life in patients and contrary to popular belief, affects adults, children and dark and fair-skinned individuals comparably (Ezzedine *et al.*, 2015; Catucci Boza *et al.*, 2016).

Oxidative stress is suspected to be a key component in triggering vitiligo (Laddha *et al.*, 2013). One possible source is the accumulation of H_2O_2 in the skin of vitiligo patients which is thought to originate from defective recycling of (6R)-5,6,7,8 tetrahydrobiopterin (Schallreuter *et al.*, 1999, 2001). Coupled with reported low levels of the H_2O_2-degrading enzyme catalase in vitiligo patients compared to healthy controls accumulating H_2O_2 may result in an elevated basal level of oxidative pressure in susceptible individuals (Schallreuter *et al*., 1991).

A disruption in the anti-oxidant system may also contribute to the diminished capacity of melanocytes from vitiligo patients to cope with (additional?) oxidative stress. Melanocytes from vitiligo patients show a diminished capacity to cope with oxidative stress generated by treatment with the vitiligo-inducing phenolic compound 4-TBP compared to normal controls (Manga *et al.*, 2006). Furthermore, reports of impaired activation of the Nrf2-ARE pathway in melanocytes from vitiligo patients in response to stress as well as rescue of stressed cells through activation of Nrf2 lend further mechanistic support for a defective antioxidant system in vitiligo-susceptible individuals (Jian *et al.*, 2014; Chang *et al.*, 2017).

As can be inferred from the treatment of affected individuals with immunosuppressive drugs as a means to halt progression of the disease, a defective melanocyte is not sufficient for

vitiligo expression – i.e. a functional immune system is required. The autoimmune pathology of vitiligo is well-established and involves humoral and cell-mediated immune components. While a variety of melanocyte-specific autoantibodies have been identified in the circulation of vitiligo patients, their role in disease initiation and progression is unclear. On the other hand, the role of cell-mediated immunity in melanocyte loss is well documented. Reports of $CD8^+$ cells in close proximity to IFN-γ^+ cells in lesional and perilesional skin while absent in non-lesional skin provide strong evidence of a T cell-driven pathology in vitiligo (Yang *et al.*, 2015). Furthermore, *ex-vivo* culture of normally pigmented skin with T cells from perilesional vitiligo skin results in melanocyte destruction (van den Boorn *et al.*, 2009).

While defects in antioxidant capacity as well as the presence of cytotoxic T cells in the active lesion are well documented, a link between the two in driving vitiligo expression remains elusive; partially due to the difficulty in sampling prior to development of disease symptoms. Induced vitiligo animal models can provide valuable mechanistic insights into the progression of vitiligo and thus present a means to test potential therapeutic interventions. However, as mentioned, vitiligo is a multifactorial disorder and therefore requires a model that shares all the characteristics with the human condition including spontaneous onset. The Smyth chicken is a well-established model for autoimmune vitiligo. Similar to humans, Smyth chickens experience a spontaneous post-natal loss of melanocytes in growing feathers through a complex interaction of genetic, environmental and immunological factors (Smyth *et al.*, 1981).

The full Smyth Line model is composed of three MHC-matched ($B^{101/101}$) lines of chicken: the vitiligo-prone Smyth chicken, the vitiligo-susceptible, parental Brown line from which the Smyth line was derived, and the vitiligo-resistant, distantly related Light Brown Leghorn line. The identification of an environmental trigger (vaccination of 1-day old chicks

with live, cell-free turkey herpesvirus) has resulted in a reliable incidence of vitiligo among hatch mates in the three lines: 80-95%, 0-2% and 0% for the Smyth line, Brown line and Light Brown Leghorn lines, respectively (Erf *et al.*, 2001).

In addition to a low incidence of vitiligo, an inherent susceptibility to vitiligo development was identified in the Brown line by i.p. injection with the DNA methylation inhibitor 5-azacytidine. When treated in this manner, the incidence of vitiligo in Brown line chickens was over 70% compared to 0% in vehicle-injected chickens. In contrast there was no change in the incidence (0%) of vitiligo in 5-azacytidine-treated Light Brown Leghorn chickens (Sreekumar, Erf and Smyth, Jr., 1996). Therefore the Smyth line, Brown line and Light Brown Leghorn lines may be considered: vitiligo-prone, -susceptible and -resistant, respectively.

Similarly to humans, genetic susceptibility is thought to be localized, in part, to the melanocyte itself. In regenerating feathers of partially depigmented Smyth chickens, melanocytes were observed with retracted dendrites and contained large pigmented vacuoles (Boissy *et al*., 1983). Similar abnormalities were observed in primary cultures of melanocytes derived from developing embryos of Smyth chickens whereas cultures from embryos of Brown line chickens appeared normal (Boissy *et al.*, 1986). However it is important to note that the inherent melanocyte defect is not sufficient for disease expression as demonstrated in immunosuppression studies on the Smyth chicken (Lamont and Smyth, 1981; Boissy *et al*, 1984; Boyle *et al*., 1987; Pardue *et al.*, 1987).

While autoantibodies have been detected to melanocyte-specific antigens (Austin *et al.*, 1992; Searle *et al.*, 1993; Austin and Boissy, 1995) in Smyth chickens, most recent evidences supports the role of cell-mediated immunity in driving the autoimmune response. The close proximity of $CD8^+$ cells to apoptotic cells in the barb ridge (anatomical location of melanocytes

in growing feathers) mimics results observed in human skin (Wang and Erf, 2004) as does the progressive elevation of IFN-γ and granzyme A in the target tissue, which can be detected within days of visual pigmentation loss (Shi and Erf, 2012). These observations, together with the *in vivo* demonstration of a melanocyte-specific cell-mediated immunity in Smyth chickens that developed vitiligo further support the notion of (Wang and Erf, 2003).

In addition to the many similarities between human and avian vitiligo, the nature and accessibility of the target tissue provides unique opportunities for the study of spontaneous autoimmune disease. Specifically, the growing feather (target tissue) is a skin derivative that contains actively pigmenting melanocytes in a defined epidermal region (barb ridge) as well as dermis for leukocyte recruitment and autoimmune activity and can be easily sampled for *ex vivo* analysis by pulling it from the follicle after which it regenerates. Hence, the value of an avian model for autoimmune vitiligo is in the ability to monitor the development of the autoimmune response beginning prior to- and continuing through complete progression. Furthermore, application of a patented growing feather-injection system to the Smyth chicken model opens new horizons as a means to study autoimmune memory or recall responses *in vivo* and directly in the target tissue. Finally, the ability to establish primary melanocyte cultures prior to disease development (and even in partially de-pigmented individuals) allows for focused, controlled study of melanocyte dysfunction *in vitro*. Therefore the overall purpose for this dissertation is to examine the primary and memory autoimmune responses in Smyth chickens as well as the role of the target cell in provoking the response according to the following objectives:

Objective 1: To gain a more comprehensive understanding of the relationship between infiltrating leukocytes and immunological activities in the evolving autoimmune lesion in growing feathers of Smyth chickens. Specifically, pulp-infiltrating leukocyte profiles were

obtained for individual vitiligo-prone Smyth and parental-control, vitiligo-susceptible but non-expressing Brown line chickens by sampling (plucking) growing feathers beginning at 1-day post-hatch and continuing two times per week until 113 days of age. Gene expression profiles were also determined on the level of the individual and utilizing cDNA derived from the whole pulp. Lastly, changes in the overall diversity of the T cell repertoire in the evolving autoimmune lesion were examined.

Objective 2: To establish a method for assessing and monitoring the melanocyte-specific memory response in growing feathers of completely de-pigmented Smyth chickens. The feather-injection system was used to re-introduce melanocytes into the target tissue via intradermal injection. Lymphocyte infiltration and gene expression profiles were obtained on an individual basis. Changes in the overall diversity of the T cell receptor repertoire was also examined in injected feathers. Injection of vehicle only into growing feathers of Smyth chickens accounted for immune activity in response to the wound created by the injection itself. In addition, growing feathers of fully pigmented (non-vitiliginous) MHC-matched Brown line chickens were also injected as above.

Objective 3: To compare the response of primary melanocytes of age-matched vitiligo-prone Smyth line, vitiligo-susceptible Brown line and vitiligo-resistant Light Brown Leghorn line chickens to oxidative stress induced by treatment with H_2O_2. Primary melanocyte cultures were established from growing feathers before the onset of vitiligo. Cell viability in response to challenge with varying doses of H_2O_2 was observed as well as the surface expression of MHC-I and –II on treated melanocytes. Relative expression of genes involved in the antioxidant response, co-stimulation of T cell signaling and inflammation were also monitored in response to H_2O_2 challenge.

References

Austin, L. M. *et al.* (1992) 'The detection of melanocyte autoantibodies in the Smyth chicken model for vitiligo.', *Clinical immunology and immunopathology*, 64(2), pp. 112–20. Available at: http://www.ncbi.nlm.nih.gov/pubmed/1643744.

Austin, L. M. and Boissy, R. E. (1995) 'Mammalian tyrosinase-related protein-1 is recognized by autoantibodies from vitiliginous Smyth chickens. An avian model for human vitiligo.', *The American journal of pathology*, 146(6), pp. 1529–41. Available at: http://www.pubmedcentral.nih.gov/articlerender.fcgi?artid=1870917&tool=pmcentrez&rendertype=abstract.

Boissy, R. E. *et al.* (1986) 'Delayed-amelanotic (DAM or Smyth) chicken: melanocyte dysfunction in vivo and in vitro.', *The Journal of investigative dermatology*, 86(2), pp. 149–156. Available at: http://www.ncbi.nlm.nih.gov/pubmed/3091704.

Boissy, R. E., Lamont, S. J. and Smyth, J. R. (1984) 'Persistence of abnormal melanocytes in immunosuppressed chickens of the autoimmune "DAM" line.', *Cell and tissue research*, 235(3), pp. 663–8. Available at: http://www.ncbi.nlm.nih.gov/pubmed/6713493.

Boissy, R. E., Smyth, J. R. and Fite, K. V (1983) 'Progressive cytologic changes during the development of delayed feather amelanosis and associated choroidal defects in the DAM chicken line. A vitiligo model.', *The American journal of pathology*, 111(2), pp. 197–212. Available at: http://www.ncbi.nlm.nih.gov/pubmed/6846502.

van den Boorn, J. G. *et al.* (2009) 'Autoimmune Destruction of Skin Melanocytes by Perilesional T Cells from Vitiligo Patients', *Journal of Investigative Dermatology*, 129(9), pp. 2220–2232. doi: 10.1038/jid.2009.32.

Boyle, M. L., Pardue, S. L. and Smyth, J. R. (1987) 'Effect of corticosterone on the incidence of amelanosis in Smyth delayed amelanotic line chickens.', *Poultry science*, 66(2), pp. 363–7. Available at: http://www.ncbi.nlm.nih.gov/pubmed/3588505.

Catucci Boza, J. *et al.* (2016) 'Quality of Life Impairment in Children and Adults with Vitiligo: A Cross-Sectional Study Based on Dermatology-Specific and Disease-Specific Quality of Life Instruments', *Dermatology*, 232(5), pp. 619–625. doi: 10.1159/000448656.

Chang, Y. *et al.* (2017) 'Simvastatin Protects Human Melanocytes from H2O2-Induced Oxidative Stress by Activating Nrf2', *Journal of Investigative Dermatology*. The Authors, 137(6), pp. 1286–1296. doi: 10.1016/j.jid.2017.01.020.

Erf, G. F. *et al.* (2001) 'Herpesvirus connection in the expression of autoimmune vitiligo in Smyth line chickens.', *Pigment cell research / sponsored by the European Society for Pigment Cell Research and the International Pigment Cell Society*, 14(1), pp. 40–46. doi: 10.1034/j.1600-0749.2001.140107.x.

Ezzedine, K. *et al.* (2015) 'Living with vitiligo: results from a national survey indicate differences between skin phototypes', *British Journal of Dermatology*, 173(2), pp. 607–609. doi: 10.1111/bjd.13839.

Ezzedine, K. *et al.* (2015) 'Vitiligo', *The Lancet*. Elsevier, 386(9988), pp. 74–84. doi: 10.1016/S0140-6736(14)60763-7.

Jian, Z. *et al.* (2014) 'Impaired activation of the Nrf2-ARE signaling pathway undermines H 2 O 2-induced oxidative stress response: A possible mechanism for melanocyte degeneration in vitiligo', *Journal of Investigative Dermatology*. Nature Publishing Group, 134(8), pp. 2221–2230. doi: 10.1038/jid.2014.152.

Laddha, N. C. *et al.* (2013) 'Vitiligo: interplay between oxidative stress and immune system.', *Experimental dermatology*, 22(4), pp. 245–50. doi: 10.1111/exd.12103.

Lamont, S. J. and Smyth, J. R. (1981) 'Effect of bursectomy on development of a spontaneous postnatal amelanosis.', *Clinical immunology and immunopathology*, 21(3), pp. 407–11. Available at: http://www.ncbi.nlm.nih.gov/pubmed/6976866.

Manga, P. *et al.* (2006) 'A role for tyrosinase-related protein 1 in 4-tert-butylphenol-induced toxicity in melanocytes: Implications for vitiligo', *American Journal of Pathology*, 169(5), pp. 1652–1662. doi: 10.2353/ajpath.2006.050769.

Pardue, S. L. *et al.* (1987) 'Enhanced integumental and ocular amelanosis following the termination of cyclosporine administration.', *The Journal of investigative dermatology*, 88(6), pp. 758–61. Available at: http://www.ncbi.nlm.nih.gov/pubmed/3585059.

Picardo, M. *et al.* (2015) 'Vitiligo', *Nature Reviews Disease Primers*, p. 15011. doi: 10.1038/nrdp.2015.11.

Schallreuter, K. U. *et al.* (1999) 'In vivo and in vitro evidence for hydrogen peroxide (H2O2) accumulation in the epidermis of patients with vitiligo and its successful removal by a UVB-activated pseudocatalase.', *The journal of investigative dermatology. Symposium proceedings*, 4(1), pp. 91–6. Available at: http://www.ncbi.nlm.nih.gov/pubmed/10537016.

Schallreuter, K. U. *et al.* (2001) 'Epidermal H(2)O(2) accumulation alters tetrahydrobiopterin (6BH4) recycling in vitiligo: identification of a general mechanism in regulation of all 6BH4-dependent processes?', *The Journal of investigative dermatology*, 116(1), pp. 167–74. doi: 10.1046/j.1523-1747.2001.00220.x.

Schallreuter, K. U., Wood, J. M. and Berger, J. (1991) 'Low catalase levels in the epidermis of patients with vitiligo.', *The Journal of investigative dermatology*, 97(6), pp. 1081–5. Available at: http://www.ncbi.nlm.nih.gov/pubmed/1748819 (Accessed: 12 July 2018).

Searle, E. A. *et al.* (1993) 'Smyth Chicken Melanocyte Autoantibodies - Cross-Species Recognition, In-Vivo Binding, And Plasma-Membrane Reactivity Of The Antiserum', *Pigment Cell Research*, 6(3), pp. 145–157.

Shi, F. and Erf, G. F. (2012) 'IFN-γ, IL-21, and IL-10 co-expression in evolving autoimmune vitiligo lesions of Smyth line chickens.', *The Journal of investigative dermatology*, 132(3 Pt 1), pp. 642–9. doi: 10.1038/jid.2011.377.

Smyth, J. R., Boissy, R. E. and Fite, K. V (1981) 'The DAM chicken: a model for spontaneous postnatal cutaneous and ocular amelanosis.', *The Journal of heredity*, 72(3), pp. 150–6. Available at: http://www.ncbi.nlm.nih.gov/pubmed/7276522.

Sreekumar, G. P., Erf, G. F. and Smyth, Jr., J. R. (1996) '5-Azacytidine Treatment Induces Autoimmune Vitiligo in Parental Control Strains of the Smyth Line Chicken Model for Autoimmune Vitiligo', *Clinical Immunology and Immunopathology*, 81(2), pp. 136–144. doi: 10.1006/clin.1996.0169.

Taïeb, A. and Picardo, M. (2009) 'Vitiligo', *New England Journal of Medicine*. Massachusetts Medical Society, 360(2), pp. 160–169. doi: 10.1056/NEJMcp0804388.

Wang, X. and Erf, G. F. (2003) 'Melanocyte-specific cell mediated immune response in vitiliginous Smyth line chickens', *Journal of Autoimmunity*, 21(2), pp. 149–160. doi: 10.1016/S0896-8411(03)00087-8.

Wang, X. and Erf, G. F. (2004) 'Apoptosis in feathers of Smyth line chickens with autoimmune vitiligo', *Journal of Autoimmunity*, 22(1), pp. 21–30. doi: 10.1016/j.jaut.2003.09.006.

Yang, L. *et al.* (2015) 'Interferon-gamma Inhibits Melanogenesis and Induces Apoptosis in Melanocytes: A Pivotal Role of CD8+ Cytotoxic T Lymphocytes in Vitiligo.', *Acta dermato-venereologica*, 95(6), pp. 664–70. doi: 10.2340/00015555-2080.

Literature Review

Vitiligo Overview

Vitiligo is an acquired depigmentation disorder characterized by the progressive loss of pigment-producing cells (melanocytes) in the skin resulting in the appearance of white patches. It is estimated to affect 0.5 – 1% of the population worldwide and has no apparent preference for race, age or gender (Taïeb and Picardo, 2009; Ezzedine *et al.*, 2015; Picardo *et al.*, 2015). Vitiligo is currently classified into two major categories: non-segmental ("vitiligo) and segmental (Ezzedine *et al.*, 2012). Non-segmental vitiligo is the most common form and is characterized by the symmetrical distribution of lesions on both sides of the body which evolve over time. In contrast, segmental vitiligo is characterized by the unilateral distribution of lesions which spread rapidly but quickly stabilize (Ezzedine *et al.*, 2012; Picardo *et al.*, 2015). The term "mixed vitiligo" refers to a condition that shares characteristics of both segmental and non-segmental vitiligo and is now considered a subgroup of segmental vitiligo (Ezzedine *et al.*, 2012).

Quality of Life Impact

While vitiligo is not a life threatening disease, it has a strong negative effect on the quality of life of patients. In a recently published survey of vitiligo patients in Korea, over 53% of responders reported feeling depressed as a result of their skin condition (Bae *et al.*, 2018). A common misconception is that individuals with darker skin carry a heavier burden due to vitiligo than those with fairer skin (Grimes and Miller, 2018). In a 2015 survey of vitiligo patients of dark and fair skin, it was found that while specific areas of concern were different between the two groups, the general self-perceived stress level was comparable (K. Ezzedine *et al.*, 2015). Vitiligo also impacts similar aspects of lifestyle and overall quality of life in adults and children including personal relationships (e.g. partners, friendships and bullying), leisure (e.g. sports,

choice of clothing, social activities) and feelings (eg. self-conscious about lesions) (Catucci Boza *et al.*, 2016). Moreover, a recent study on the association of quality of life and location of vitiligo lesions found the greatest impact when the hands were affected (Florez-Pollack *et al.*, 2017).

Management of Vitiligo

As there is no cure for vitiligo, a management strategy is often presented to patients with two goals in mind: halt progression of the disease and stimulate re-pigmentation (Whitton *et al*., 2016). Repeated exposure to narrow-band ultraviolet B radiation is currently the preferred method for stimulating re-pigmentation in vitiligo patients. Administration of immunosuppressive agents such as corticosteroids is often conducted in conjunction with phototherapy as a means to halt progression of vitiligo (Bae *et al.*, 2017). Surgical intervention, such as transplantation of fully pigmented skin, is often the next step in a treatment schedule followed by depigmentation therapies such as administration of monobenzyl ether of hydroquinone (Taïeb and Picardo, 2009; Picardo *et al.*, 2015). Novel therapies targeting IFN-γ signaling through the use of JAK/STAT inhibitors are emerging, however their efficacy is unclear (Craiglow and King, 2015; Kim *et al.*, 2018; Nguyen *et al.*, 2018).

Pathophysiology of Vitiligo

The most widely accepted view of vitiligo etiopathogenesis is that disease onset is triggered through a complex interaction between genetic, environmental and immunological factors with specific causal mechanisms varying between individuals (Le Poole *et al.*, 1993; Ezzedine *et al.*, 2015).

The most extensive work on the underlying genetic susceptibility to vitiligo has come from Dr. Richard Spritz at the University of Colorado. In a meta-analysis of data from three separate genome-wide association studies (GWAS) SNPs were found on several loci of

immunologically relevant genes such as *CD80-ADPRH*, *CTLA4*, *FASLG*, *IL2RA*, *GZMB*, *HLA-A* and *HLA-DRB* – all of which affect T cell function (Jin *et al.*, 2016). CTLA-4 protein inhibits T cell activation through binding and removal of co-stimulatory receptors B7-1 (CD80) and B7-2 (CD86) on antigen-presenting cells (Linsley *et al.*, 1994; Qureshi *et al.*, 2011). The *CD80-ADPRH* gene refers to an enhancer region on the CD80 gene. Interleukin-2 receptor alpha (IL2RA) is a portion of the high-affinity interleukin-2 receptor complex and is transiently expressed on activated T cells as well as constitutively on regulatory T cells. *FASLG* and *GZMB* are both directly involved in mediating direct cytotoxicity by T cells. While GWAS represents a powerful tool to identify susceptibility loci, the authors estimate that results only account for a mere 22.5% of heritability of vitiligo (Jin *et al.*, 2016). Moreover, despite computational predictions, further work is needed to confirm the consequences (i.e. functional vs. regulatory, causal vs. non-causal) of the observed genetic variations.

Oxidative stress is suspected to be a key component in triggering vitiligo (Laddha *et al.*, 2013). Accumulation of epidermal H_2O_2 in the skin of patients with active vitiligo was first reported by Schallreuter *et al.* in 1999. Potential causes of H_2O_2 accumulation include defective recycling of (6R)-5,6,7,8 tetrahydrobiopterin ($6BH_4$) as well as low levels of catalase – both of which have been documented in tissue extracts derived from skin of vitiligo patients (Schallreuter *et al.*, 1991; Schallereuter *et al.*, 1994). $6BH_4$ is a co-factor for the enzyme phenylalanine hydroxylase which catalyzes the first step in L-phenylalanine metabolism yielding L-tyrosine (precursor of melanin synthesis) and 4a-hydroxy-BH_4. 4a-hydroxy-BH_4 is converted to quinonoid dihydro-6-biopterin (q-BH_2) which itself is converted back to 6-BH_4 (Schallereuter *et al.*, 1994). The conversion of L-phenylalanine to 4a-hydroxy-BH_4 by phenylalanine hydroxylase involves the intermediate 4a-peroxy-BH_4 which can breakdown into q-BH_2 and

H_2O_2 (Davis and Kaufman, 1989; Schallereuter *et al.*, 1994). Additionally, in the absence of 4a-hydroxy-BH_4, dehydratase which converts 4a-hydroxy-BH_4 to q-BH_2, 4a-hydroxy-BH_4 can non-enzymatically yield 7-BH_4 (an alternative isomer of 6-BH_4). Lower levels of 4a-hydroxy-BH_4, dehydratase in cell extracts from the skin of vitiligo patients and melanocytes from one vitiligo patient compared to normal skin have been reported (Harada *et al.*, 1993). Diminished activity of 4a-hydroxy-BH_4, dehydratase lead to the accumulation of 7-BH_4 and an increase in *de novo* synthesis of 6-BH_4. Combined with reported diminished levels of catalase (Schallreuter *et al*., 1991; Maresca *et al.*, 1997), dysfunction in $6BH_4$ recycling may continually generate H_2O_2, leading to its accumulation which would apply an elevated level of potential oxidative stress in melanocytes. Further evidence for an elevated "baseline" level of oxidative pressure was observed in the membrane lipid peroxidation of melanocytes from vitiligo patients in conjunction with elevated production of reactive oxygen species (ROS) in non-lesional skin relative to normal controls (Dell'Anna *et al.*, 2007). The presence of allantonin (a product of H_2O_2 and uric acid) has also been observed in skin extracts derived from vitiligo patients while the product was absent in normal skin (Shalbaf *et al.*, 2008).

An elevated level of basal oxidative stress would explain the reported increased susceptibility of melanocyte from vitiligo patients to cope with oxidative stress *in vitro* (Maresca *et al.*, 1997; Manga *et al.*, 2006). However, another possibility is a defective anti-oxidant system in melanocytes from genetically susceptible individuals. Nrf2 is a transcription factor that under normal conditions is sequestered in the cytoplasm by Keap1 and promotes its degradation by ubiquitination. Under stressful conditions cysteine residues on Keap1 are reduced permitting its dissociation from Nrf2 which translocates to the nucleus where it binds ARE sites on target genes and promotes their transcription (Loboda *et al.*, 2016).

The Nrf2-ARE (nuclear factor E2-related factor 2; Nrf2-antioxidant response element) pathway has emerged as a major player in protecting melanocytes against damage induced by oxidative stress. Activation of the Nrf2-ARE pathway has been demonstrated to protect melanocytes from oxidative stress induced by exposure to the vitiligo-inducing phenol monobenzone (Arowojolu *et al.*, 2017). In addition, it appears that expression of the Nrf2-target hemeoxygenase-1 (HMOX1, HO-1) is the key protective enzyme in melanocyte response to oxidtative stress. HMOX1 catalyzes the rate-limiting step of heme degradation which generates, in part, biliverdin which is converted the potent antioxidant bilirubin (Loboda *et al.*, 2016). Several reports have observed a protective effect of HMOX1 expression as a result of activation of the Nrf2 pathway in oxidative stress-challenged melanocytes (Elassiuty *et al.*, 2011; Jian *et al.*, 2011, 2016; Chang *et al.*, 2017; Jung *et al.*, 2017). In 2014 Jian *et al.* were the first to report an impaired response of the Nrf2-ARE pathway in H_2O_2-challenged melanocytes from vitiligo skin in comparison to those from normal skin. In these cells it appeared that Nrf2 itself was, at least partially, retained in the cytoplasm after oxidative challenge thereby limiting the expression of HMOX1.

While recent evidence of impaired activation of the Nrf2-ARE pathway in melanocytes from vitiligo patients supports the notion of a diminished capacity to cope with oxidative stress in susceptible individuals, a functional immune system is required for progression of vitiligo (i.e. melanocyte dysfunction is not sufficient for disease expression). An immune-driven pathology in vitiligo is evidenced by use of immunosuppressive drugs that often are prescribed either as a mono- or combination therapy in an attempt to halt progression of the disease and re-stimulate pigmentation (Bae *et al.*, 2017; Kim *et al.*, 2018; Nguyen *et al.*, 2018). Vitiligo is also associated

with other autoimmune disorders including thyroid disease, alopecia areata, diabetes systemic lupus erythematosus psoriasis and rheumatoid arthritis (Dahir and Thomsen, 2018).

The presence of melanocyte-specific autoantibodies in vitiligo patients has been known since at least 1977 (Hertz *et al.*). Since that time the presence of a wide variety of circulating melanocyte-specific autoantibodies have been reported with specificities ranging from: tyrosinase (Baharav *et al.*, 1996; Helen Kemp *et al.*, 1999), Trp-1 (Kemp *et al.*, 1998), pmel17 (Kemp *et al.*, 1998) and melanin-concentrating hormone receptor 1 (Kemp *et al.*, 2002). The cytotoxic potential of anti-melanocyte antibodies has been demonstrated *in vitro* (Norris *et al.*, 1988; Gilhar *et al.*, 1995; Ruiz-Argüelles *et al.*, 2007). However, the precise role autoantibodies play in the initiation and progression of vitiligo remains unclear. Furthermore, their use as a marker for disease activity is controversial (Kroon *et al.*, 2013).

In contrast, the correlation between a T cell infiltrate and melanocyte loss was first described in 1996 by Le Poole *et al.* and is now well-established. Several reports have documented the presence of $CD8^+$ T cells in active and stable vitiligo lesions. Gene expression profiles of lesional skin from vitiligo patients has revealed expression of chemokines reflective of a T_H1 (cell-mediated) immune response (Rashighi *et al.*, 2014). Furthermore, immunohistochemical staining of lesional and perilesional skin biopsies from vitiligo patients revealed a close association between IFN-γ^+ and $CD8^+$ cells whereas these cells were absent in and non-lesional skin provide strong evidence of a role for activated cytotoxic T cells in melanocyte loss (Yang *et al.*, 2015). Analysis of $CD8^+$ cells isolated from perilesional skin biopsy tissues obtained from vitiligo patients revealed an elevated production of IFN-γ relative to those from non-lesional skin (Wańkowicz-Kalińska *et al.*, 2003). Direct evidence of T cell-mediated cytotoxicity has been observed in the *ex-vivo* culture and expansion of perilesional T

cells followed by co-culture with skin explants. Only co-cultures that contained $CD8^+$ cells induced apoptosis in Gp-100^+ (a melanocyte-marker) cells in non-lesional skin. No signs of apoptosis were observed in lesional skin incubated with total T cells (also contain $CD8^+$ cells) indicating a melanocyte-specific cytotoxicity (van den Boorn *et al.*, 2009). However, a separate report on the co-culture of isolated perilesional $CD8^+$ cells with primary melanocytes suggests a cytotoxic role of IFN-γ itself (Wu *et al.*, 2013). Clearly, IFN-γ can affect melanocytes as demonstrated by numerous reports reporting its alteration of pigmentation, growth and expression of immunologically-relevant molecules (Yohn *et al.*, 1990; Le Poole, Mutis, *et al.*, 1993; Dwivedi *et al.*, 2013; Natarajan *et al.*, 2014; L Yang *et al.*, 2015) however its precise role in the initiation of the disease remains undefined.

In addition to the activation of autoreactive $CD8^+$ cells, there is also evidence of an impaired regulatory T cell (Treg) compartment in vitiligo patients. Reduced numbers of circulating and skin-resident Tregs have been reported in vitiligo patients (Lili *et al.*, 2012a; Abdallah *et al.*, 2014; Lin *et al.*, 2014; Hegab and Attia, 2015; Kidir *et al.*, 2017). In addition, impaired suppressive abilities of circulating Tregs from vitiligo patients have been observed in co-culture assays with globally-activated (anti-CD3/CD28) T cells (Ben Ahmed *et al.*, 2012; Lili *et al.*, 2012b; Lin *et al.*, 2014). However, a separate report found that circulating Tregs from vitiligo patients were fully functional in their suppressive abilities. Instead, expression of the chemokine CCL22 was found to be reduced in vitiligo skin compared to healthy controls. Therefore Tregs, whose CCR4 (receptor for CCL22) expression was no different from controls, were not sufficiently recruited to the inflamed tissue (Klarquist *et al.*, 2010). The ability of autoreactive cytotoxic T cells to be recruited to the tissue through the CCL22-CCR4 axis was not

addressed. If confirmed, a diminished Treg compartment likely permits the development of autoimmune vitiligo.

Despite strong evidence of a T cell-driven immunopathology in autoimmune vitiligo, there are very few studies on the generation of memory T cells. This is surprising since, as mentioned earlier, one of the key strategies in vitiligo management is the stimulation of re-pigmentation – presumably through the regeneration of melanocytes from progenitor cells. MelanA/MART-1-specific T cells with a memory phenotype have been isolated from the periphery (Ogg *et al.*, 1998; Mantovani *et al.*, 2003). In a 2017 report, a high proportion of skin resident T cells from stable and active vitiligo lesions were found to display an effector memory ($CD45RO^{+}CCR7^{-}$) phenotype.

While the link between impaired anti-oxidant responses in vitiligo melanocytes and melanocyte-specific autoimmune targeting remains undiscovered, it is possible that the melanocyte itself may play a role in initiating the immune response. There is evidence of the capability of melanocytes to express immunologically relevant molecules such as: CD40 (Lu *et al.*, 2002), MHC-II (Le Poole *et al.*, 1993) and interleukin-6 and -8 (Toosi *et al*., 2012; Yao *et al.*, 2012). However, their role in initiating or provoking the immune response in vitiligo is unknown.

Findings from Mouse Models of Vitiligo

The role of heat shock protein 70 (HSP70) in the initiation of vitiligo was uncovered in a mouse model utilizing gene gun vaccination as a means to induce the disease. Interestingly, induction of vitiligo was global in these mice as depigmentation was not reserved to the vaccination site (Denman *et al.*, 2008). Inducible HSP70 (HSP70i) was also demonstrated to be required for depigmentation in a HSP70i-knockout mouse model vaccinated with optimized Trp-

1 – a highly immunogenic melanocyte-specific target molecule (Mosenson *et al.*, 2012). The most compelling evidence for involvement of HSP70i is the ability of a mutated form of the protein to reverse depigmentation in mouse models of vitiligo. *In vitro*, the mutated form of HSP70i failed to activate dendritic cells as evidenced by decreased MHC-II, CD80, CD86 and CD83 surface expression (Mosenson *et al.*, 2013). Based on these results it is thought that HSP70i is released from melanocytes, perhaps in response to stress, and is recognized by nearby dendritic cells which in turn activate T cells.

The Krt14-Kitl* mouse, also known as K14-SCF, expresses a mutated form of kit-ligand (stem cell factor) under the control of the keratinocyte-specific keratin 14 (K14) promoter. As murine keratinocytes do not normally express kit-ligand, expression of a membrane-bound form in Krt14-Kitl* mice retains melanocytes in the epidermis and, in contrast to melanocytes from normal mice which are exclusive to hair follicles, more closely mimics human skin (Kunisada *et al.*, 1998). The requirement of IFN-γ in the initiation and progression of vitiligo has also been demonstrated in an adoptive transfer model utilizing the Krt14-Kitl* transgenic mouse. Vitiligo in these mice is induced by the adoptive transfer of melanocyte-specific (PMEL) $CD8^+$ T cells purified from the spleen of PMEL TCR transgenic mice into transgenic Krt14-Kitl* mice. Analysis of depigmented skin of recipient mice revealed elevated IFN-γ expression which was demonstrated to originate from infiltrating $CD8^+$ T cells. Furthermore, post-induction administration of an IFN-γ-neutralizing antibody resulted in the prevention of depigmentation by inhibiting the accumulation of auto-reactive T cells in the skin (Harris *et al.*, 2012).

Gene expression profiling of lesional skin revealed an IFN-γ-dependent chemokine signature similar to that seen in skin from vitiligo patients. Specifically, CXCL10 appears to be essential to the recruitment of $CXCR3^+$ T cells to the skin. In mice receiving either T cells from a

Cxcr3$^{-/-}$ PMEL TCR transgenic mice or wild-type PMEL TCR T cells with a CXCL10 neutralizing antibody, CD8^{+} T cells failed to accumulate in the skin thus preventing and even reversing de-pigmentation (Rashighi *et al.*, 2014). Similar effects were seen by the administration of simvastatin – an inhibitor of STAT1 which is required for IFN-γ signaling (Agarwal *et al.*, 2015). Indeed, expression of CXCL10 may serve as a clinical marker for vitiligo (Rashighi *et al.*, 2014). Moreover, blockade of the IFN-γ/CXCL10/CXCL3 axis is currently being explored as a treatment option in the clinic. Results thus far have been mixed (Craiglow and King, 2015; Kim *et al.*, 2018; Nguyen *et al.*, 2018).

As seen above, most murine models of vitiligo involve the induction of the disease and therefore do not fully represent the human condition. In 2012 a transgenic mouse model for T cell-mediated immunotherapy utilizing a tyrosinase-specific, HLA-A2-restricted T cell receptor derived from a tumor-infiltrating CD4^{+} HLA-A2-restricted T cell of a metastatic melanoma patient was described. To the surprise of the authors, the majority of T cells in the periphery and spleen were not only CD4^{-}CD8^{-} but were fully functional; capable of cytokine secretion in response to stimuli. In addition, the mice (termed h3TA2) gradually developed spontaneous autoimmune vitiligo (Mehrotra *et al.*, 2012). Crossing h3TA2 with Krt14-Kitl* mice yielded the Vitesse mouse which spontaneously develops anti-melanocyte cell-mediated immunity to epidermal melanocytes. Interestingly, depigmentation in the Vitesse mouse was followed by spotted re-pigmentation which is associated with increased numbers of FoxP3^{+} T cells (regulatory) suggesting an establishment of peripheral tolerance (Eby *et al.*, 2014).

The Smyth chicken model for autoimmune vitiligo

The Smyth line of chicken was originally described in 1977 by J Robert Smith Jr from the University of Massachusetts and began with a single of the Massachusetts Brown line of

chicken who exhibited a complete loss of pigment in her adult plumage. Genetic selection for the "amelanosis trait", as it was referred to then, involved crossing with other Brown line males as well as males from three non-related lines: Barred Plymouth Rocks, random-breeding meat stock and Light Brown Leghorn lines (Smyth *et al*., 1981). Pigment loss in Smyth chickens closely mimics that seen in vitiligo patients. Similarly to humans, Smyth chickens experience a spontaneous post-natal loss of melanocytes in growing feathers through a complex interaction of genetic, environmental and immunological factors (Smyth *et al.*, 1981). In addition, some vitiliginous Smyth chickens experience erratic episodes of de- and re-pigmentation. Furthermore, as in humans, vitiligo in Smyth chickens is closely associated with hypothyroidism and an alopecia-like feathering defect (Smyth, Jr., 1989).

The full Smyth Line model is composed of three MHC-matched ($B^{101/101}$) lines of chicken: the vitiligo-prone Smyth chicken (incidence 80-95%), the vitiligo-susceptible, parental Brown line (incidence 0-2%) and the vitiligo-resistant, distantly related Light Brown Leghorn line (incidence 0%). The inherent genetic susceptibility to autoimmune vitiligo was revealed by i.p. injection with the DNA methylation inhibitor 5-azacytidine. When treated in this manner, the incidence of vitiligo in Brown line chickens was over 70% compared to 0% in vehicle-injected chickens. In contrast there was no change in the incidence (0%) of vitiligo in Light Brown Leghorn chickens (Sreekumar, Erf and Smyth, Jr., 1996).

As in humans, the genetic susceptibility in Smyth chickens is localized, at least in part, to an inherent abnormality in melanocytes. Melanocyte cultures derived from the neural crest of developing Smyth chicken embryos were initially morphologically identical to those from Brown line and Light Brown Leghorn line chickens but by 4 – 6 weeks had developed large, pigmented vacuoles in their cytoplasm. In addition, by 12 weeks the cells became enlarged and

less dendritic with increased numbers of pigmented vacuoles (Boissy *et al.*, 1986). These observations mimic those observed in long term cultures of melanocytes from vitiligo patients (Boissy *et al.*, 1991). Similar abnormalities were also observed in growing feathers of Smyth chickens in the lead up to visual onset of vitiligo. At least two weeks prior to vitiligo onset, melanocytes at the barb ridge (anatomical location of melanocytes in feathers) had retracted their dendrites and contained large pigmented clumps (Boissy *et al*., 1983).

As in humans, the inherent dysfunction of melanocytes is not sufficient for disease expression. In bursectomized (bursa of Fabricius is the site of B cell development in birds) Smyth chickens dysfunctional melanocytes were retained which argues for the requirement of a functional immune system in vitiligo expression (Boissy *et al*., 1984). Further evidence was provided by the administration of corticosterone (an immunosuppressive steroid) which resulted in a significant reduction in vitiligo incidence compared to untreated controls (Boyle *et al.*, 1987). In administration of cyclosporine A which, as an inhibitor of IL-2 release, resulted in a significant delay in the age of onset presumably from the inhibition of antigen-primed T cells. Withdrawal of the treatment resulted in a sharp rise in the incidence of vitiligo (Pardue *et al.*, 1987).

While the exact roles of cell-mediated and humoral immunity in initiating autoimmune vitiligo are unclear, current evidence strongly argues for a T cell-driven etiology. Although evidence for a humoral response in Smyth chickens is well documented (Lamont *et al.*, 1982; Austin *et al.*, 1992; Searle *et al.*, 1993; Austin and Boissy, 1995), it does not appear to be necessary for disease expression as removal of the bursa of Fabricius resulted in a delay but not a prevention of vitiligo (Boissy *et al.*, 1984). Furthermore, while infiltration of both T and B cells

into regenerating feathers of vitiliginous Smyth chickens have been observed, T cell levels remained elevated post-onset while those of B cells returned to baseline.

In growing feathers plucked from Smyth chickens with vitiligo, $CD8^+$ T cells were found at the dermal/epidermal junction (anatomical location of melanocytes) in close proximity to apoptotic cells (Wang and Erf, 2004). Additionally, leukocyte infiltration into wattles of completely depigmented Smyth chickens injected with feather-derived melanocyte lysates was dominated by T cells, providing strong evidence of a melanocyte-specific cell-mediated immune response (Wang and Erf, 2003). A microarray study examining pools of cDNA from growing feathers of Smyth chickens also found evidence of both humoral (Ig-J chain, CXCL13) and cell-mediated (CCL19, GZMA, IL21R) immune activities prior-to vitiligo onset (Shi *et al.*, 2012). More convincing evidence for a cell-mediated immune response came from a study examining the relationship between infiltrating leukocytes (estimated by immunohistochemical staining of frozen tissue sections) and cytokine gene expression profiles in growing feathers obtained prior-to and throughout vitiligo progression. Elevated IFN-γ expression as well as a dominant presence of $CD8^+$ cells leading up to visual onset, suggests a Th1-like, cell-mediated polarization in the active lesion (Shi and Erf, 2012).

References

Abdallah, M. *et al.* (2014) 'Assessment of tissue FoxP3 $^{+}$, CD4 $^{+}$ and CD8 $^{+}$ T-cells in active and stable nonsegmental vitiligo', *International Journal of Dermatology*, 53(8), pp. 940–946. doi: 10.1111/ijd.12160.

Agarwal, P. *et al.* (2015) 'Simvastatin Prevents and Reverses Depigmentation in a Mouse Model of Vitiligo', *Journal of Investigative Dermatology*, 135(4), pp. 1080–1088. doi: 10.1038/jid.2014.529.

Ben Ahmed, M. *et al.* (2012) 'Functional defects of peripheral regulatory T lymphocytes in patients with progressive vitiligo', *Pigment Cell & Melanoma Research*, 25(1), pp. 99–109. doi: 10.1111/j.1755-148X.2011.00920.x.

Arowojolu, O. A. *et al.* (2017) 'The nuclear factor (erythroid-derived 2)-like 2 (NRF2) antioxidant response promotes melanocyte viability and reduces toxicity of the vitiligo-inducing phenol monobenzone', *Experimental Dermatology*, 26(7), pp. 637–644. doi: 10.1111/exd.13350.

Austin, L. M. *et al.* (1992) 'The detection of melanocyte autoantibodies in the Smyth chicken model for vitiligo.', *Clinical immunology and immunopathology*, 64(2), pp. 112–20. Available at: http://www.ncbi.nlm.nih.gov/pubmed/1643744.

Austin, L. M. and Boissy, R. E. (1995) 'Mammalian tyrosinase-related protein-1 is recognized by autoantibodies from vitiliginous Smyth chickens. An avian model for human vitiligo.', *The American journal of pathology*, 146(6), pp. 1529–41. Available at: http://www.pubmedcentral.nih.gov/articlerender.fcgi?artid=1870917&tool=pmcentrez&rendertype=abstract.

Bae, J. M. *et al.* (2017) 'Phototherapy for Vitiligo', *JAMA Dermatology*. American Medical Association, 153(7), p. 666. doi: 10.1001/jamadermatol.2017.0002.

Bae, J. M. *et al.* (2018) 'Factors affecting quality of life in patients with vitiligo: a nationwide study', *British Journal of Dermatology*, 178(1), pp. 238–244. doi: 10.1111/bjd.15560.

Baharav, E. *et al.* (1996) 'Tyrosinase as an autoantigen in patients with vitiligo.', *Clinical and experimental immunology*, 105(1), pp. 84–8. Available at: http://www.ncbi.nlm.nih.gov/pubmed/8697641 (Accessed: 12 July 2018).

Boissy, R. E. *et al.* (1986) 'Delayed-amelanotic (DAM or Smyth) chicken: melanocyte dysfunction in vivo and in vitro.', *The Journal of investigative dermatology*, 86(2), pp. 149–156. Available at: http://www.ncbi.nlm.nih.gov/pubmed/3091704.

Boissy, R. E. *et al.* (1991) 'Structural aberration of the rough endoplasmic reticulum and melanosome compartmentalization in long-term cultures of melanocytes from vitiligo patients', *Journal of Investigative Dermatology*, 97(3), pp. 395–404. doi: 10.1111/1523-1747.ep12480976.

Boissy, R. E., Lamont, S. J. and Smyth, J. R. (1984) 'Persistence of abnormal melanocytes in immunosuppressed chickens of the autoimmune "DAM" line.', *Cell and tissue research*, 235(3), pp. 663–8. Available at: http://www.ncbi.nlm.nih.gov/pubmed/6713493.

Boissy, R. E., Smyth, J. R. and Fite, K. V (1983) 'Progressive cytologic changes during the development of delayed feather amelanosis and associated choroidal defects in the DAM chicken line. A vitiligo model.', *The American journal of pathology*, 111(2), pp. 197–212. Available at: http://www.ncbi.nlm.nih.gov/pubmed/6846502.

van den Boorn, J. G. *et al.* (2009) 'Autoimmune Destruction of Skin Melanocytes by Perilesional T Cells from Vitiligo Patients', *Journal of Investigative Dermatology*, 129(9), pp. 2220–2232. doi: 10.1038/jid.2009.32.

Boyle, M. L., Pardue, S. L. and Smyth, J. R. (1987) 'Effect of corticosterone on the incidence of amelanosis in Smyth delayed amelanotic line chickens.', *Poultry science*, 66(2), pp. 363–7. Available at: http://www.ncbi.nlm.nih.gov/pubmed/3588505.

Catucci Boza, J. *et al.* (2016) 'Quality of Life Impairment in Children and Adults with Vitiligo: A Cross-Sectional Study Based on Dermatology-Specific and Disease-Specific Quality of Life Instruments', *Dermatology*, 232(5), pp. 619–625. doi: 10.1159/000448656.

Chang, Y. *et al.* (2017) 'Simvastatin Protects Human Melanocytes from H2O2-Induced Oxidative Stress by Activating Nrf2', *Journal of Investigative Dermatology*. The Authors, 137(6), pp. 1286–1296. doi: 10.1016/j.jid.2017.01.020.

Craiglow, B. G. and King, B. A. (2015) 'Tofacitinib citrate for the treatment of Vitiligo a pathogenesis-directed therapy', *JAMA Dermatology*, 151(10), pp. 1110–1112. doi: 10.1001/jamadermatol.2015.1520.

Dahir, A. M. and Thomsen, S. F. (2018) 'Comorbidities in vitiligo: comprehensive review', *International Journal of Dermatology*. doi: 10.1111/ijd.14055.

Davis, M. D. and Kaufman, S. (1989) 'Evidence for the formation of the 4a-carbinolamine during the tyrosine-dependent oxidation of tetrahydrobiopterin by rat liver phenylalanine hydroxylase.', *The Journal of biological chemistry*, 264(15), pp. 8585–96. Available at: http://www.ncbi.nlm.nih.gov/pubmed/2722790.

Dell'Anna, M. L. *et al.* (2007) 'Membrane Lipid Alterations as a Possible Basis for Melanocyte Degeneration in Vitiligo', *Journal of Investigative Dermatology*. Elsevier, 127(5), pp. 1226–1233. doi: 10.1038/SJ.JID.5700700.

Denman, C. J. *et al.* (2008) 'HSP70i accelerates depigmentation in a mouse model of autoimmune vitiligo', *Journal of Investigative Dermatology*, 128(8), pp. 2041–2048. doi: 10.1038/jid.2008.45.

Dwivedi, M. *et al.* (2013) 'Involvement of Interferon-Gamma Genetic Variants and Intercellular Adhesion Molecule-1 in Onset and Progression of Generalized Vitiligo', *Journal of Interferon & Cytokine Research*, 33(11), pp. 646–659. doi: 10.1089/jir.2012.0171.

Eby, J. M. *et al.* (2014) 'Immune responses in a mouse model of vitiligo with spontaneous epidermal de- and repigmentation.', *Pigment cell & melanoma research*, 27(6), pp. 1075–85. doi: 10.1111/pcmr.12284.

Elassiuty, Y. E. *et al.* (2011) 'Heme oxygenase-1 expression protects melanocytes from stress-induced cell death: implications for vitiligo', *Experimental Dermatology*, 20(6), pp. 496–501. doi: 10.1111/j.1600-0625.2010.01232.x.

Ezzedine, K. *et al.* (2012) 'Revised classification/nomenclature of vitiligo and related issues: the Vitiligo Global Issues Consensus Conference', *Pigment Cell & Melanoma Research*. Wiley/Blackwell (10.1111), 25(3), pp. E1–E13. doi: 10.1111/j.1755-148X.2012.00997.x.

Ezzedine, K. *et al.* (2015) 'Living with vitiligo: results from a national survey indicate differences between skin phototypes', *British Journal of Dermatology*, 173(2), pp. 607–609. doi: 10.1111/bjd.13839.

Ezzedine, K. *et al.* (2015) 'Vitiligo', *The Lancet*. Elsevier, 386(9988), pp. 74–84. doi: 10.1016/S0140-6736(14)60763-7.

Ezzedine, K., Whitton, M. and Pinart, M. (2016) 'Interventions for Vitiligo', *JAMA*. American Medical Association, 316(16), p. 1708. doi: 10.1001/jama.2016.12399.

Florez-Pollack, S. *et al.* (2017) 'Association of Quality of Life and Location of Lesions in Patients With Vitiligo', *JAMA Dermatology*. American Medical Association, 153(3), p. 341. doi: 10.1001/jamadermatol.2016.4670.

Gilhar, A. *et al.* (1995) 'In vivo destruction of melanocytes by the IgG fraction of serum from patients with vitiligo.', *The Journal of investigative dermatology*, 105(5), pp. 683–6. Available at: http://www.ncbi.nlm.nih.gov/pubmed/7594644 (Accessed: 12 July 2018).

Grimes, P. E. and Miller, M. M. (2018) 'Vitiligo: Patient stories, self-esteem, and the psychological burden of disease', *International Journal of Women's Dermatology*. Elsevier, 4(1), pp. 32–37. doi: 10.1016/J.IJWD.2017.11.005.

Harada, T. *et al.* (1993) 'Feedback regulation mechanisms for the control of GTP cyclohydrolase I activity.', *Science (New York, N.Y.)*. American Association for the Advancement of Science, 260(5113), pp. 1507–10. doi: 10.1126/science.8502995.

Harris, J. E. *et al.* (2012) 'A Mouse Model of Vitiligo with Focused Epidermal Depigmentation Requires IFN-γ for Autoreactive CD8+ T-Cell Accumulation in the Skin', *Journal of Investigative Dermatology*, 132(7), pp. 1869–1876. doi: 10.1038/jid.2011.463.

Hegab, D. S. and Attia, M. A. S. (2015) 'Decreased Circulating T Regulatory Cells in Egyptian Patients with Nonsegmental Vitiligo: Correlation with Disease Activity', *Dermatology Research and Practice*, 2015, pp. 1–7. doi: 10.1155/2015/145409.

Helen Kemp, E. *et al.* (1999) 'Identification of Epitopes on Tyrosinase which are Recognized by Autoantibodies from Patients with Vitiligo', *Journal of Investigative Dermatology*, 113(2), pp. 267–271. doi: 10.1046/j.1523-1747.1999.00664.x.

Hertz, K. C. *et al.* (1977) 'Autoimmune vitiligo: detection of antibodies to melanin-producing cells.', *New England Journal of Medicine*, 297(12), pp. 634–637. doi: 10.1056/NEJM197709222971204.

Jian, Z. *et al.* (2011) 'Heme Oxygenase-1 Protects Human Melanocytes from H2O2-Induced Oxidative Stress via the Nrf2-ARE Pathway', *Journal of Investigative Dermatology*. Nature Publishing Group, 131(7), pp. 1420–1427. doi: 10.1038/jid.2011.56.

Jian, Z. *et al.* (2014) 'Impaired activation of the Nrf2-ARE signaling pathway undermines H 2 O 2-induced oxidative stress response: A possible mechanism for melanocyte degeneration in vitiligo', *Journal of Investigative Dermatology*. Nature Publishing Group, 134(8), pp. 2221–2230. doi: 10.1038/jid.2014.152.

Jian, Z. *et al.* (2016) 'Aspirin induces Nrf2-mediated transcriptional activation of haem oxygenase-1 in protection of human melanocytes from H2O2-induced oxidative stress', *Journal of Cellular and Molecular Medicine*, 20(7), pp. 1307–1318. doi: 10.1111/jcmm.12812.

Jin, Y. *et al.* (2016) 'Genome-wide association studies of autoimmune vitiligo identify 23 new risk loci and highlight key pathways and regulatory variants', *Nature Genetics*, 48(11), pp. 1418–1424. doi: 10.1038/ng.3680.

Jung, E. *et al.* (2017) 'Melanocyte-protective effect of afzelin is mediated by the Nrf2-ARE signalling pathway via GSK-3β inactivation', *Experimental Dermatology*, 26(9), pp. 764–770. doi: 10.1111/exd.13277.

Kemp, E. H. *et al.* (1998) 'Autoantibodies to human melanocyte-specific protein pmel17 in the sera of vitiligo patients: a sensitive and quantitative radioimmunoassay (RIA).', *Clinical and experimental immunology*, 114(3), pp. 333–8. Available at: http://www.ncbi.nlm.nih.gov/pubmed/9844040 (Accessed: 12 July 2018).

Kemp, E. H. *et al.* (2002) 'The melanin-concentrating hormone receptor 1, a novel target of autoantibody responses in vitiligo', *Journal of Clinical Investigation*, 109(7), pp. 923–930. doi: 10.1172/JCI14643.

Kidir, M. *et al.* (2017) 'Regulatory T-cell cytokines in patients with nonsegmental vitiligo', *International Journal of Dermatology*, 56(5), pp. 581–588. doi: 10.1111/ijd.13564.

Kim, S. R. *et al.* (2018) 'Rapid Repigmentation of Vitiligo Using Tofacitinib Plus Low-Dose, Narrowband UV-B Phototherapy', *JAMA Dermatology*. American Medical Association, 154(3), p. 370. doi: 10.1001/jamadermatol.2017.5778.

Klarquist, J. *et al.* (2010) 'Reduced skin homing by functional Treg in vitiligo', *Pigment Cell & Melanoma Research*, 23(2), pp. 276–286. doi: 10.1111/j.1755-148X.2010.00688.x.

Kroon, M. W. *et al.* (2013) 'Melanocyte antigen-specific antibodies cannot be used as markers for recent disease activity in patients with vitiligo', *Journal of the European Academy of Dermatology and Venereology*, 27(9), pp. 1172–1175. doi: 10.1111/j.1468-3083.2012.04501.x.

Kunisada, T. *et al.* (1998) 'Murine cutaneous mastocytosis and epidermal melanocytosis induced by keratinocyte expression of transgenic stem cell factor.', *The Journal of experimental medicine*, 187(10), pp. 1565–73. Available at: http://www.ncbi.nlm.nih.gov/pubmed/9584135.

Laddha, N. C. *et al.* (2013) 'Vitiligo: interplay between oxidative stress and immune system.', *Experimental dermatology*, 22(4), pp. 245–50. doi: 10.1111/exd.12103.

Lamont, S. J., Boissy, R. E. and Smyth, J. R. J. (1982) 'Humoral immune response and expression of spontaneous postnatal amelanosis in DAM line chickens.', *Immunological communications*, 11(2), pp. 121–127.

Lili, Y. *et al.* (2012a) 'Global activation of CD8+ cytotoxic T lymphocytes correlates with an impairment in regulatory T cells in patients with generalized Vitiligo', *PLoS ONE*, 7(5). doi: 10.1371/journal.pone.0037513.

Lili, Y. *et al.* (2012b) 'Global Activation of CD8+ Cytotoxic T Lymphocytes Correlates with an Impairment in Regulatory T Cells in Patients with Generalized Vitiligo', *PLoS ONE*. Edited by D. Unutmaz, 7(5), p. e37513. doi: 10.1371/journal.pone.0037513.

Lin, M. *et al.* (2014) 'Regulatory T cells from active non-segmental vitiligo exhibit lower suppressive ability on CD8+CLA+ T cells.', *European journal of dermatology : EJD*, 24(6), pp. 676–82. doi: 10.1684/ejd.2014.2436.

Linsley, P. S. *et al.* (1994) 'Human B7-1 (CD80) and B7-2 (CD86) bind with similar avidities but distinct kinetics to CD28 and CTLA-4 receptors.', *Immunity*, 1(9), pp. 793–801. Available at: http://www.ncbi.nlm.nih.gov/pubmed/7534620 (Accessed: 12 July 2018).

Loboda, A. *et al.* (2016) 'Role of Nrf2/HO-1 system in development, oxidative stress response and diseases: an evolutionarily conserved mechanism', *Cellular and Molecular Life Sciences*, 73(17), pp. 3221–3247. doi: 10.1007/s00018-016-2223-0.

Lu, Y. *et al.* (2002) 'Melanocytes are potential immunocompetent cells: evidence from recognition of immunological characteristics of cultured human melanocytes.', *Pigment cell research*, 15(6), pp. 454–60. Available at: http://www.ncbi.nlm.nih.gov/pubmed/12453188 (Accessed: 10 July 2018).

Manga, P. *et al.* (2006) 'A role for tyrosinase-related protein 1 in 4-tert-butylphenol-induced toxicity in melanocytes: Implications for vitiligo', *American Journal of Pathology*, 169(5), pp. 1652–1662. doi: 10.2353/ajpath.2006.050769.

Mantovani, S. *et al.* (2003) 'Molecular and functional bases of self-antigen recognition in long-term persistent melanocyte-specific CD8+T cells in one vitiligo patient', *Journal of Investigative Dermatology*. Elsevier Masson SAS, 121(2), pp. 308–314. doi: 10.1046/j.1523-1747.2003.12368.x.

Maresca, V. *et al.* (1997) 'Increased sensitivity to peroxidative agents as a possible pathogenic factor of melanocyte damage in vitiligo.', *The Journal of investigative dermatology*, 109(3), pp. 310–3. Available at: http://www.ncbi.nlm.nih.gov/pubmed/9284096 (Accessed: 10 July 2018).

Mehrotra, S. *et al.* (2012) 'A coreceptor-independent transgenic human TCR mediates anti-tumor and anti-self immunity in mice.', *Journal of immunology (Baltimore, Md. : 1950)*. American Association of Immunologists, 189(4), pp. 1627–38. doi: 10.4049/jimmunol.1103271.

Mosenson, J. A. *et al.* (2012) 'HSP70i is a critical component of the immune response leading to vitiligo', *Pigment Cell and Melanoma Research*, 25(1), pp. 88–98. doi: 10.1111/j.1755-148X.2011.00916.x.

Mosenson, J. A. *et al.* (2013) 'Mutant HSP70 reverses autoimmune depigmentation in vitiligo', *Science Translational Medicine*, 5(174). doi: 10.1126/scitranslmed.3005127.

Natarajan, V. T. *et al.* (2014) 'IFN-γ signaling maintains skin pigmentation homeostasis through regulation of melanosome maturation.', *Proceedings of the National Academy of Sciences of the United States of America*, 111(6), pp. 2301–6. doi: 10.1073/pnas.1304988111.

Nguyen, S. *et al.* (2018) 'Atorvastatin in Combination With Narrowband UV-B in Adult Patients With Active Vitiligo', *JAMA Dermatology*. American Medical Association, 154(6), p. 725. doi: 10.1001/jamadermatol.2017.6401.

Norris, D. A. *et al.* (1988) 'Evidence for immunologic mechanisms in human vitiligo: patients' sera induce damage to human melanocytes in vitro by complement-mediated damage and antibody-dependent cellular cytotoxicity.', *The Journal of investigative dermatology*, 90(6), pp. 783–9. Available at: http://www.ncbi.nlm.nih.gov/pubmed/3373009 (Accessed: 12 July 2018).

Ogg, G. S. *et al.* (1998) 'High frequency of skin-homing melanocyte-specific cytotoxic T lymphocytes in autoimmune vitiligo.', *The Journal of experimental medicine*, 188(6), pp. 1203–8. Available at: http://www.ncbi.nlm.nih.gov/pubmed/9743539 (Accessed: 13 July 2018).

Pardue, S. L. *et al.* (1987) 'Enhanced integumental and ocular amelanosis following the termination of cyclosporine administration.', *The Journal of investigative dermatology*, 88(6), pp. 758–61. Available at: http://www.ncbi.nlm.nih.gov/pubmed/3585059.

Picardo, M. *et al.* (2015) 'Vitiligo', *Nature Reviews Disease Primers*, p. 15011. doi: 10.1038/nrdp.2015.11.

Le Poole, I. C., Mutis, T., *et al.* (1993) 'A novel, antigen-presenting function of melanocytes and its possible relationship to hypopigmentary disorders.', *Journal of immunology (Baltimore, Md. : 1950)*, 151(12), pp. 7284–92. Available at: http://www.ncbi.nlm.nih.gov/pubmed/8258725.

Le Poole, I. C., Das, P. K., *et al.* (1993) 'Review of the etiopathomechanism of vitiligo: a convergence theory.', *Experimental dermatology*, 2(4), pp. 145–53. Available at: http://www.ncbi.nlm.nih.gov/pubmed/8162332.

Le Poole, I. C. *et al.* (1996) 'Presence of T cells and macrophages in inflammatory vitiligo skin parallels melanocyte disappearance.', *The American journal of pathology*, 148(4), pp. 1219–28.

Qureshi, O. S. *et al.* (2011) 'Trans-endocytosis of CD80 and CD86: a molecular basis for the cell-extrinsic function of CTLA-4.', *Science (New York, N.Y.)*, 332(6029), pp. 600–3. doi: 10.1126/science.1202947.

Rashighi, M. *et al.* (2014) 'CXCL10 Is Critical for the Progression and Maintenance of Depigmentation in a Mouse Model of Vitiligo', *Science Translational Medicine*, 6(223), p. 223ra23-223ra23. doi: 10.1126/scitranslmed.3007811.

Ruiz-Argüelles, A. *et al.* (2007) 'Apoptosis of melanocytes in vitiligo results from antibody penetration', *Journal of Autoimmunity*, 29(4), pp. 281–286. doi: 10.1016/j.jaut.2007.07.012.

Schallereuter, K. U. *et al.* (1994) 'Defective tetrahydrobiopterin and catecholamine biosynthesis in the depigmentation disorder vitiligo', *BBA - Molecular Basis of Disease*, 1226(2), pp. 181–192. doi: 10.1016/0925-4439(94)90027-2.

Schallreuter, K. U. *et al.* (1999) 'In vivo and in vitro evidence for hydrogen peroxide (H2O2) accumulation in the epidermis of patients with vitiligo and its successful removal by a UVB-activated pseudocatalase.', *The journal of investigative dermatology. Symposium proceedings*, 4(1), pp. 91–6. Available at: http://www.ncbi.nlm.nih.gov/pubmed/10537016.

Schallreuter, K. U. *et al.* (2001) 'Epidermal H(2)O(2) accumulation alters tetrahydrobiopterin (6BH4) recycling in vitiligo: identification of a general mechanism in regulation of all 6BH4-dependent processes?', *The Journal of investigative dermatology*, 116(1), pp. 167–74. doi: 10.1046/j.1523-1747.2001.00220.x.

Schallreuter, K. U., Wood, J. M. and Berger, J. (1991) 'Low catalase levels in the epidermis of patients with vitiligo.', *The Journal of investigative dermatology*, 97(6), pp. 1081–5. Available at: http://www.ncbi.nlm.nih.gov/pubmed/1748819 (Accessed: 12 July 2018).

Searle, E. A. *et al.* (1993) 'Smyth Chicken Melanocyte Autoantibodies - Cross-Species Recognition, In-Vivo Binding, And Plasma-Membrane Reactivity Of The Antiserum', *Pigment Cell Research*, 6(3), pp. 145–157.

Shalbaf, M. *et al.* (2008) 'Presence of epidermal allantoin further supports oxidative stress in vitiligo', *Experimental Dermatology*. Wiley/Blackwell (10.1111), 17(9), pp. 761–770. doi: 10.1111/j.1600-0625.2008.00697.x.

Shi, F. *et al.* (2012) 'Understanding mechanisms of vitiligo development in Smyth line of chickens by transcriptomic microarray analysis of evolving autoimmune lesions', *BMC Immunology*. BioMed Central Ltd, 13(1), p. 18. doi: 10.1186/1471-2172-13-18.

Shi, F. and Erf, G. F. (2012) 'IFN-γ, IL-21, and IL-10 co-expression in evolving autoimmune vitiligo lesions of Smyth line chickens.', *The Journal of investigative dermatology*, 132(3 Pt 1), pp. 642–9. doi: 10.1038/jid.2011.377.

Smyth, Jr., J. R. (1989) 'The Smyth chicken: A model for autoimmune amelanosis', *Critical reviews in poultry biology*, 2, pp. 1–19.

Smyth, J. R., Boissy, R. E. and Fite, K. V (1981) 'The DAM chicken: a model for spontaneous postnatal cutaneous and ocular amelanosis.', *The Journal of heredity*, 72(3), pp. 150–6. Available at: http://www.ncbi.nlm.nih.gov/pubmed/7276522.

Sreekumar, G. P., Erf, G. F. and Smyth, Jr., J. R. (1996) '5-Azacytidine Treatment Induces Autoimmune Vitiligo in Parental Control Strains of the Smyth Line Chicken Model for Autoimmune Vitiligo', *Clinical Immunology and Immunopathology*, 81(2), pp. 136–144. doi: 10.1006/clin.1996.0169.

Taïeb, A. and Picardo, M. (2009) 'Vitiligo', *New England Journal of Medicine*. Massachusetts Medical Society, 360(2), pp. 160–169. doi: 10.1056/NEJMcp0804388.

Toosi, S., Orlow, S. J. and Manga, P. (2012) 'Vitiligo-inducing phenols activate the unfolded protein response in melanocytes resulting in upregulation of IL6 and IL8', *Journal of Investigative Dermatology*, 132(11), pp. 2601–2609. doi: 10.1038/jid.2012.181.

Wang, X. and Erf, G. F. (2003) 'Melanocyte-specific cell mediated immune response in vitiliginous Smyth line chickens', *Journal of Autoimmunity*, 21(2), pp. 149–160. doi: 10.1016/S0896-8411(03)00087-8.

Wang, X. and Erf, G. F. (2004) 'Apoptosis in feathers of Smyth line chickens with autoimmune vitiligo', *Journal of Autoimmunity*, 22(1), pp. 21–30. doi: 10.1016/j.jaut.2003.09.006.

Wańkowicz-Kalińska, A. *et al.* (2003) 'Immunopolarization of CD4+ and CD8+ T cells to Type-1-like is associated with melanocyte loss in human vitiligo.', *Laboratory investigation; a journal of technical methods and pathology*, 83(5), pp. 683–95. Available at: http://www.ncbi.nlm.nih.gov/pubmed/12746478 (Accessed: 12 July 2018).

WU, J. *et al.* (2013) 'CD8+ T cells from vitiligo perilesional margins induce autologous melanocyte apoptosis', *Molecular Medicine Reports*, 7(1), pp. 237–241. doi: 10.3892/mmr.2012.1117.

Yang, L. *et al.* (2015) 'Interferon-gamma Inhibits Melanogenesis and Induces Apoptosis in Melanocytes: A Pivotal Role of CD8+ Cytotoxic T Lymphocytes in Vitiligo.', *Acta dermato-venereologica*, 95(6), pp. 664–70. doi: 10.2340/00015555-2080.

Yang, L. *et al.* (2015) 'Interferon-gamma Inhibits Melanogenesis and Induces Apoptosis in Melanocytes: A Pivotal Role of CD8+ Cytotoxic T Lymphocytes in Vitiligo', *Acta Dermato Venereologica*, 95(6), pp. 664–670. doi: 10.2340/00015555-2080.

Yao, L. *et al.* (2012) 'Subtoxic levels hydrogen peroxide-induced expression of interleukin-6 by epidermal melanocytes.', *Archives of dermatological research*, 304(10), pp. 831–8. doi: 10.1007/s00403-012-1277-6.

Yohn, J. J. *et al.* (1990) ‘Modulation of melanocyte intercellular adhesion molecule-1 by immune cytokines.’, *The Journal of investigative dermatology*, 95(2), pp. 233–7. Available at: http://www.ncbi.nlm.nih.gov/pubmed/1974278 (Accessed: 12 July 2018).

Chapter I

Spontaneous immunological activities in the target tissue of vitiligo-prone Smyth and vitiligo-susceptible Brown lines of chicken

Introduction

Vitiligo is a common (0.5-1% worldwide population), acquired depigmentation disorder characterized by the progressive loss of pigment-producing cells (melanocytes) in the skin (Ezzedine *et al.*, 2012). Vitiligo is generally considered an autoimmune disorder with spontaneous disease onset suspected to result from a complex interaction of genetic, environmental and immunological factors (Ezzedine *et al.*, 2015). Evidence of melanocyte-specific cell-mediated and humoral immune responses have been well documented in humans (Bystryn, 1989; Harning, Cui and Bystryn, 1991; Ogg *et al.*, 1998; Luiten *et al.*, 2009; Wu *et al.*, 2013; Zhu *et al.*, 2015; Jimenez-Brito *et al.*, 2016). Additionally, the use of immunosuppressive drugs is often prescribed either as a mono- or combination therapy in an attempt to halt progression of the disease and re-stimulate pigmentation (Bae *et al.*, 2017; Kim *et al.*, 2018; Nguyen *et al.*, 2018). Unfortunately, preventative measures are lacking due in part to the difficulty in collecting data before onset of the disease.

The Smyth line of chicken was originally described in 1977 and has since been well established as an excellent model for autoimmune vitiligo. Similarly to humans, Smyth chickens experience a spontaneous post-natal loss of melanocytes in growing feathers through a complex interaction of genetic, environmental and immunological factors (Smyth *et al.*, 1981). In addition, the identification of an environmental trigger (vaccination of 1-day old chicks with live, cell-free turkey herpesvirus) has resulted in a reliable incidence of vitiligo (80-95%) among Smyth chicken hatch mates (Erf *et al.*, 2001).

As mentioned, in chickens melanocytes are located in growing feathers which are derived from the skin. The living portion of growing feathers (pulp) consists of a column of dermis surrounded by epithelial tissue (epidermis) which includes melanocytes and

keratinocytes. The dermal and epidermal pulp tissue is generated from the dermal papilla and epidermal collar of the feather follicle, respectively, around which the connective tissue sheath is formed that encases the 8-10 mm column of the growing feather pulp tissue. At the proximal end (2-3 mm newest growth), melanocytes are located in an area of modified epidermis, which is subdivided into barb ridges. Each barb ridge is made up epidermal melanocytes and columns of keratinocytes. The cell bodies of the epidermal melanocytes can be observed facing the dermis at the epidermal-dermal junction, forming a circle around the dermis, and their dendrites extend along the keratinocyte columns for melanosome transfer.

The enclosed, sterile environment of a growing feather is easily removed (plucked) and allows for the continuous monitoring of local immune responses by repeat-sampling of the same individual over the course of an experiment. In fact, the growing feather is currently being utilized as a cutaneous test-tissue to gain temporal insights into tissue/cellular responses to test materials injected into its dermis (Erf and Ramachandran, 2016; Erf *et al.*, 2017; Sullivan and Erf, 2017). Thus, the Smyth line of chicken represents an ideal model to study the initiating events of spontaneously-occurring autoimmune vitiligo in growing feathers.

The full Smyth Line model is composed of three lines of chicken: the vitiligo-prone Smyth chicken (incidence 80-95%), the vitiligo-susceptible, parental Brown line (incidence 0-2%) and the vitiligo-resistant, distantly related Light Brown Leghorn line (incidence 0%). The inherent genetic susceptibility to autoimmune vitiligo was revealed by i.p. injection with the DNA methylation inhibitor 5-azacytidine. When treated in this manner, the incidence of vitiligo in Brown line chickens was over 70% compared to 0% in vehicle-injected chickens. In contrast there was no change in the incidence (0%) of vitiligo in Light Brown Leghorn chickens (Sreekumar, Erf and Smyth, Jr., 1996).

As in humans, the progression of vitiligo in Smyth chickens requires a functional immune system. This was demonstrated by the administration of corticosterone (an immunosuppressive steroid) which resulted in a significant reduction in vitiligo incidence compared to untreated controls (Boyle *et al.*, 1987). Furthermore, while evidence for a humoral response in Smyth chickens is well documented (Lamont *et al.*, 1982; Austin *et al.*, 1992; Searle *et al.*, 1993; Austin and Boissy, 1995), it does not appear to be necessary for disease expression as removal of the bursa of Fabricius (site of B cell development in birds) resulted in a delay but not a prevention of vitiligo (Boissy *et al.*, 1984). Similar delays in onset were seen by the administration of cyclosporine A which, as an inhibitor of IL-2 release, has a marked effect on antigen-specific T cell proliferation (Pardue *et al.*, 1987).

While the exact roles of cell-mediated and humoral immunity in initiating autoimmune vitiligo are unclear, current evidence strongly argues for a T cell-driven etiology. In growing feathers plucked from Smyth chickens with vitiligo, $CD8^+$ T cells were found at the dermal/epidermal junction (anatomical location of melanocytes) in close proximity to apoptotic cells (Wang and Erf, 2004). Additionally, memory response-like leukocyte infiltration into wattles of completely depigmented Smyth chickens injected with feather-derived melanocyte lysates was dominated by T cells, although B cells were also detected (Wang and Erf, 2003). A microarray study examining pools of cDNA from growing feathers of Smyth chickens also found evidence of both humoral (Ig-J chain, CXCL13) and cell-mediated (CCL19, GZMA, IL21R) immune activities prior-to vitiligo onset (Shi *et al.*, 2012). More convincing evidence for a cell-mediated immune response came from a study examining the relationship between infiltrating leukocytes (estimated by immunohistochemical staining of frozen tissue sections) and cytokine gene expression profiles in growing feathers obtained prior-to and throughout vitiligo

progression. Elevated IFN-γ expression as well as a dominant presence of $CD8^+$ cells leading up to visual onset, suggests a Th1-like, cell-mediated polarization in the active lesion (Shi and Erf, 2012).

The T cell compartment of a given individual is comprised of a variety (repertoire) of clones each with its own unique T cell receptor (TCR) capable of recognizing its own unique antigen displayed on MHC molecules of antigen-presenting cells. Upon its first encounter with an antigen-MHC complex, an activated T cell will undergo multiple rounds of proliferation, in essence skewing the repertoire. T cell receptors themselves are heterodimers with either an α- and β-chain or a γ- and a δ-chain. Antigen-specificity of the TCR is largely determined by a hypervariable region on the β and δ chains designated as the complementarity-determining region 3 (CDR3) which is generated by the random somatic recombination of varying alleles of germline-encoded variable (V), diversity (D) and joining (J) gene segments. The CDR3 itself results from the random addition and deletion of nucleotides at the junction of V-D and D-J gene segments (junctional diversity). The process yields T cell clone- and antigen-specific TCR β- and δ-chain genes with CDR3-regions that vary in their physical length. Therefore the distribution of lengths in a pool of recombined TCR β- and δ-chain genes can be used as a low resolution but fully comprehensive measure of T cell antigen-specificity diversity in the evolving autoimmune lesion (Gorochov *et al.*, 1998; Bour *et al.*, 1999; Matsumoto *et al.*, 2006).

Building on the information from the previously mentioned studies, our objective was to gain a more comprehensive understanding of the relationship between infiltrating leukocytes and immunological activities in the evolving autoimmune lesion in growing feathers of Smyth chickens. To obtain individual profiles of pulp-infiltrating leukocytes and gene expression activities, sampling began before the onset of vitiligo and continued through complete

depigmentation. Starting at 1-day post-hatch, growing feathers were sampled from individual chickens and continued two times per week until day 113. Single cell suspensions were prepared from the entire pulp of growing feathers and pulp-infiltrating leukocyte levels were determined by flow cytometry. Gene expression profiles were also determined using the whole pulp and on the level of the individual. Lastly, changes in the overall diversity of the T cell repertoire in the evolving autoimmune lesion were examined. Separate individual profiles of all parameters were also obtained for parental control, vitiligo-susceptible but non-expressing Brown line chickens. Results from this study will not only provide population-level insights into the initiating events of autoimmune vitiligo in Smyth chickens but will also allow for the study of the homogeneity of the response using data at the level of the individual.

Materials and Methods

Animal care

All chickens used in this study were from the Smyth and Brown line populations maintained by G. F. Erf at the Arkansas Experiment Station Poultry Farm in Fayetteville, AR. Fourteen vitiligo-prone Smyth and six MHC-matched ($B^{101/101}$) parental-control Brown line chicks (straight-run) were initially selected from a replacement hatch for the study. All chicks were vaccinated against Marek's disease with live herpesvirus of turkey (Fort Dodge Animal Health, Fort Dodge, IA) at 1-day post-hatch and kept on floor pens with wood shavings and free access to food and water at the Arkansas Agricultural Experiment Station Poultry Farm at the University of Arkansas, Division of Agriculture, Fayetteville, AR. All studies were conducted with the approval of the University of Arkansas Institutional Animal Care and Use Committee (IACUC) as outlined in protocol 15015.

Vitiligo scoring and feather sampling

Prior to sampling, all chickens were visually scored for signs of depigmentation (indicative of vitiligo onset). Specifically, scoring was done by close examination of the most proximal end (newest growth) of growing feather shafts for signs of depigmentation – paying particular attention to the area covered by skin. Both, scoring and feather sampling began at 1-day post-hatch and continued twice a week until day 113 (approximately 16 weeks). Samples taken during days 1-26 were plucked from the wing and thereafter (days 29-113) from the breast track. For each chicken and each time point, three growing feather samples were taken with one being placed in D-PBS on ice, and the other two in Tissue-Tek® O.C.T. Compound (Sakura of America, Hayward, CA) and snap-frozen in liquid nitrogen. Samples stored in D-PBS were used for same-day population analysis of pulp infiltrating leukocytes (see below). Samples snap-frozen in O.C.T. were stored at -80°C until use.

Population analysis of infiltrating leukocytes

Single-cell suspensions were obtained from the feather pulp as previously described (Erf and Ramachandran, 2016). Briefly, a longitudinal slit was made along the feather sheath and the pulp was removed, placed in a D-PBS solution containing 0.1% collagenase (type IV, Life Technologies, Carlsbad, CA) and 0.1% dispase II (Boehringer Mannheim, Mannheim, Germany) and incubated for one hour at 40°C. Infiltrating cells were liberated from the digested pulp tissue by passage through a 60µm nylon mesh and washed in a D-PBS solution containing 1% bovine serum albumin (VWR, Randor, PA) and 0.1% sodium azide (VWR, Randor, PA). Leukocyte populations in prepared single-cell suspensions were immunofluorescently stained using the following chicken-specific mouse-monoclonal antibodies: total leukocytes (CD45-SPRD), macrophages (KUL01-rPE), B cells (Bu-1-FITC), γδ T cells (TCR1-FITC), $\alpha\beta_1$ T cells (TCR2-FITC), $\alpha\beta_2$ T cells (TCR3-rPE), T-helper cells (CD4-FITC) and cytotoxic T cells (CD8α-rPE)

(SouthernBiotech, Birmingham, AL). To control for non-specific binding and identify negative populations for gating, a pool of all samples was prepared and incubated with a cocktail of mouse IgG1 isotype-control antibodies (FITC-, rPE- and SPRD-conjugated). Pooled samples were also single-stained with anti-CD45-FITC, -rPE and –SPRD antibodies in order to set compensation. Stained samples were acquired (10,000 events) on a Becton Dickinson FACSort flow cytometer equipped with a 488nm laser. Data analysis was performed using FlowJo software (FlowJo, LLC, Ashland, OR). Forward- versus side-scatter dot plots were used to filter out debris and data were expressed as the percentage of all acquired events (% pulp cells).

RNA extraction and cDNA synthesis

Frozen feathers sampled from 1d – 61d were processed for RNA extraction. To ensure complete removal of O.C.T., frozen feather samples were thawed in 70% ethanol. Once thawed the pulp was removed as above and immediately placed in TRI Reagent® (Zymo Research, Irvine, CA). Extracted pulp tissue was homogenized in TRI Reagent using a Tissue-Tearor™ (BioSpec Products, Bartlesville, OK, model# 985370-395) and total RNA was isolated using the Direct-zol™ RNA Miniprep kit (Zymo Research, Irvine, CA) with on-column DNase digestion according to the manufacturer's instructions. RNA was eluted in 30µL DEPC-treated molecular-grade water (VWR, Radnor, PA) and quantity and purity was assessed by absorbance at 260nm and 280nm on a BioTek Synergy HT (Winooski, VT). One microgram of RNA was reverse transcribed to cDNA in a 20µL sample volume (50ng/µL) using the High Capacity cDNA Reverse Transcription kit (Applied Biosystems, Foster City, CA) according to the manufacturer's instructions. Synthesized cDNA was diluted to 10ng/µL using DEPC-free molecular-grade water (VWR, Radnor, PA) and stored at -20°C until use.

Gene expression analysis

Quantitative real-time PCR was performed as previously described using the TaqMan™ system with modifications (Hamal *et al.*, 2010). Target primer and probe sequences are listed in Table 1. Reactions were carried out in a 12µL sample volume using 20ng of cDNA and were run on an Applied Biosystems® 7500 Real-Time PCR System using manufacturer-programmed cycling conditions. Relative gene expression was determined by the efficiency-calibrated ΔCt method (Pfaffl, 2001) and is expressed as fold change relative to the calibrator sample. To obtain gene expression profiles for individual chickens, results were calculated using individual-specific day 29 samples as calibrators and 28S as a reference gene.

Amplification of CDR3-containing regions of T cell receptor β-chains

Complementarity-determining region 3 (CDR3)-containing regions of the T cell receptor-β_1 (TCR-β_1) and –β_2 (TCR-β_2) chain genes were amplified from individual cDNA samples (prepared above) by end-point PCR. Using all available coding sequences in the NCBI database, fluorescently-labeled (forward) primers were designed against conserved 5'-variable (V) gene segments of TCR-β_1 (TCR-$V_\beta1$) and TCR-β_2 (TCR-$V_\beta2$) genes. An unlabeled (reverse) primer was designed in a similar manner against a conserved 3'-constant (C) region shared by the two genes. Specificity of TCR-$V_\beta1$ and TCR-$V_\beta2$ forward primers was confirmed by testing against cDNA derived from TCR1 (γδ T)-, TCR2 ($\alpha\beta_1$ T)- and TCR3 ($\alpha\beta_2$ T)-sorted PBMCs. Primer sequences and labels are listed in Table 2. Reactions were carried out in a 20µL sample volume using 20ng cDNA, 0.5µM primers and Phusion™ High-Fidelity PCR Master Mix (Thermo Scientific, Waltham, MA). Cycling conditions were as follows: 98°C for 20 seconds (initial denaturation), 98°C for 10 seconds (denaturation), 60°C for 30 seconds (annealing), 72°C for 30 seconds (extension), 72°C for 5 minutes (final extension) and held at 4°C.

Quantification of changes in the T cell receptor repertoire

Fluorescently-labeled PCR products amplified from individual cDNA samples were sent to the DNA Analysis Facility on Science Hill at Yale University (New Haven, CT) for size-separation by capillary electrophoresis on a 3730xl DNA Analyzer (Applied Biosystems, Foster City, CA). Analysis of raw spectrographs (fluorescence signal versus size) for each sample was performed using GeneMapper® 4.0 (Applied Biosystems, Foster City, CA) with fluorescence height as the measure of quantity (Figure 4a, b). To discount non-specific fluctuations in the fluorescence signal, initial peak detection was performed using thresholds of 100 and 50 for TCR-$V_\beta 1$ and -$V_\beta 2$ samples respectively. Alleles were defined based on an overlay of all spectrographs and were separated by approximately three base pairs (Figure 4c). Each individual CDR3 length profile was then converted to a frequency distribution by dividing the fluorescence height of a specific allele by the total fluorescence of all alleles in the sample (Figure 4d). To quantify overall changes in CDR3 frequency distributions over time the Hamming-distance (D-score) was calculated against a reference sample. Specifically, the absolute values of the difference in frequencies for every allele relative to samples taken at 1 day of age were summed and then divided by 2 (theoretical minimum and maximum: 0% and 100% respectively; Gorochov et al. 1998).

Statistical analysis

Prior to statistical testing, gene expression (fold change) data were converted from an exponential to a linear scale by $\log_2$ transformation. No transformation was required for leukocyte infiltration (% pulp cells) or T cell receptor diversity data (D-score). Data for vitiligo-expressing Smyth chickens were aligned and averaged according to time (days) with respect to

vitiligo onset (set to 0d). Data for non-expressing Brown line chickens were reported and averaged based on age (days). To determine the trend with respect to time on all measurements, a mixed-effects regression model was used. Time was identified as a fixed effect and individual chickens as a random effect using a residual covariance structure. When a significant effect was found, post-hoc multiple means comparisons were made against the -36 d sample using the Tukey-Kramer p-value adjustment. Correlation analysis was done using Spearman's method. Differences were considered significant when $P \leq 0.05$. All statistical analysis was done using JMP Pro 13 (SAS Institute Inc., Cary, NC).

Results

Vitiligo incidence

At the conclusion of the study 10 Smyth chickens had developed signs of vitiligo. One Smyth chicken with no signs of vitiligo died at 26 days and was replaced with another chicken, also with no signs of vitiligo, at the following time point (29 days). Two Smyth and one Brown line chicken had signs of sporadic progression of vitiligo, however, only samples from Smyth chickens which had progressed from fully pigmented to fully depigmented (n = 8) and Brown line chickens that remained fully pigmented (n = 5) were selected for further analysis. As expected, individual Smyth chickens developed vitiligo at different ages: two at 43 days, three at 47 days, one at 54 days and two at 57 days.

Infiltration of leukocytes into growing feathers of Smyth chickens relative to vitiligo onset

For statistical analysis, data points for vitiligo-expressing Smyth chickens were aligned and averaged with respect to time (days) of vitiligo onset (set to 0 d). In order to increase the power of statistical testing, time points with less than 3 data points were excluded which resulted in an analysis range of 39 days prior through 68 days post-vitiligo onset (-39 d – 68 d). In order

to determine periods of significant infiltration, multiple means comparisons were made against the -39 d time point.

Highly significant ($P < 0.0001$) changes in total leukocytes (CD45+), macrophages (KUL01+), B cells (Bu-1+), γδ T cells (TCR1+), $\alpha\beta_1$ T cells (TCR2+) and $\alpha\beta_2$ T cells (TCR3+) levels were detected over time in growing feathers of vitiligo-expressing Smyth chickens (Figure 1). Baseline (-39 d) levels of total leukocytes averaged 10.8 ± 2.1 % pulp cells. Two weeks prior to visual onset (-15 d) leukocyte levels were roughly double (21 ± 4.8 % pulp cells) and by -4 d had risen to statistical significance (32.8 ± 3.5 % pulp cells; $P < 0.05$) reaching a maximum of 46.0 ± 1.2 % pulp cells ($P < 0.05$) 3 days post visual onset (3 d). Total leukocyte levels remained statistically elevated until 17 days post onset (32.3 ± 7.5 % pulp cells; $P < 0.05$) at which point they lowered to roughly double the baseline levels (~20% pulp cells).

At -39 d, macrophages accounted for over 45% of total leukocytes (4.9 ± 0.9 % pulp cells), but by visual onset (0d) had dropped down to 8.2% of total leukocytes (3.3 ± 0.5 % pulp cells). While no significant differences relative to the baseline (4.9 ± 0.9 % pulp cells) were found, the percentage of macrophages in the growing feather continued to decline throughout complete depigmentation.

At -39 d, B cell levels were a mere 0.5 ± 0.1 % pulp cells, however by visual onset their numbers increased to 9.0 ± 1.0 % pulp cells, having more than doubled from the previous time point (-4 d; 4.4 ± 1.0; $P < 0.05$). After reaching a maximum of 11.9 ± 1.6 % pulp cell 6 days post onset ($P < 0.05$), B cells, while still numerically above baseline, declined to non-significant levels.

At -39 d, γδ, $\alpha\beta_1$ and $\alpha\beta_2$ T cells measured 0.1 ± 0.0, 0.6 ± 0.3 and 0.2 ± 0.1 % pulp cells respectively. Significant infiltration of $\alpha\beta_1$ T cells were detected as early as -11 d (5.6 ± 1.1 %

pulp cells; $P < 0.05$) and remained statistically elevated until 41 d (6.1 ± 0.8 % pulp cells; $P < 0.05$) having reached maximum levels at 3 d (9.4 ± 0.8 % pulp cells; $P<0.05$). In contrast, statistically elevated levels of $\alpha\beta_2$ T cells were not seen until -4 d (1.6 ± 0.4 % pulp cells; $P < 0.05$) and did not reach their maximum until 62 days post onset (4.8 ± 1.4 % pulp cells; $P<0.05$). Significant changes in γδ T cells were not detected until 41 and 55 days post visual onset (2.0 ± 0.6 and 2.4 ± 0.6 % pulp cells respectively; $P < 0.05$.

Infiltration of leukocytes into growing feathers of non-vitiligo-expressing Brown line chickens

Data points for Brown line controls (n = 5) were aligned and averaged by age (days) with multiple means comparisons being made against the sample collected at 8 days of age. Highly significant changes in total leukocytes ($P=0.0019$), macrophages ($P < 0.0001$), γδ T ($P = 0.0001$), $\alpha\beta_1$ T ($P < 0.0001$) and $\alpha\beta_2$ T cells ($P < 0.0001$) were also observed in growing feathers of non-expressing Brown line control chickens (Figure 2). In contrast to levels in growing feathers of Smyth chickens, total leukocytes never rose above 21% total pulp cells and there were no significant increases found relative to 8 d samples. Similarly to Smyth chickens macrophage levels steadily declined over the course of the study. In particular between 12 d and 15 d macrophages level dropped from 8.3 ± 1.6 to 4.4 ± 0.5 % pulp cells ($P < 0.05$). Interestingly, a transient elevation in $\alpha\beta_1$ and $\alpha\beta_2$ T cell levels was observed at 61 d (3.9 ± 1.3 and 1.6 ± 0.3 % pulp cells, respectively; $P < 0.05$) and 64 d (4.6 ± 1.3 and 1.6 ± 0.3 % pulp cells, respectively) . In complete contrast to Smyth chickens no increases in B cells were observed in growing feathers from Brown line chickens ($P = 0.2385$).

Infiltration of $CD4^+$, $CD8\alpha^+$ and $CD4^+CD8a^+$ cells in growing feathers of Smyth chickens and non-vitiligo-expressing Brown line chickens

Highly significant changes in the levels of $CD4^+CD8\alpha^-$, $CD4^-CD8\alpha^+$ and $CD4^+CD8\alpha^+$ T cells were detected over time in growing feathers of vitiligo-expressing Smyth chickens (P=0.0003, <0.0001 and <0.0001 respectively; Figure 3a). At -39 d $CD4^+CD8\alpha^-$, $CD4^-CD8\alpha^+$ and $CD4^+CD8\alpha^+$ cells accounted for 3.1 ± 0.6, 0.8 ± 0.4 and 0.1 ± 0.0 % pulp cells, respectively. $CD4^-CD8\alpha^+$ cells were significantly elevated as early as -8d (5.0 ± 1.4 % pulp cells; $P < 0.05$) and reached their maximum at 17 d and 55 d (8.3 ± 0.6 and 2.0 % pulp cells, respectively; $P < 0.05$). Interestingly, while $CD4^+CD8\alpha^-$ cells reached their maximum level at onset (0 d; 5.4 ± 0.7 % pulp cells), these increases were not statistically significant. $CD4^+CD8\alpha^+$ cells (phenotypically CD8α-low) were transiently elevated from -4 d (2.0 ± 0.3 % pulp cells; $P < 0.05$) to 17 d (2.1 ± 0.3 % pulp cells; $P < 0.05$).

Highly significant changes in the levels of $CD4^+CD8\alpha^-$, $CD4^-CD8\alpha^+$ and $CD4^+CD8\alpha^+$ T cells were also detected in growing feathers of Brown line chickens ($P < 0.0001$, < 0.0001 and = 0.0003 respectively; Figure 3b). Transient increases in $CD4^-CD8\alpha^+$ were seen from 36 d – 47 d ($P < 0.05$) and again from 61 d – 64 d ($P < 0.05$) though levels never rose above 4% of pulp cells. A similar increase from 61 d – 64 d ($P < 0.05$) was found in $CD4^+CD8\alpha^+$ cells though levels never rose above 1.5% of pulp cells. Similar to Smyth chickens, no significant differences in the levels of CD4+ cells were found relative to the 8 d of age samples.

Alterations in the T cell repertoire in growing feathers precede visual onset of vitiligo in Smyth chickens

To examine overall changes in the diversity within the TCR repertoire (D-score) with respect to vitiligo onset in growing feathers of Smyth chickens, cDNA from samples collected

between 45 days before and 13 days post-onset were used (Figure 5a). D-scores for TCR-β1 ranged from 23.1 ± 4.2% (-45 d) to 36.8 ± 6.6% (-36 d) ($P = 0.0335$), however no sample differed significantly from -39 d. In contrast D-scores for TCR-β2 ranged from 14.5 ± 2.2% (-45d) to 38.5 ± 2.4% (10d) ($P < 0.0001$) with significant overall changes seen at -18 d (35.6 ± 4.0%; $P < 0.05$) and -8 d through 10 d ($P < 0.05$).

Alterations in the T cell repertoire in growing feathers of non-expressing Brown line chickens

To examine overall changes in the diversity within the TCR repertoire (D-score) with respect to age in growing feathers of Brown line chickens, cDNA from samples collected between ages 5 d and 61 d were used (Figure 5b). D-scores for TCR-β1 ranged from 21.3 ± 3.8% (5 d) to 39.8 ± 8.9% (26 d) ($P = 0.0403$). In contrast to Smyth chickens, two samples (29 d and 43 d; $P < 0.05$) differed significantly from 5 d with several others differing just below statistical significance. Significant changes in TCR-β2 diversity were also found ($P = 0.0028$). D-scores ranged from 16.8 ± 1.7% (5 d) to 39.4 ± 7.6% (47 d) however no sample differed significantly from 5 day samples. Interestingly, variability in TCR-β2 D-score profile in individual Brown line chickens increased substantially after 26 d of age.

Association of overall changes in the TCR repertoire with infiltrating T cell subsets

To determine whether increases in overall changes in the T cell receptor repertoire (D-score) were associated with levels of T cells and their subsets in growing feather samples from vitiligo-expressing Smyth and non-expressing Brown line chickens, D-scores and pulp-infiltration data were tested for correlation by Spearman's method (Table 3). Highly significant, positive correlations between the D-score of TCR-β2 and infiltrating $\alpha\beta_2$ T ($P < 0.0001$), $CD4^-$ $CD8\alpha^+$ ($P < 0.0001$) and $CD4^+CD8\alpha^+$ ($P = 0.0003$) cells were found in data obtained from vitiligo-expressing Smyth chickens (Table 3). No significant correlations between TCR-β1 D-

scores and infiltrating T cells were found in samples from Smyth chickens. In growing feather samples from Brown line chickens, a highly significant negative correlation between the D-score of TCR-β2 and infiltrating $CD4^{+}CD8\alpha^{-}$ T cells was found (P = 0.0001). No significant correlations between TCR-β1 D-score and infiltrating T cells were found in samples from Brown line chickens.

Association of overall changes in the TCR repertoire with specific allele groups

To determine whether increases in overall changes in the T cell receptor repertoire were associated with relative quantities of specific allele groups in growing feather samples from vitiligo-expressing Smyth and non-expressing Brown line chickens, D-scores and allele frequency data were tested for correlation by Spearman's method (Table 4). In growing feathers from Smyth chickens, increases in two alleles (251, P = 0.0413; 268, P = 0.047) were significantly correlated with changes in TCR-β1 diversity. Rises in the frequency of a single allele group was positively correlated to overall changes in TCR-β2 diversity (284, P=0.0008) in growing feathers obtained from vitiligo-expressing Smyth chickens. Interestingly, increases in frequency of the same allele group was significantly and positively correlated to changes in TCR-β2 (284, P = 0.0498) diversity in growing feathers obtained from non-expressing Brown line controls.

Early markers of immunological activities in growing feathers of Smyth chickens relative to vitiligo onset

Targeted gene expression was carried out on cDNA prepared from samples collected between 45 days before and 13 days post-vitiligo onset from Smyth chickens. Highly significant changes in expression of *CTLA4* and *IL21R* were found in growing feathers of vitiligo-expressing Smyth chickens (P < 0.0001; Figure 6). Both genes demonstrated a similar trend of a

steady increase leading up to vitiligo onset (0 d), reaching peak levels 3 days post-onset and maintaining a sustained elevation thereafter. The earliest signs of immunological activity were in the significant increased expression of the anti-inflammatory co-receptor CLTA4 (-32 d; $P < 0.05$) with the significant increase in *IL21R* expression seen three days later (-29 d; $P < 0.05$). Interestingly, while significant changes in overall gene expression were found for type-1 interferons (*IFNA*, $P = 0.1020$; *IFNB*, $P = 0.0120$) no differences were found relative to -39 d samples.

Markers of pro-inflammatory and recruitment activities in growing feathers of Smyth chickens relative to vitiligo onset

Highly significant changes in the expression of recruitment and homing-related genes *CCL19*, *CCR7*, *CXCL8* and *IL21R* were found in growing feathers of vitiligo-expressing Smyth chickens ($P < 0.0001$; Figure 7). Initial increases for all four genes began 22 days before visual onset ($P < 0.05$) after which levels continued to rise reaching maximum expression 3 days post-onset and remained elevated thereafter. Highly significant changes in the expression of pro-inflammatory genes *IL1B* and *IL18* ($P < 0.0001$) were also found (Figure 7). Beginning 18 days before visual onset, levels of *IL1B* and *IL18* were significantly increased and similar to the chemokine genes, reached maximum expression 3 days post onset and remained elevated thereafter.

Markers of T cell activation and anti-inflammatory activities in growing feathers of Smyth chickens relative to vitiligo onset

Highly significant changes in the expression of T cell activation-related genes *IFNG*, *FASLG*, *GZMA* and *IL21* and anti-inflammatory genes *IL10* and *TGFB1* were found in growing feathers of vitiligo-expressing Smyth chickens ($P < 0.0001$; Figure 8). All genes demonstrated a

similar trend upwards leading up to vitiligo onset reaching maximum levels 3 days post onset and maintaining a sustained elevation thereafter. Interestingly, significant expression of the anti-inflammatory cytokine *IL10* preceded significant elevation of T cell activation markers. Eighteen days prior to visual onset saw the first significant increase in *IL10* ($P < 0.05$) followed by significant elevation of *IL21*, a cytokine responsible for the maintenance of activated T cells, three days later (-15 d, $P < 0.05$). *IFNG*, the signature cytokine of a cell-mediated immune response was significantly elevated starting at -11d followed by increases in cytotoxic T cell markers *FASLG* and *GZMA* three days later (-8 d, $P < 0.05$). Lastly, significant expression of the anti-inflammatory cytokine *TGFB1* was seen at 3 d and 6 d ($P < 0.05$).

Expression of recruitment and anti-inflammatory genes in growing feathers from Brown line chickens

Gene expression was carried out on cDNA prepared from samples collected between 8 and 61 days of age from growing feathers of non-expressing Brown line chickens. Of all genes measured only *CTLA4*, *IL10* and *CXCL8* were found to change significantly with age ($P = 0.0241$, 0.005 and 0.0038 respectively; Figure 8, Table 5). In contrast to Smyth chickens, individual variability was quite high and therefore no sample varied significantly from 8d samples.

Immunoregulatory activities in growing feathers from Brown line chickens

To determine if significant differences found in growing feathers of Brown line chickens were the results of outliers, individual plots of cell infiltration and gene expression were examined (Figure 9). Three of the five chickens analyzed had substantial, yet transient rises in $\alpha\beta_1$T and CD4+ cells (1231, 1234 and 1244, Figure 7, a). In the cell infiltration profiles of two of these three individuals (1231 and 1234, Figure 7, a)) a small, transient increase in $\alpha\beta_2$T and

CD8α+ cells was also observed. None of the chickens with CD4+ cell infiltration showed any obvious changes in *IFNG* gene expression, however all showed substantial rises in *CTLA4* and *IL10* (Figure 4, b).

Discussion

The Smyth chicken represents a unique opportunity to examine the temporal quantitative and qualitative aspects of a variety of parameters in the evolving autoimmune vitiligo lesion. The anatomical location of the target tissue (a growing feather) allows for the repeated sampling of the same individual prior to- and throughout diseases development. This unique feature of the model allows for the assessment of immunological activities before the emergence of symptoms which is essential to identifying predisposing factors. The availability of the MHC-matched ($B^{101/101}$) genetically-susceptible but non-vitiligo-expressing Brown line is an added benefit allowing for direct comparisons between lines which may prove valuable in identifying preventative mechanisms inherent in individual chickens. The data presented here serve to provide a sequence of immunologically significant events in the lead up to and progression of autoimmune vitiligo in Smyth chickens.

The first signs of immunological activity in growing feathers of Smyth chickens occurred a full month prior to visual onset, and, surprisingly, were regulatory in nature. *CTLA4* is constitutively expressed in regulatory T cells (Tregs) but is also induced in activated T cells (Freeman *et al.*, 1992; Linsley *et al.*, 1992). In competition with the co-stimulatory CD28 receptor, CTLA4 binds the co-stimulatory ligands B7-1 (CD80) and B7-2 (CD86) on the surface of antigen-presenting cells. Once bound, the CTLA4-expressing cell removes B7-1 (CD80) and B7-2 (CD86) thereby preventing its binding to CD28 and in essence preventing co-stimulation (Qureshi *et al.*, 2011). With no significant increases in T cells seen at these early time points, it is

logical to assume a tissue-resident source for *CTLA4* expression and, as no other signs of T cell activation were detected, the observed expression implies a regulatory T cell response. However the lack of significant increases in *TGFB1* expression argues against the presence of Tregs at this stage of the disease, although, it is possible that other isoforms of TGF (*TGFB2*, *TGFB3*; not measured) are involved. It is also possible that effects of TGF-β cannot be seen at the transcription level as the protein is synthesized and secreted in an inactive form that must be acted on by other proteins. Unfortunately, positive identification of Tregs is difficult in the chicken as the canonical marker, FoxP3, has yet to be identified leaving CD25 (IL2R)/CD4 co-expression as the accepted method for detection of these cells (Shanmugasundaram and Selvaraj, 2011).

Three days later (29 days prior to onset), a significant elevation of *IL21R* gene expression was observed. Activated T cells express *IL21R* as a means to respond to IL-21 which is a form of co-stimulation and a means of sustaining their effector state (Parrish-Novak *et al.*, 2000; Elsaesser *et al.*, 2009). However the lack effector activities, including *IL21* itself, detected during this time makes them an unlikely candidate for the source of increased expression. Jüngel *et al.* noted the expression of *IL21R* without *IL21* in synovial fibroblasts and macrophages from patients with rheumatoid arthritis (Jüngel *et al.*, 2004). Another likely possibility for the source of *IL21R* expression are dendritic cells. As demonstrated in IL21 receptor-deficient non-obese diabetic (NOD) mouse models for autoimmune (type 1) diabetes, IL21 signaling is indispensable for disease onset (Sutherland *et al.*, 2009). Furthermore, in a virus-induced mouse model for type-1 diabetes on the NOD background, a dramatic reduction in diabetes incidence on IL-21 receptor-deficient mice was reversed with the addition of IL-21 receptor sufficient dendritic

cells. The authors noted the failure of IL-21 deficient dendritic cells to acquire CCR7 which would impede their migration to lymph nodes (Van Belle *et al.*, 2012).

The first signs of leukocyte recruitment activities were seen 22 days prior to visual onset. At this time *CCR7* along with its ligand *CCL19* were both significantly elevated suggesting an active recruitment of naïve T cells, which were detect but not elevated at this time. It is also possible that, perhaps dendritic cells (not measured) acquired *CCR7* as suggested in Van Belle *et al.* (2012). Further evidence of active recruitment was seen in the elevated expression of *CXCL8*. Interestingly, while CXCL8 is a potent heterophil (neutrophil in mammals) and monocyte attractant (Poh *et al.*, 2008), no obvious infiltration of these cells was seen at this time (data not shown for heterphils). In fact, significant levels of cell infiltration were not seen in any measured leukocyte at this time point which suggests a tissue-resident (specifically, the pulp) source of these activities and therefore an induction of expression.

Local activation of tissue-resident T cells would explain the significant increase in *IL2R* expression. Activated T cells induce expression of IL2R in order to respond to IL-2 which enables their proliferation. Further evidence for local activation of T cells was seen in the significant alteration of the TCR-β_2, without significant elevation of $\alpha\beta_2$ T cell levels, four days later. In addition to signs of local T cell activation eighteen days prior to onset, the significant increase in the closely related cytokines *IL1B* and *IL18* represents a clear shift in the growing feather towards a pro-inflammatory state. Interestingly the potent anti-inflammatory cytokine *IL10* was also significantly upregulated at this time. Interleukin-10 can also be produced by activated T cells, including Tregs (Koni *et al.*, 2013) as well as B cells (Mielle *et al.*, 2018). Lastly, significant elevation of *IL21* further argues for T cell activation in the growing feather at this time. In addition to well established roles in sustaining the effector phenotype of activated T

cells, IL-21 is also suspected to play a role in the formation of memory T cells (Chen *et al.*, 2013; Yuan, Yang and Huang, 2017), B cell activation and plasma cell generation (Kuchen *et al.*, 2007).

The 11-15 days before visual onset appear to set the stage for a Th-1-like, cell-mediated autoimmune response which reached its peak three days post onset. The earliest rises of infiltrating leukocytes were seen in the levels of $\alpha\beta_1$T cells 11 days prior to visual onset, clearly preceding the first significant increase in B cells, further supporting the notion that vitiligo is a T cell-driven disorder. Rises in $\alpha\beta_1$T cells were accompanied by significant increases in *IFNG* which is thought to play a central role in driving the progression of autoimmune vitiligo (Harris *et al.*, 2012; Shi and Erf, 2012; Yang *et al.*, 2015). Indeed production of IFN-γ has served as a reliable marker for CD8α+ T cell activation (Byrne *et al.*, 2014). Other possible sources of IFN-γ include natural killer cells which were not measured.

Eight to four days prior to visual onset saw the further development of the autoimmune response with significant increases CD8α+ cells which are likely cytotoxic T cells based on the simultaneous increases in *FASLG* and *GZMA* expression seen at this time point. Also increased were total leukocytes (CD45+), $\alpha\beta_2$T and CD4+CD8α+ cells. While the $CD4^+CD8\alpha^+$ lymphocytes are a relatively minor component of the T cell compartment, the emergence of additional cells (phenotypically CD8-low) in the active lesion is notable. Chicken-specific studies suggest that they are of a CD4+ T cell origin (Luhtala *et al.*, 1997) and that their presence in the periphery increases with age (Erf *et al.*, 1998). Unfortunately, follow up studies on the source and function of these cells are lacking.

B cell levels were not significantly increased until visual onset of vitiligo (0d). The late entry of B cells further supports the notion of the generation of autoantibodies as a consequence

and not a cause of melanocyte destruction. It should be noted that "onset" was defined by the depigmentation at the most proximal end of the feather which would be indicative of melanocyte loss.

The "peak" of the response in terms of levels of activity occurred 3-6 days post visual onset. Here, maximum levels of nearly every measured parameter were reached. However, post-onset both B and $CD4^+CD8\alpha^+$ cells eventually returned to basal levels while $CD8^+$ T cells maintained a significantly elevated presence in the feather, perhaps having made the transition to memory cells. Additionally, significantly elevated levels of *CCL19*, *CCR7*, *CTLA4*, *CXCL8*, *FASLG*, *GZMA*, *IFNG*, *IL1B*, *IL2R*, *IL10*, *IL18*, *IL21* and *IL21R* were also maintained in the tissue until at least 13 days post onset (the last time point measured) while those of *TGFB1* returned to basal levels six days post onset.

Regarding alterations in the T cell repertoire in both Smyth and Brown line chickens, a repeat study utilizing a sample of naïve T cells (e.g. from the periphery) would likely provide a cleaner measurement of the alterations in diversity. Although early samples were chosen as references for comparison, their TCR-length distribution patterns were not normal (i.e. Gaussian) which implies that the pool of TCRs in the tissue may already be skewed relative to a pool of naïve T cells from the periphery, which would be expected to demonstrate a normal distribution of TCR lengths. In addition, while we opted for a low resolution but fully comprehensive approach to monitoring the T cell repertoire, the number of TCR β-chains is relatively small compared to humans (2 vs. 52) and therefore the ability of AFLP to detect changes is likely diminished. In agreement with past studies, the T cell infiltrate was dominated by $\alpha\beta_1$ T (TCR2+) cells (Shresta *et al.*, 1997). It is likely that the relatively larger numbers of TCR2+ cells (vs. TCR3+ $\alpha\beta_2$ T cells) in the tissue contributed to the inability to detect an overall effect of time on

T cell diversity relative to vitiligo onset. Be that as it may, we were able to detect positive correlations between infiltrating T cells and changes in their T cell receptor diversity which is indicative of clonal expansion. We were also able to correlate changes in the repertoire with the increased frequency of specific allele groups, reiterating the notion of a clonal shift in T cell diversity in the target tissue. The possibility of a common T cell receptor-specificity in Smyth and Brown line chickens is indicated by a common allele group that was positively correlated with overall changes in TCR-β_2 diversity, although sequencing data would be required to confirm as a single allele group contains a large variety of alleles.

Lastly, while the parental-control Brown line has long been known to be susceptible to vitiligo (Sreekumar, Erf and Smyth, Jr., 1996), this is the first report to suggest a role for immunoregulatory mechanisms in preventing disease onset in this line of chickens. It is interesting that in this case, *CTLA4* and *IL10* expression are likely to have succeeded in preventing the initiation of the immune response, especially as their expression was not followed or accompanied by increases in *IFNG* and *IL21* – in contrast to Smyth chickens. In the non-obese diabetic mouse model, alternative isoforms of *CTLA4* (e.g. soluble, B7-independent) have been identified and are suspected to have a role in type 1 diabetes onset through impaired Treg function (Vijayakrishnan *et al.*, 2004; Chikuma *et al.*, 2005; Araki *et al.*, 2009; Gerold *et al.*, 2011; Stumpf *et al.*, 2013). Moreover a 2012 report documented a negative correlation between cytotoxic T cells and Tregs in the blood of patients with generalized vitiligo (Lili *et al.*, 2012).

If the immunosuppressive roles of *CTLA4* and *IL10* in Brown line chickens are confirmed, this would imply a common melanocyte-specific triggering of a T cell-driven immune response in both vitiligo-prone Smyth and -susceptible Brown line chickens with the former progressing to a cell-mediated autoimmune response and the later to an

immunoregulatory response, perhaps resulting in the establishment of peripheral tolerance (anergy). Future studies should work to test this hypothesis as it would represent a clear paradigm shift for the Smyth chicken model and warrant its further development for the study of autoimmune vitiligo.

References

Araki, M. *et al.* (2009) 'Genetic evidence that the differential expression of the ligand-independent isoform of CTLA-4 is the molecular basis of the Idd5.1 type 1 diabetes region in nonobese diabetic mice.', *Journal of immunology (Baltimore, Md. : 1950)*. American Association of Immunologists, 183(8), pp. 5146–57. doi: 10.4049/jimmunol.0802610.

Austin, L. M. *et al.* (1992) 'The detection of melanocyte autoantibodies in the Smyth chicken model for vitiligo.', *Clinical immunology and immunopathology*, 64(2), pp. 112–20. Available at: http://www.ncbi.nlm.nih.gov/pubmed/1643744.

Austin, L. M. and Boissy, R. E. (1995) 'Mammalian tyrosinase-related protein-1 is recognized by autoantibodies from vitiliginous Smyth chickens. An avian model for human vitiligo.', *The American journal of pathology*, 146(6), pp. 1529–41. Available at: http://www.pubmedcentral.nih.gov/articlerender.fcgi?artid=1870917&tool=pmcentrez&rendertype=abstract.

Bae, J. M. *et al.* (2017) 'Phototherapy for Vitiligo', *JAMA Dermatology*. American Medical Association, 153(7), p. 666. doi: 10.1001/jamadermatol.2017.0002.

Van Belle, T. L. *et al.* (2012) 'Interleukin-21 Receptor-Mediated Signals Control Autoreactive T Cell Infiltration in Pancreatic Islets', *Immunity*, 36(6), pp. 1060–1072. doi: 10.1016/j.immuni.2012.04.005.

Boissy, R. E., Lamont, S. J. and Smyth, J. R. (1984) 'Persistence of abnormal melanocytes in immunosuppressed chickens of the autoimmune "DAM" line.', *Cell and tissue research*, 235(3), pp. 663–8. Available at: http://www.ncbi.nlm.nih.gov/pubmed/6713493.

Bour, H. *et al.* (1999) 'T-cell repertoire analysis in chronic plaque psoriasis suggests an antigen-specific immune response.', *Human immunology*, 60(8), pp. 665–76. Available at: http://www.ncbi.nlm.nih.gov/pubmed/10439312.

Boyle, M. L., Pardue, S. L. and Smyth, J. R. (1987) 'Effect of corticosterone on the incidence of amelanosis in Smyth delayed amelanotic line chickens.', *Poultry science*, 66(2), pp. 363–7. Available at: http://www.ncbi.nlm.nih.gov/pubmed/3588505.

Byrne, K. T. *et al.* (2014) 'Autoimmune Vitiligo Does Not Require the Ongoing Priming of Naive CD8 T Cells for Disease Progression or Associated Protection against Melanoma', *The Journal of Immunology*, 192(4), pp. 1433–1439. doi: 10.4049/jimmunol.1302139.

Bystryn, J. C. (1989) 'Serum antibodies in vitiligo patients.', *Clinics in dermatology*, 7(2), pp. 136–45. Available at: http://www.ncbi.nlm.nih.gov/pubmed/2667738.

Chen, X.-L. *et al.* (2013) 'Induction of autoimmune diabetes in non-obese diabetic mice requires interleukin-21-dependent activation of autoreactive CD8 $^{+}$ T cells', *Clinical & Experimental Immunology*, 173(2), pp. 184–194. doi: 10.1111/cei.12108.

Chikuma, S., Abbas, A. K. and Bluestone, J. A. (2005) 'B7-Independent Inhibition of T Cells by CTLA-4', *The Journal of Immunology*, 175(1), pp. 177–181. doi: 10.4049/jimmunol.175.1.177.

Elsaesser, H., Sauer, K. and Brooks, D. G. (2009) 'IL-21 is required to control chronic viral infection.', *Science (New York, N.Y.)*. American Association for the Advancement of Science, 324(5934), pp. 1569–72. doi: 10.1126/science.1174182.

Erf, G. F. *et al.* (2001) 'Herpesvirus connection in the expression of autoimmune vitiligo in Smyth line chickens.', *Pigment cell research / sponsored by the European Society for Pigment Cell Research and the International Pigment Cell Society*, 14(1), pp. 40–46. doi: 10.1034/j.1600-0749.2001.140107.x.

Erf, G. F. *et al.* (2017) 'T lymphocytes dominate local leukocyte infiltration in response to intradermal injection of functionalized graphene-based nanomaterial', *Journal of Applied Toxicology*, 37(11), pp. 1317–1324. doi: 10.1002/jat.3492.

Erf, G. F., Bottje, W. G. and Bersi, T. K. (1998) 'CD4, CD8 and TCR defined T-cell subsets in thymus and spleen of 2- and 7-week old commercial broiler chickens.', *Veterinary immunology and immunopathology*, 62(4), pp. 339–48. Available at: http://www.ncbi.nlm.nih.gov/pubmed/9646438 (Accessed: 31 May 2018).

Erf, G. F. and Ramachandran, I. R. (2016) 'The growing feather as a dermal test site: Comparison of leukocyte profiles during the response to *Mycobacterium butyricum* in growing feathers, wattles, and wing webs', *Poultry Science*, 95(9), pp. 2011–2022. doi: 10.3382/ps/pew122.

Ezzedine, K. *et al.* (2012) 'Revised classification/nomenclature of vitiligo and related issues: the Vitiligo Global Issues Consensus Conference', *Pigment Cell & Melanoma Research*. Wiley/Blackwell (10.1111), 25(3), pp. E1–E13. doi: 10.1111/j.1755-148X.2012.00997.x.

Ezzedine, K. *et al.* (2015) 'Vitiligo', *The Lancet*. Elsevier, 386(9988), pp. 74–84. doi: 10.1016/S0140-6736(14)60763-7.

Freeman, G. J. *et al.* (1992) 'CTLA-4 and CD28 mRNA are coexpressed in most T cells after activation. Expression of CTLA-4 and CD28 mRNA does not correlate with the pattern of lymphokine production.', *Journal of immunology (Baltimore, Md. : 1950)*, 149(12), pp. 3795–801. Available at: http://www.ncbi.nlm.nih.gov/pubmed/1281186 (Accessed: 31 May 2018).

Gerold, K. D. *et al.* (2011) 'The soluble CTLA-4 splice variant protects from type 1 diabetes and potentiates regulatory T-cell function', *Diabetes*, 60(7), pp. 1955–1963. doi: 10.2337/db11-0130.

Gorochov, G. *et al.* (1998) 'Perturbation of CD4+ and CD8+ T-cell repertoires during progression to AIDS and regulation of the CD4+ repertoire during antiviral therapy.', *Nature medicine*, 4(2), pp. 215–21. Available at: http://www.ncbi.nlm.nih.gov/pubmed/9461196 (Accessed: 31 May 2018).

Hamal, K. R. *et al.* (2010) 'Differential gene expression of proinflammatory chemokines and cytokines in lungs of ascites-resistant and -susceptible broiler chickens following intravenous cellulose microparticle injection.', *Veterinary immunology and immunopathology*, 133(2–4), pp. 250–5. doi: 10.1016/j.vetimm.2009.07.011.

Harning, R., Cui, J. and Bystryn, J. C. (1991) 'Relation between the incidence and level of pigment cell antibodies and disease activity in vitiligo.', *The Journal of investigative dermatology*, 97(6), pp. 1078–80. Available at: http://www.ncbi.nlm.nih.gov/pubmed/1748818.

Harris, J. E. *et al.* (2012) 'A Mouse Model of Vitiligo with Focused Epidermal Depigmentation Requires IFN-γ for Autoreactive CD8+ T-Cell Accumulation in the Skin', *Journal of Investigative Dermatology*. Elsevier, 132(7), pp. 1869–1876. doi: 10.1038/JID.2011.463.

He, H. *et al.* (2012) 'Co-stimulation with TLR3 and TLR21 ligands synergistically up-regulates Th1-cytokine IFN-γ and regulatory cytokine IL-10 expression in chicken monocytes', *Developmental and Comparative Immunology*. Elsevier Ltd, 36(4), pp. 756–760. doi: 10.1016/j.dci.2011.11.006.

Jimenez-Brito, G. *et al.* (2016) 'Serum Antibodies to Melanocytes in Patients With Vitiligo Are Predictors of Disease Progression.', *Skinmed*, 14(1), pp. 17–21. Available at: http://www.ncbi.nlm.nih.gov/pubmed/27072723.

Jüngel, A. *et al.* (2004) 'Expression of Interleukin-21 Receptor, but Not Interleukin-21, in Synovial Fibroblasts and Synovial Macrophages of Patients with Rheumatoid Arthritis', *Arthritis and Rheumatism*, 50(5), pp. 1468–1476. doi: 10.1002/art.20218.

Kaiser, P., Underwood, G. and Davison, F. (2003) 'Differential Cytokine Responses following Marek ' s Disease Virus Infection of Chickens Differing in Resistance to Marek ' s Disease', *Journal of virology*, 77(1), pp. 762–768. doi: 10.1128/JVI.77.1.762.

Kim, S. R. *et al.* (2018) 'Rapid Repigmentation of Vitiligo Using Tofacitinib Plus Low-Dose, Narrowband UV-B Phototherapy', *JAMA Dermatology*. American Medical Association, 154(3), p. 370. doi: 10.1001/jamadermatol.2017.5778.

Kogut, M. H. *et al.* (2005) 'Expression and function of Toll-like receptors in chicken heterophils', *Developmental and Comparative Immunology*, 29(9), pp. 791–807. doi: 10.1016/j.dci.2005.02.002.

Koni, P. A. *et al.* (2013) 'Constitutively CD40-Activated B Cells Regulate CD8 T Cell Inflammatory Response by IL-10 Induction', *The Journal of Immunology*, 190(7), pp. 3189–3196. doi: 10.4049/jimmunol.1203364.

Kuchen, S. *et al.* (2007) 'Essential Role of IL-21 in B Cell Activation, Expansion, and Plasma Cell Generation during CD4+ T Cell-B Cell Collaboration', *The Journal of Immunology*, 179(9), pp. 5886–5896. doi: 10.4049/jimmunol.179.9.5886.

Lamont, S. J., Boissy, R. E. and Smyth, J. R. J. (1982) 'Humoral immune response and expression of spontaneous postnatal amelanosis in DAM line chickens.', *Immunological communications*, 11(2), pp. 121–127.

Lili, Y. *et al.* (2012) 'Global activation of CD8+ cytotoxic T lymphocytes correlates with an impairment in regulatory T cells in patients with generalized Vitiligo', *PLoS ONE*, 7(5). doi: 10.1371/journal.pone.0037513.

Linsley, P. S. *et al.* (1992) 'Coexpression and functional cooperation of CTLA-4 and CD28 on activated T lymphocytes.', *The Journal of experimental medicine*, 176(6), pp. 1595–604. Available at: http://www.ncbi.nlm.nih.gov/pubmed/1334116 (Accessed: 31 May 2018).

Luhtala, M. *et al.* (1997) 'A novel peripheral CD4+ CD8+ T cell population: inheritance of CD8alpha expression on CD4+ T cells.', *European journal of immunology*, 27(1), pp. 189–93. doi: 10.1002/eji.1830270128.

Luiten, R. M. *et al.* (2009) 'Autoimmune destruction of skin melanocytes by perilesional T cells from vitiligo patients', *Journal of Investigative Dermatology*. Nature Publishing Group, 129(9), pp. 2220–2232. doi: 10.1038/jid.2009.32.

Matsumoto, Y. *et al.* (2006) 'CDR3 spectratyping analysis of the TCR repertoire in myasthenia gravis.', *Journal of immunology (Baltimore, Md. : 1950)*, 176(8), pp. 5100–7. Available at: http://www.ncbi.nlm.nih.gov/pubmed/16585608.

Mielle, J. *et al.* (2018) 'IL-10 Producing B Cells Ability to Induce Regulatory T Cells Is Maintained in Rheumatoid Arthritis.', *Frontiers in immunology*, 9, p. 961. doi: 10.3389/fimmu.2018.00961.

Nguyen, S. *et al.* (2018) 'Atorvastatin in Combination With Narrowband UV-B in Adult Patients With Active Vitiligo', *JAMA Dermatology*. doi: 10.1001/jamadermatol.2017.6401.

Ogg, B. G. S. *et al.* (1998) 'Cytotoxic T Lymphocytes in Autoimmune Vitiligo', *Analysis*, 188(6).

Pardue, S. L. *et al.* (1987) 'Enhanced integumental and ocular amelanosis following the termination of cyclosporine administration.', *The Journal of investigative dermatology*, 88(6), pp. 758–61. Available at: http://www.ncbi.nlm.nih.gov/pubmed/3585059.

Parrish-Novak, J. *et al.* (2000) 'Interleukin 21 and its receptor are involved in NK cell expansion and regulation of lymphocyte function.', *Nature*, 408(6808), pp. 57–63. doi: 10.1038/35040504.

Pfaffl, M. W. (2001) 'A new mathematical model for relative quantification in real-time RT-PCR', *Nucleic Acids Research*, 29(9), p. 45e–45. doi: 10.1093/nar/29.9.e45.

Poh, T. Y. *et al.* (2008) 'Re-evaluation of chicken CXCR1 determines the true gene structure: CXCLi1 (K60) and CXCLi2 (CAF/interleukin-8) are ligands for this receptor.', *The Journal of biological chemistry*, 283(24), pp. 16408–15. doi: 10.1074/jbc.M800998200.

Qureshi, O. S. *et al.* (2011) 'Trans-endocytosis of CD80 and CD86: a molecular basis for the cell-extrinsic function of CTLA-4.', *Science (New York, N.Y.)*, 332(6029), pp. 600–3. doi: 10.1126/science.1202947.

Rothwell, L. *et al.* (2004) 'Cloning and Characterization of Chicken IL-10 and Its Role in the Immune Response to Eimeria maxima', *The Journal of Immunology*, 173(4), pp. 2675–2682. doi: 10.4049/jimmunol.173.4.2675.

Searle, E. A. *et al.* (1993) 'Smyth Chicken Melanocyte Autoantibodies - Cross-Species Recognition, In-Vivo Binding, And Plasma-Membrane Reactivity Of The Antiserum', *Pigment Cell Research*, 6(3), pp. 145–157.

Shanmugasundaram, R. and Selvaraj, R. K. (2011) 'Regulatory T Cell Properties of Chicken CD4+CD25+ Cells', *The Journal of Immunology*, 186(4), pp. 1997–2002. doi: 10.4049/jimmunol.1002040.

Shi, F. *et al.* (2012) 'Understanding mechanisms of vitiligo development in Smyth line of chickens by transcriptomic microarray analysis of evolving autoimmune lesions', *BMC Immunology*. BioMed Central Ltd, 13(1), p. 18. doi: 10.1186/1471-2172-13-18.

Shi, F. and Erf, G. F. (2012) 'IFN-γ, IL-21, and IL-10 co-expression in evolving autoimmune vitiligo lesions of Smyth line chickens.', *The Journal of investigative dermatology*, 132(3 Pt 1), pp. 642–9. doi: 10.1038/jid.2011.377.

Shresta, S., Smyth, J. R. and Erf, G. F. (1997) 'Profiles of pulp infiltrating lymphocytes at various times throughout feather regeneration in Smyth line chickens with vitiligo.', *Autoimmunity*, 25(4), pp. 193–201. Available at: http://www.ncbi.nlm.nih.gov/pubmed/9344327.

Smyth, J. R., Boissy, R. E. and Fite, K. V (1981) 'The DAM chicken: a model for spontaneous postnatal cutaneous and ocular amelanosis.', *The Journal of heredity*, 72(3), pp. 150–6. Available at: http://www.ncbi.nlm.nih.gov/pubmed/7276522.

Sreekumar, G. P., Erf, G. F. and Smyth, Jr., J. R. (1996) '5-Azacytidine Treatment Induces Autoimmune Vitiligo in Parental Control Strains of the Smyth Line Chicken Model for Autoimmune Vitiligo', *Clinical Immunology and Immunopathology*, 81(2), pp. 136–144. doi: 10.1006/clin.1996.0169.

Stumpf, M., Zhou, X. and Bluestone, J. A. (2013) 'The B7-Independent Isoform of CTLA-4 Functions To Regulate Autoimmune Diabetes', *The Journal of Immunology*, 190(3), pp. 961–969. doi: 10.4049/jimmunol.1201362.

Sullivan, K. S. and Erf, G. F. (2017) 'CD4+ T cells dominate the leukocyte infiltration response initiated by intra-dermal injection of phytohemagglutinin into growing feathers in chickens', *Poultry Science*, 96(10), pp. 3574–3580. doi: 10.3382/ps/pex135.

Sutherland, A. P. R. *et al.* (2009) 'Interleukin-21 is required for the development of type 1 diabetes in NOD mice.', *Diabetes*. American Diabetes Association, 58(5), pp. 1144–55. doi: 10.2337/db08-0882.

Vijayakrishnan, L. *et al.* (2004) 'An autoimmune disease-associated CTLA-4 splice variant lacking the B7 binding domain signals negatively in T cells', *Immunity*, 20(5), pp. 563–575. doi: 10.1016/S1074-7613(04)00110-4.

Wang, X. and Erf, G. F. (2003) 'Melanocyte-specific cell mediated immune response in vitiliginous Smyth line chickens', *Journal of Autoimmunity*, 21(2), pp. 149–160. doi: 10.1016/S0896-8411(03)00087-8.

Wang, X. and Erf, G. F. (2004) 'Apoptosis in feathers of Smyth line chickens with autoimmune vitiligo', *Journal of Autoimmunity*, 22(1), pp. 21–30. doi: 10.1016/j.jaut.2003.09.006.

Wu, J. *et al.* (2013) 'CD8+ T cells from vitiligo perilesional margins induce autologous melanocyte apoptosis', *Molecular Medicine Reports*, 7(1), pp. 237–241. doi: 10.3892/mmr.2012.1117.

Yang, L. *et al.* (2015) 'Interferon-gamma Inhibits Melanogenesis and Induces Apoptosis in Melanocytes: A Pivotal Role of CD8+ Cytotoxic T Lymphocytes in Vitiligo.', *Acta dermato-venereologica*, 95(6), pp. 664–70. doi: 10.2340/00015555-2080.

Yuan, Y., Yang, Y. and Huang, X. (2017) 'IL-21 is required for CD4 memory formation in response to viral infection', *JCI Insight*, 2(7), p. e90652. doi: 10.1172/jci.insight.90652.

Zhu, M. C. *et al.* (2015) 'Detection of serum anti-melanocyte antibodies and identification of related antigens in patients with vitiligo.', *Genetics and molecular research : GMR*, 14(4), pp. 16060–73. doi: 10.4238/2015.December.7.19.

Table 1. **Target gene primer[1] and probe[2] sequences**

Target	Accession NO.	Primer/Probe	Sequence (5'-3')
28S[3]	X59733	Forward	GGCGAAGCCAGAGGAAACT
		Reverse	GACGACCGATTTGCACGTC
		Probe	AGGACCGCTACGGACCTCCACCA
CCL19[8]	NM_001302168.1	Forward	GCTGCGCCTCCGAGAGA
		Reverse	ACACTTCTGCAGAGCCTAATTGC
		Probe	CAGCTCTGCCAGGAAGGTCCCAAATC
CCR7[8]	NM_001198752.1	Forward	ACCATGGACGGCGGTAAA
		Reverse	ATGGTGGTGTTGGCGTCATA
		Probe	TGTGCTGGGAACAACGTCACCGAC
CTLA4[8]	NM_001040091.1	Forward	GGGTCACCGTGAGCTTTCTC
		Reverse	GCCTGTTGGCCAGTACTATTGC
		Probe	CGCAGCCACCGCCACTGC
FASLG[8]	NM_001031559.1	Forward	CCAGTGAAAAAGGAAGCAAGGA
		Reverse	GAGACAGGTTCCCACTCCAATG
		Probe	CAGCACACTTAACAGGAAACCCCACACAG
GZMA[8]	NM_204457.1	Forward	CAGCTGCTCATTGCAATCTGA
		Reverse	GGACAGTAGTCTGGGTAGCGAATT
		Probe	CAGAGTTATTCTTGGAGCCCATTCACGGAC
IFNA3[6] (IFN-α, IFNA)	NM_205427.1	Forward	GACAGCCAACGCCAAAGC
		Reverse	GTCGCTGCTGTCCAAGCATT
		Probe	CTCAACCGGATCCACCGCTACACC
IFNW1[6] (IFN-β, IFNB)	NM_001024836.1	Forward	CCTCCAACACCTCTTCAACATG
		Reverse	TGGCGTGTGCGGTCAAT
		Probe	TTAGCAGCCCACACACTCCAAAACACTG
IFNG[3]	NM_205149.1	Forward	GTGAAGAAGGTGAAAGATATCATGGA
		Reverse	GCTTTGCGCTGGATTCTCA
		Probe	TGGCCAAGCTCCCGATGAACGA
IL1B[3]	NM_204524.1	Forward	GCTCTACATGTCGTGTGTGATGAG
		Reverse	TGTCGATGTCCCGCATGA
		Probe	CCACACTGCAGCTGGAGGAAGCC
IL8L2[5] (IL8, CXCL8)	NM_205498.1	Forward	GCCCTCCTCCTGGTTTCAG
		Reverse	TGGCACCGCAGCTCATT
		Probe	CTTTACCAGCGTCCTACCTTGCGACA
IL10[4]	NM_001004414.2	Forward	CATGCTGCTGGGCCTGAA
		Reverse	CGTCTCCTTGATCTGCTTGATG
		Probe	CGACGATGCGGCGCTGTCA
IL18[8]	NM_204608.1	Forward	GGCAGTGGAATGTACTTCGACAT
		Reverse	ACCTGGACGCTGAATGCAA
		Probe	ACTGTTACAAAACCACCGCGCCTTCA
IL21[7]	NM_001024835.1	Forward	GTGGTGAAAGATAAGGATGTCGAA
		Reverse	TGCCATTCTGGAAGCAGGTT
		Probe	TGCTGCATACACCAGAAAACCCTGGG
IL2RA[8] (CD25)	NM_204596.1	Forward	GCCAGCAAGACAAACCCAAA
		Reverse	GGCATACCGCAAAAACTTGAA
		Probe	CCCAGCACCTCCGAAGCAAGCA

Table 1. **(Cont.)**

Target	Accession NO.	Primer/Probe	Sequence (5'-3')
IL21R[8]	NM_001030640.1	Forward	CAGTACTCCACGTGTCACGAAAA
		Reverse	TGGCACCCAGGTCATTCCT
		Probe	ACTATGTGCAGACCCTGTCGTGCCTCC
TGFB1[8]	NM_001318456.1	Forward	GGTTATATGGCCAACTTCTGCAT
		Reverse	CCCCGGGTTGTGTTGGT
		Probe	AGCGCCGACACGCAGTACACCA

[1] All oligos were synthesized by Eurofins Genomics, Louisville, KY

[2] Probes were labeled with FAM and TAMARA on the 5'- and 3'-ends respectively

[3, 4, 5, 6, 7] Sequences from Kaiser *et al*., 2003; Rothwell *et al.*, 2004; Kogut *et al.*, 2005; He *et al.*, 2012 and Shi and Erf, 2012, respectively

[8] Primers and probes were designed using Primer Express 3.0 (Applied Biosystems, Foster City, CA.)

Table 2. **Primers[1] used for T cell receptor spectratyping**

Gene segment	Accession NO.	Primers	Sequence (5'-3')
TCR Variable-β_1	EF554743.1	Forward[2]	GTGGGACTAAGGAGAAATCC
	EF554744.1		
	EF554745.1		
	EF554746.1		
	EF554747.1		
	EF554748.1		
	EF554749.1		
	EF554750.1		
	EF554751.1		
	EF554752.1		
	EF554753.1		
	EF554754.1		
	EF554755.1		
	EF554756.1		
	EF554757.1		
	M81147.1		
	M37802.1		
	M37803.1		
	M37804.1		
	M37805.1		
TCR Variable-β_2	EF554759.1	Forward[3]	GCGATATTCACACCGGATAC
	EF554760.1		
	EF554761.1		
	EF554763.1		
	EF554764.1		
	EF554765.1		
	EF554768.1		
	EF554769.1		
	EF554772.1		
	EF554773.1		
	EF554774.1		
	EF554775.1		
	EF554776.1		
	EF554777.1		
	EF554778.1		
	EF554779.1		
	EF554780.1		
	EF554782.1		
	M37806.1		
	M81149.1		
	M81148.1		
	M81150.1		
	M81151.1		
TCR Constant-β	EF554742.1	Reverse	GATCAGGGAAGAAACCAGAG

[1] Oligos were synthesized by Applied Biosystems, Foster City, CA

[2] Contains a 5'-VIC label

[3] Contains a 5'-FAM label

Table 3. **Spearman correlation coefficients relating perturbations in T cell repertoire (D-score) with infiltrating T cell and T cell subsets in growing feathers of vitiligo-expressing Smyth and non-expressing Brown line chickens.**

Line	D-score	T cell	Spearman ρ	P-value[1]
Brown line	TCR-β_1	$\alpha\beta_1$ T	0.0394	0.7498
		$CD4^+$	-0.0836	0.4979
		$CD8\alpha^+$	0.0880	0.4757
		$CD4^+CD8\alpha^+$	-0.0425	0.7306
	TCR-β_2	$\alpha\beta_2$ T	0.1079	0.3811
		$CD4^+$	-0.4514	0.0001*
		$CD8\alpha^+$	0.0047	0.9696
		$CD4^+CD8\alpha^+$	-0.1724	0.1598
Smyth line	TCR-β_1	$\alpha\beta_1$ T	0.1093	0.2494
		$CD4^+$	-0.0035	0.9710
		$CD8\alpha^+$	0.0900	0.3430
		$CD4^+CD8\alpha^+$	0.1031	0.2772
	TCR-β_2	$\alpha\beta_2$ T	0.4064	<0.0001*
		$CD4^+$	-0.0240	0.8008
		$CD8\alpha^+$	0.4350	<0.0001*
		$CD4^+CD8\alpha^+$	0.3353	0.0003*

[1]P-values <0.05 were considered statistically significant (*)

Table 4. **Spearman correlation coefficients relating perturbations in T cell repertoire (D-score) with T cell receptor allele group frequency in growing feathers of vitiligo-expressing Smyth and non-expressing Brown line chickens.**

Line	D-score	Allele group	Spearman ρ	P-value[1]
Brown line	TCR-β_1	246	-0.1209	0.2763
		248	-0.5031	<0.0001*
		251	0.1437	0.1950
		254	-0.5202	<0.0001*
		257	-0.2109	0.0556
		260	0.4912	<0.0001*
		262	-0.0792	0.4768
		265	-0.6450	<0.0001*
		268	-0.4010	0.0002*
		271	0.0230	0.8368
		274	-0.0585	0.5991
		277	0.0337	0.7625
		279	-0.2994	0.0060*
	TCR-β_2	273	0.0638	0.5665
		276	-0.1737	0.1163
		279	-0.5772	<0.0001*
		282	-0.1944	0.0782
		284	0.2160	0.0498*
		287	-0.4840	<0.0001*
		290	-0.3928	0.0002*
		293	-0.2370	0.0310
		295	-0.4557	<0.0001*
		298	-0.1190	0.2841
		301	-0.1569	0.1566
		304	-0.0393	0.7241
Smyth line	TCR-β_1	246	0.0542	0.5432
		248	-0.3054	0.0005*
		251	0.1806	0.0413*
		254	-0.1447	0.1032
		257	-0.2640	0.0026*
		260	-0.0063	0.9436
		262	-0.1869	0.0346*
		265	-0.1193	0.1797
		268	0.1759	0.0470*
		271	0.1140	0.1999
		274	-0.1204	0.1759
		277	-0.2423	0.0059*
		279	-0.0718	0.4206
	TCR-β_2	273	0.0525	0.5562

Table 4. **(Cont.)**

Line	D-score	Allele group	Spearman ρ	P-value[1]
		276	-0.2209	0.0122*
		279	-0.6595	<0.0001*
		282	-0.2558	0.0036*
		284	0.2922	0.0008*
		287	-0.1367	0.1239
		290	-0.3627	<0.0001*
		293	-0.3431	<0.0001*
		295	-0.5266	<0.0001*
		298	0.0394	0.6588
		301	0.0217	0.8076
		304	0.0023	0.9798

[1]P-values <0.05 were considered statistically significant (*)

Table 5. **Genes with no overall changes in expression relative to age in growing feathers of parental-control, non-expressing Brown line chickens**

Gene	P-value
CCL19	0.1518
CCR7	0.3619
FASLG	0.6281
GZMA	0.6149
INFA	0.6772
IFNB	0.4729
IFNG	0.6055
IL1B	0.6360
IL2R	0.0864
IL18	0.7660
IL21	0.3447
IL21R	0.2106
TGFB1	0.6912

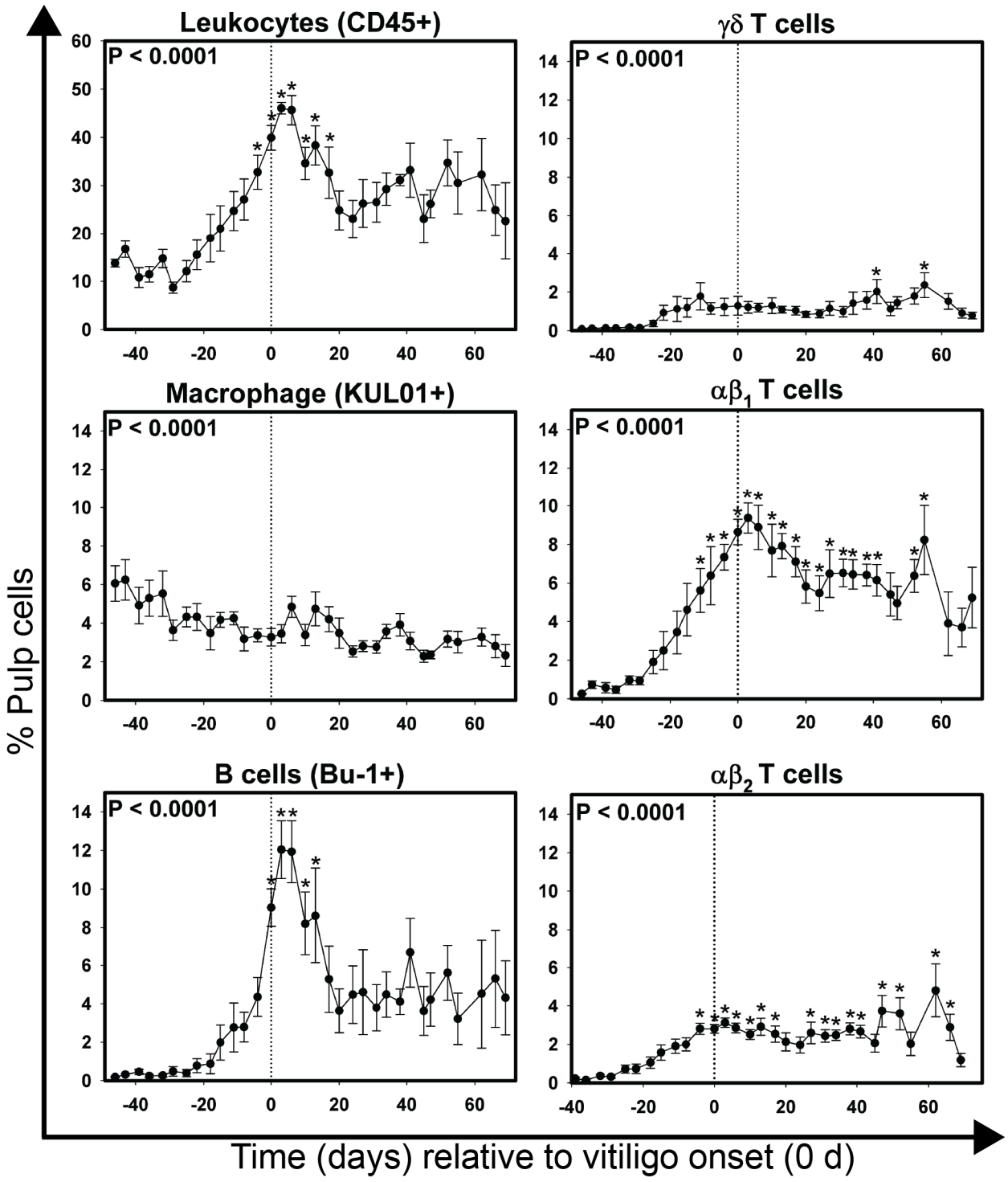
Leukocytes (CD45+)
P < 0.0001
γδ T cells
P < 0.0001
Macrophage (KUL01+)
P < 0.0001
αβ1 T cells
P < 0.0001
B cells (Bu-1+)
P < 0.0001
αβ2 T cells
P < 0.0001
% Pulp cells
Time (days) relative to vitiligo onset (0 d)

Figure 1. **Cell infiltration profiles for total leukocytes, macrophages, B cells and T cells in growing feathers of vitiligo-expressing Smyth.** Growing feathers were sampled from Smyth beginning at 1 day post-hatch and continued twice a week for 113 days. Single-cell suspensions were prepared from feather samples and immunofluorescently-stained for total leukocytes (CD45), macrophages (KUL01), B cells (Bu-1), γδ T cells (TCR1), $\alpha\beta_1$ T cells (TCR2) and $\alpha\beta_2$ T cells (TCR3) using mouse monoclonal chicken-specific antibodies. Population analysis was performed by flow cytometry. Data were aligned by time (days) relative to age of vitiligo onset (set to 0 d and indicated by vertical dashed line). The overall effect of time relative to vitiligo onset was determined using a mixed effects regression model setting time and individual bird as a fixed and random effect respectively. When a significant time effect was found, post-hoc multiple means comparisons were made against the -39 d sample using the Tukey-Kramer p-value adjustment. Differences were considered significant at $P < 0.05$ (*). Data are plotted as mean ± SEM; n = 3 to 8 chickens per time point.

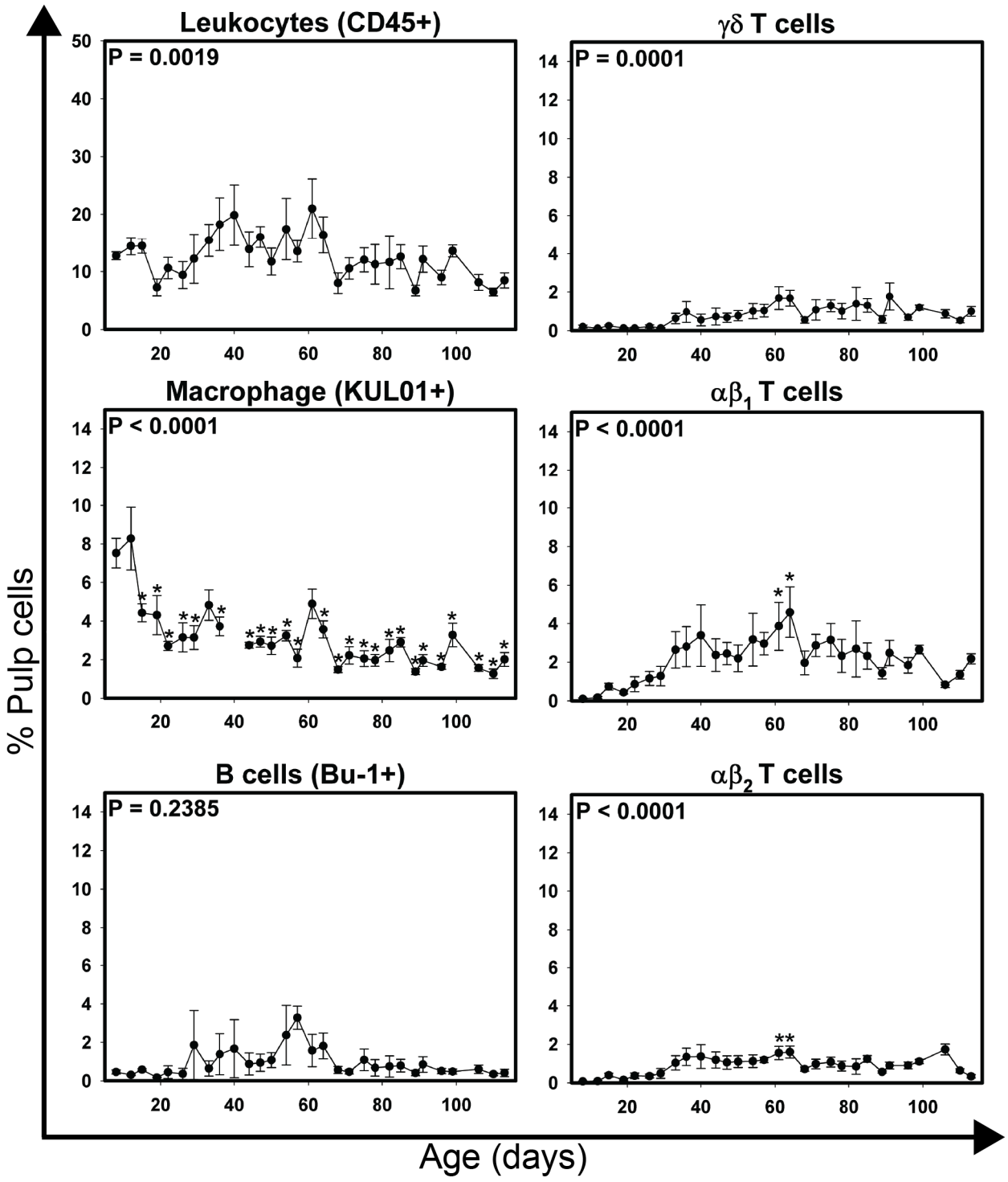
Leukocytes (CD45+)
P = 0.0019
γδ T cells
P = 0.0001
Macrophage (KUL01+)
P < 0.0001
αβ1 T cells
P < 0.0001
B cells (Bu-1+)
P = 0.2385
αβ2 T cells
P < 0.0001
% Pulp cells
Age (days)

Figure 2. **Cell infiltration profiles for total leukocytes, macrophages, B cells and T cells in growing feathers of parental control, non-expressing Brown line chickens.** Growing feathers were sampled from Brown line chickens beginning at 1 day post-hatch and continued twice a week for 113 days. Single-cell suspensions were prepared from feather samples and immunofluorescently-stained for total leukocytes (CD45), macrophages (KUL01), B cells (Bu-1), γδ T cells (TCR1), $\alpha\beta_1$ T cells (TCR2) and $\alpha\beta_2$ T cells (TCR3) using mouse monoclonal chicken-specific antibodies. Population analysis was performed by flow cytometry. Data were aligned and averaged by age (days). The overall effect of time was determined using a mixed effects regression model setting age and individual bird as a fixed and random effect respectively. When a significant time effect was found, post-hoc multiple means comparisons were made against the 8 d sample using the Tukey-Kramer p-value adjustment. Differences were considered significant at $P < 0.05$ (*). Data are plotted as mean ± SEM; n = 5 chickens per time point.

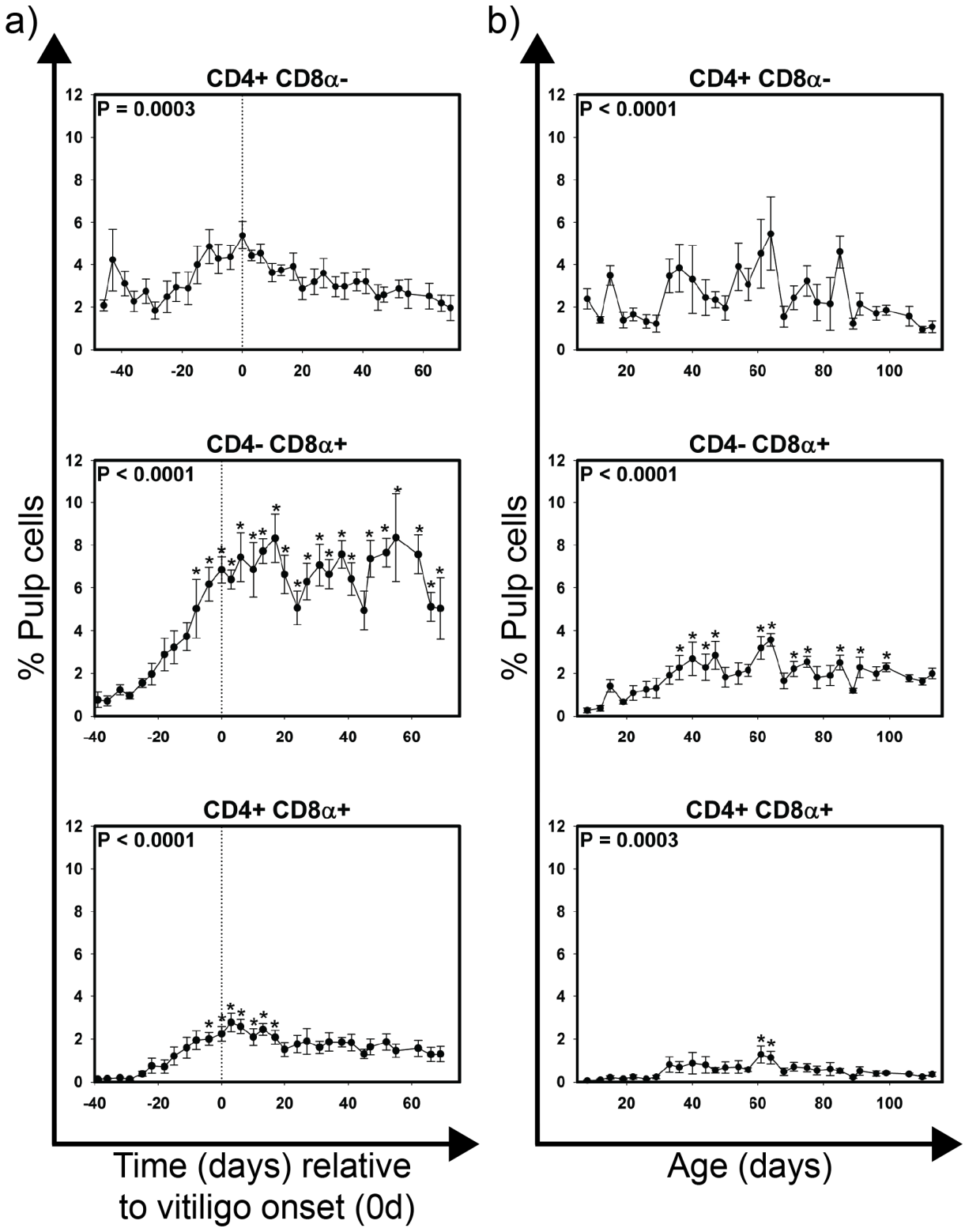
a)
b)
CD4+ CD8α-
P = 0.0003
P < 0.0001
CD4- CD8α+
P < 0.0001
P < 0.0001
CD4+ CD8α+
P < 0.0001
P = 0.0003
% Pulp cells
% Pulp cells
Time (days) relative to vitiligo onset (0d)
Age (days)

Figure 3. **Cell infiltration profiles for T cell subsets in growing feathers of vitiligo-expressing Smyth and parental-control, non-expressing Brown line chickens.** Growing feathers were sampled from Smyth and Brown line chickens beginning at 1 day post-hatch and continued twice a week for 113 days. Single-cell suspensions were prepared from feather samples and immunofluorescently-stained for CD4 and CD8α using mouse monoclonal chicken-specific antibodies. Population analysis was performed by flow cytometry. a) Data for vitiligo-expressing Smyth chickens were aligned by time (days) relative to age of vitiligo onset (set to 0 d and indicated by vertical dashed line). b) Data for non-expressing Brown line chickens were aligned and averaged by age (days). The overall effect of time was determined using a mixed effects regression model setting time and individual bird as a fixed and random effect respectively. When a significant time effect was found, post-hoc multiple means comparisons were made against the -39 d and 8 d samples for Smyth and Brown line respectively, using the Tukey-Kramer p-value adjustment. Differences were considered significant at $P < 0.05$ (*). Data are plotted as mean ± SEM; n = 3 to 8 and 5 chickens per time point for Smyth and Brown line respectively.

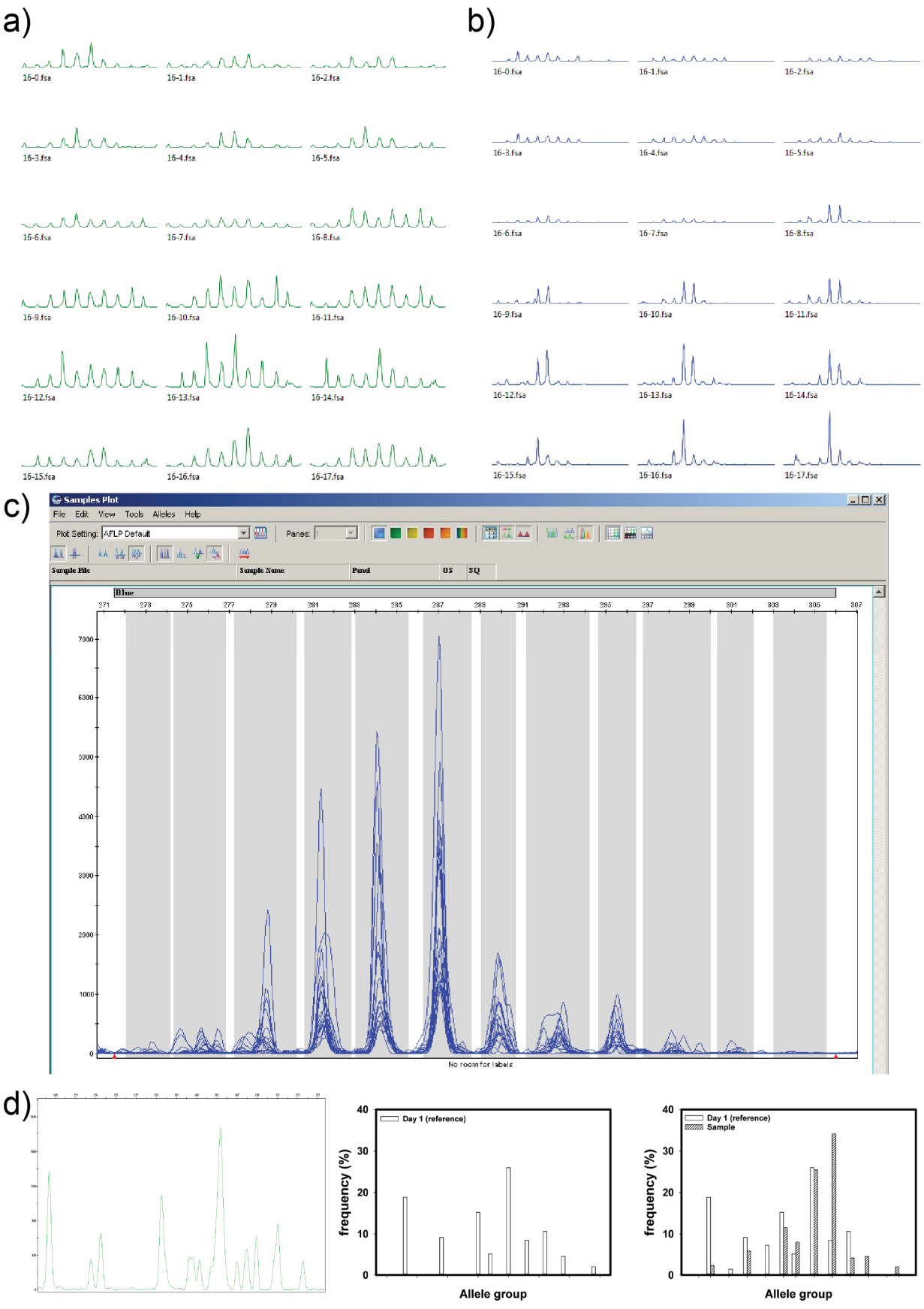
a)
16-0.fsa
16-1.fsa
16-2.fsa
16-3.fsa
16-4.fsa
16-5.fsa
16-6.fsa
16-7.fsa
16-8.fsa
16-9.fsa
16-10.fsa
16-11.fsa
16-12.fsa
16-13.fsa
16-14.fsa
16-15.fsa
16-16.fsa
16-17.fsa
b)
16-0.fsa
16-1.fsa
16-2.fsa
16-3.fsa
16-4.fsa
16-5.fsa
16-6.fsa
16-7.fsa
16-8.fsa
16-9.fsa
16-10.fsa
16-11.fsa
16-12.fsa
16-13.fsa
16-14.fsa
16-15.fsa
16-16.fsa
16-17.fsa
c)
Samples Plot
File Edit View Tools Alleles Help
Plot Setting: AFLP Default
Panes:
Sample File
Sample Name
Panel
OS
SQ
Blue
No room for labels
d)
Day 1 (reference)
frequency (%)
Allele group
Day 1 (reference)
Sample
frequency (%)
Allele group

Figure 4. **Quantification of changes in the T cell receptor repertoire.** Complementarity-determining 3-containing regions of the T cell receptor-β_1 (TCR-β_1) and –β_2 (TCR-β_2) genes were amplified from individual cDNA samples by end-point PCR using fluorescently-labeled (forward) primers against conserved 5' regions of the variable (V) gene segments of the TCR-β_1 and -β_2 genes and an unlabeled (reverse) primer against a conserved 3' constant (C) region shared by the two genes. The resulting fluorescently-labeled products were then size-separated by capillary electrophoresis and the quantity of each group of alleles was determined using GeneMapper® 4.0. a), b) Sample size profiles of TCR-β_1 and TCR-β_2 genes respectively (fluorescence signal versus size). c) Alleles were defined based on an overlay of all spectrographs and were separated by approximately three base pairs and the height of the fluorescence signal was used as the measure of quantity of each allele group. d) Each quantification profile (left) was converted to a frequency distribution (middle) and the Hamming-distance (D-score) between individual day 1 samples was calculated. D-scores were obtained by summing the absolute difference of each allele group relative to individual day 1 samples (right) and then dividing by 2.

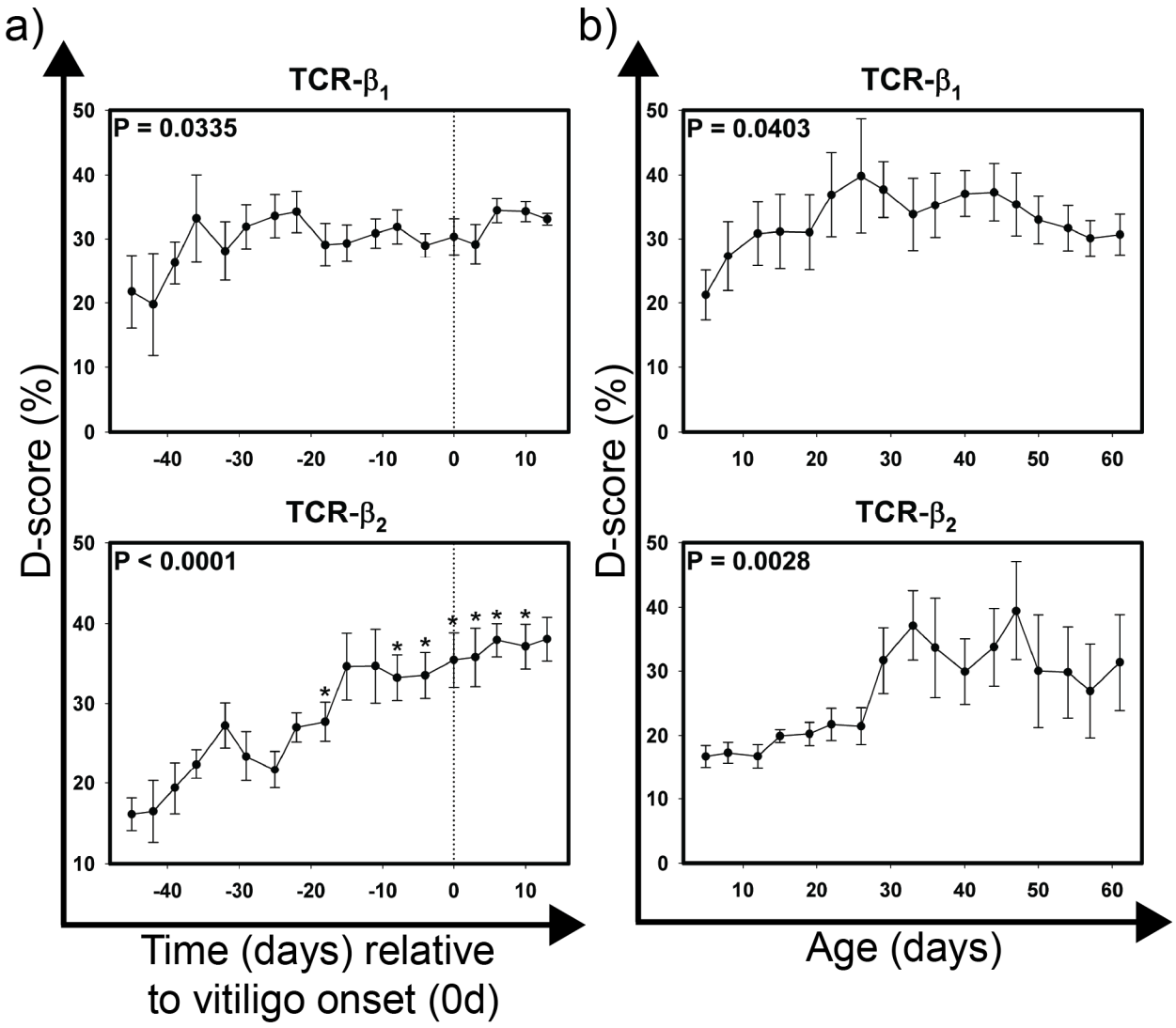
a)
b)
TCR-β1
P = 0.0335
TCR-β2
P < 0.0001
TCR-β1
P = 0.0403
TCR-β2
P = 0.0028
D-score (%)
Time (days) relative to vitiligo onset (0d)
Age (days)

Figure 5. **Alterations in the T cell receptor repertoire in growing feathers of vitiligo-expressing Smyth and non-expressing Brown line chickens.** Growing feathers were sampled from Smyth beginning at 1 day post-hatch and continued twice a week for 113 days. Complementarity-determining 3-containing regions of the T cell receptor-variable β_1 (TCR-β_1) and -variable β_2 (TCR-β_2) genes were amplified from cDNA derived from growing feather samples by end-point PCR using fluorescently-labeled forward primers specific to conserved 5' regions of variable (V) gene segments and an unlabeled reverse primer specific to conserved 3' constant regions shared by the two genes. The resulting fluorescently-labeled products were size-separated by capillary electrophoresis and the quantities of each group of alleles estimated based on fluorescence intensity. Quantification profiles for each sample was converted to a frequency distribution and the Hamming-distance (D-score) was calculated by summing the absolute difference of each allele group relative to a reference sample and then dividing by 2. a) cDNA from samples collected from 45 days prior to- through 13 days post-vitiligo onset were analyzed for alterations in the T cell receptor repertoire. Data for vitiligo-expressing Smyth line chickens were aligned by time (days) relative to age of vitiligo onset (set to 0 d). b) cDNA from samples collected from 5 days through 61 days of age were analyzed for alterations in the T cell receptor repertoire. Data for Brown line controls were aligned and averaged by age (days).The overall effect of time was determined using a mixed effects regression model setting time and individual bird as a fixed and random effect respectively. When a significant time effect was found, post-hoc multiple means comparisons were made against the -39 d and 8 d samples for Smyth and Brown line respectively, using the Tukey-Kramer p-value adjustment. Differences were considered significant at $P < 0.05$ (*). Data are plotted as mean ± SEM; n = 3 to 8 and 5 chickens per time point for Smyth and Brown line respectively.

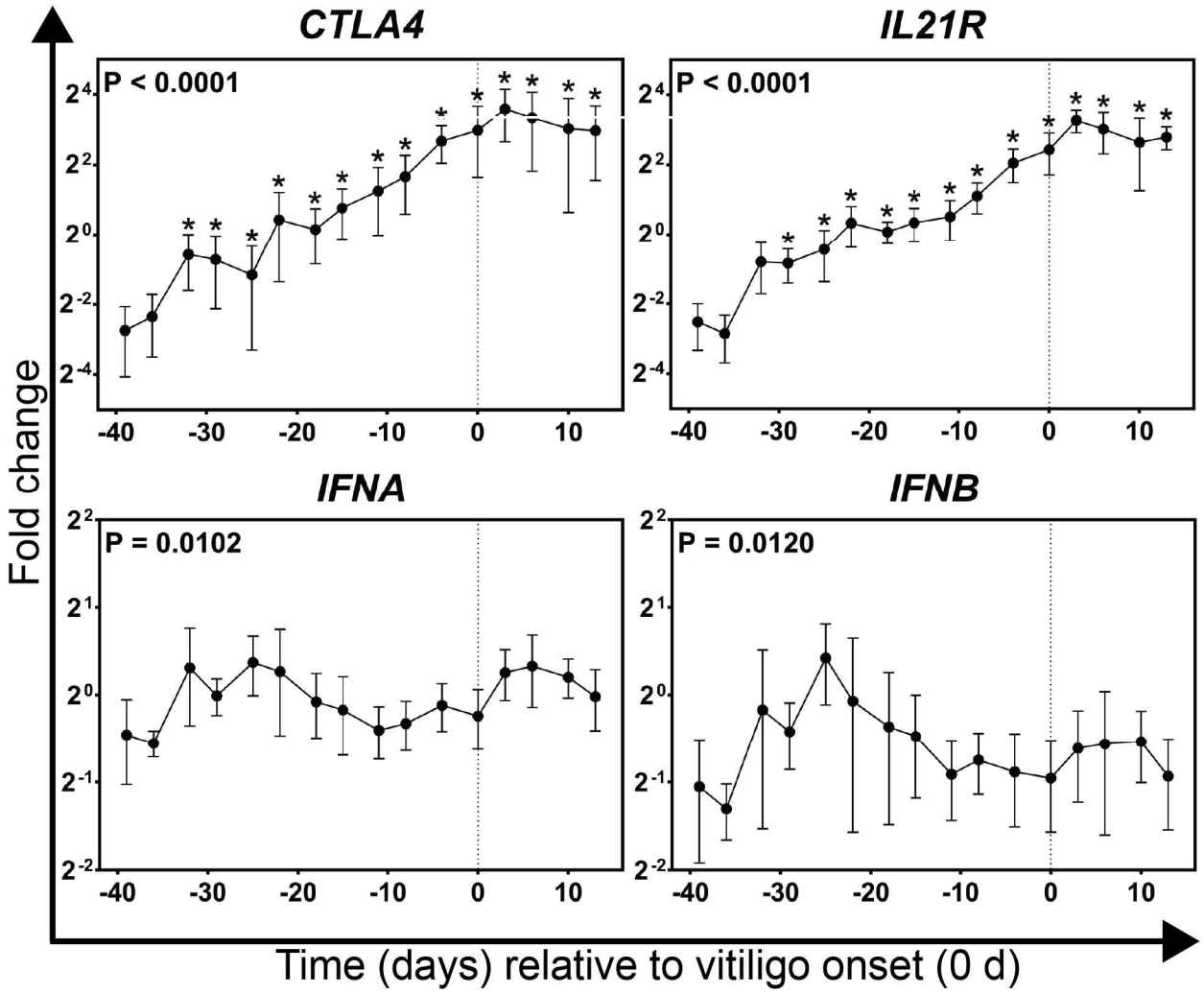

Figure 6. **Gene expression profiles for potential early markers of immunological activities in growing feathers of vitiligo-expressing Smyth line chickens.** Growing feather samples were taken from Smyth beginning at 1 day post-hatch and continuing twice a week for 113 days. cDNA from samples collected from 39 days prior to- through 13 days post-vitiligo onset were analyzed for relative gene expression of *CTLA4*, *IL21R*, *IFNA* and *IFNB*. Relative gene expression was determined by the efficiency-calibrated ΔCt method (Pfaffl, 2001) and is expressed as fold change relative to the calibrator sample. Gene expression profiles were obtained for individual chickens, using individual-specific day 29 samples as calibrators and 28S as a reference gene. Data were aligned and averaged by time (days) relative to age of vitiligo onset (set to 0 d; indicated by vertical dashed line). The overall effect of time was determined using a mixed effects regression model setting time and individual bird as a fixed and random effect respectively. When a significant time effect was found, post-hoc multiple means comparisons were made against the -39 d samples using the Tukey-Kramer p-value adjustment. Differences were considered significant at $P < 0.05$ (*). Data are plotted as mean ± SEM; n = 3 to 8 chickens per time point.

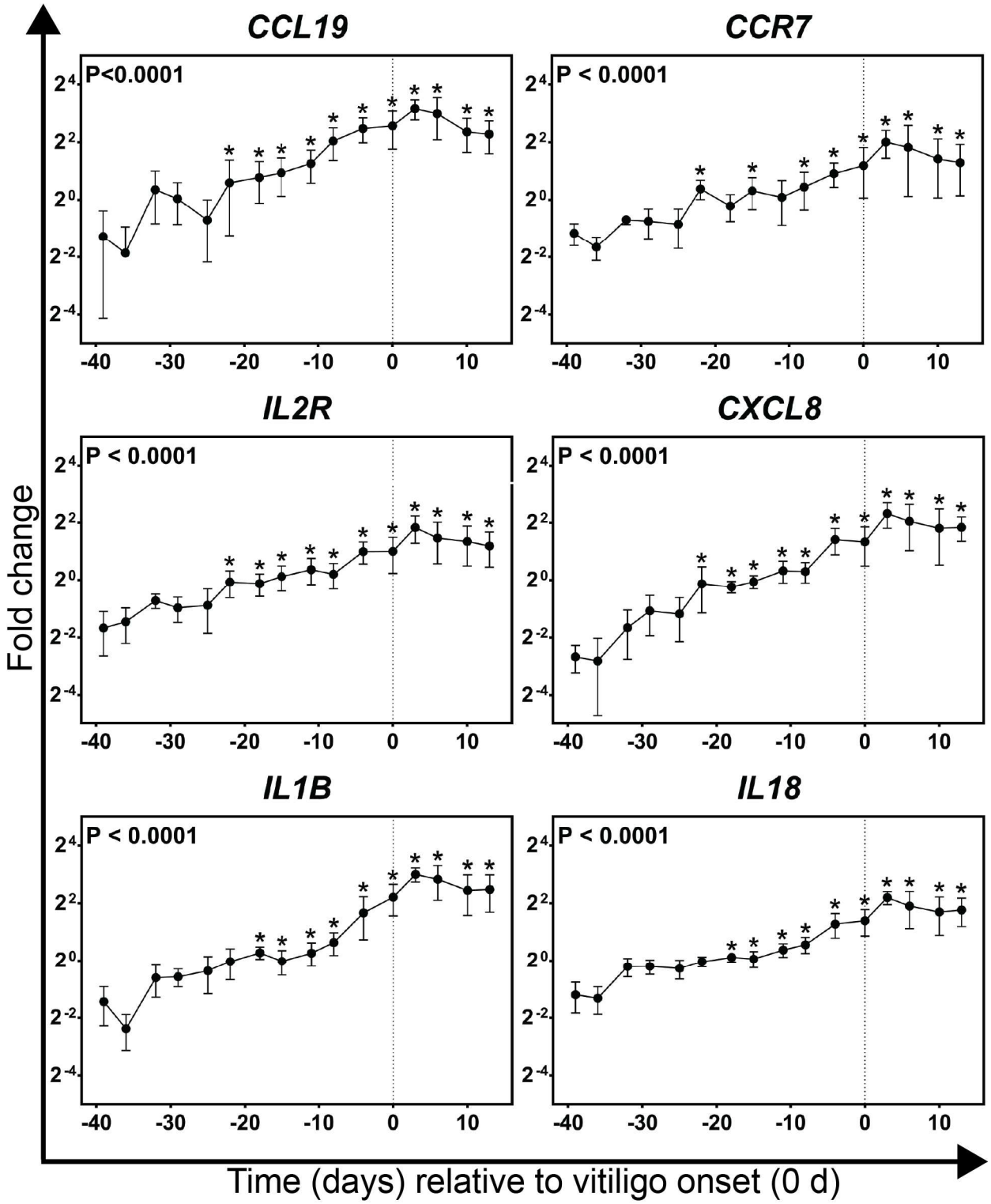
CCL19
P<0.0001
CCR7
P < 0.0001
IL2R
P < 0.0001
CXCL8
P < 0.0001
IL1B
P < 0.0001
IL18
P < 0.0001
Fold change
Time (days) relative to vitiligo onset (0 d)

Figure 7. **Gene expression profiles for markers of pro-inflammatory and recruitment activities in growing feathers of vitiligo-expressing Smyth line chickens.** Growing feather samples were taken from Smyth beginning at 1 day post-hatch and continuing twice a week for 113 days. cDNA from samples collected from 39 days prior to- through 13 days post-vitiligo onset were analyzed for relative gene expression of *CCL19*, *CCR7*, *IL2R*, *CXCL8*, *IL1B* and *IL18*. Relative gene expression was determined by the efficiency-calibrated ΔCt method (Pfaffl, 2001) and is expressed as fold change relative to the calibrator sample. Gene expression profiles were obtained for individual chickens, using individual-specific day 29 samples as calibrators and 28S as a reference gene. Data were aligned and averaged by time (days) relative to age of vitiligo onset (set to 0 d; indicated by vertical dashed line). The overall effect of time was determined using a mixed effects regression model setting time and individual bird as a fixed and random effect respectively. When a significant time effect was found, post-hoc multiple means comparisons were made against the -39 d samples using the Tukey-Kramer p-value adjustment. Differences were considered significant at $P < 0.05$ (*). Data are plotted as mean ± SEM; n = 3 to 8 chickens per time point.

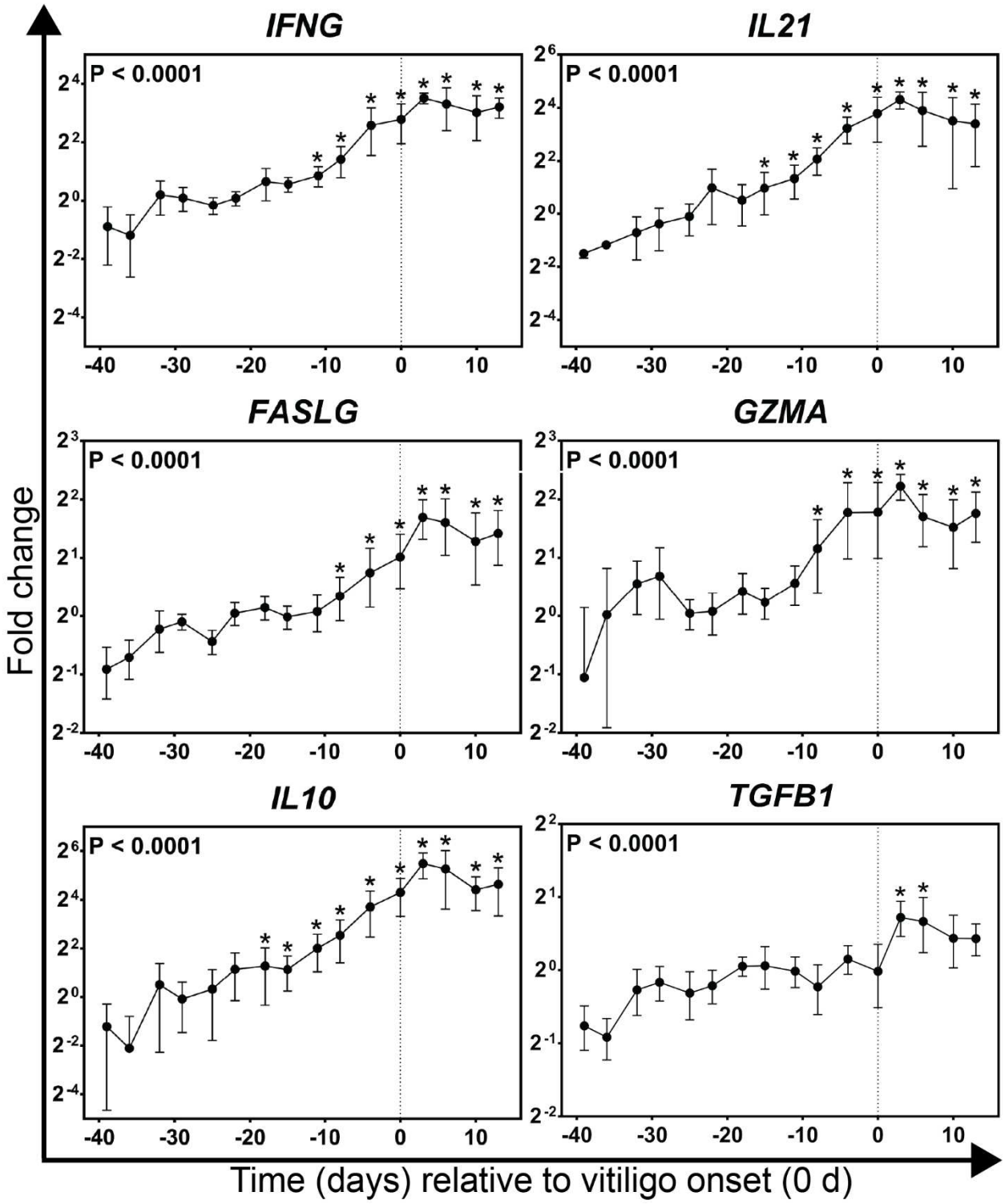
IFNG
IL21
FASLG
GZMA
IL10
TGFB1
P < 0.0001
Fold change
Time (days) relative to vitiligo onset (0 d)

Figure 8. **Gene expression profiles for markers of cell-mediated immunity and anti-inflammatory activities in growing feathers of vitiligo-expressing Smyth line chickens.** Growing feather samples were taken from Smyth beginning at 1 day post-hatch and continuing twice a week for 113 days. cDNA from samples collected from 39 days prior to- through 13 days post-vitiligo onset were analyzed for relative gene expression of *IFNG*, *IL21*, *FASLG*, *GZMA*, *IL10* and *TGFB1*. Relative gene expression was determined by the efficiency-calibrated ΔCt method (Pfaffl, 2001) and is expressed as fold change relative to the calibrator sample. Gene expression profiles were obtained for individual chickens, using individual-specific day 29 samples as calibrators and 28S as a reference gene. Data were aligned and averaged by time (days) relative to age of vitiligo onset (set to 0 d; indicated by vertical dashed line). The overall effect of time was determined using a mixed effects regression model setting time and individual bird as a fixed and random effect respectively. When a significant time effect was found, post-hoc multiple means comparisons were made against the -39 d samples using the Tukey-Kramer p-value adjustment. Differences were considered significant at $P < 0.05$ (*). Data are plotted as mean ± SEM; n = 3 to 8 chickens per time point.

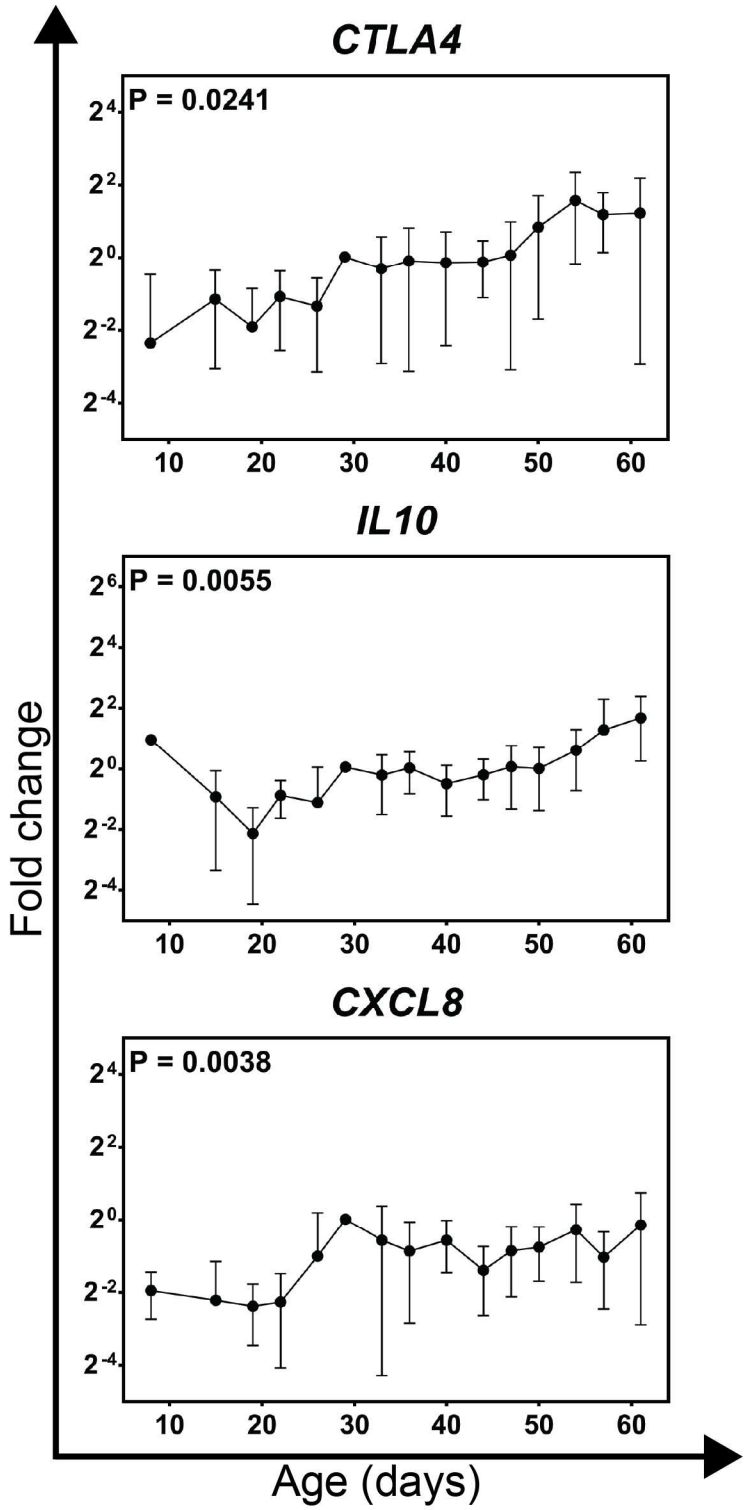
CTLA4
P = 0.0241
IL10
P = 0.0055
CXCL8
P = 0.0038
Fold change
Age (days)
10
20
30
40
50
60

Figure 9. **Expression profiles for genes significantly affected by age in growing feathers of parental-control, non-expressing Brown line chickens.** Growing feather samples were taken from Brown line chickens beginning at 1 day post-hatch and continuing twice a week for 113 days. cDNA from samples collected from 8 – 61 days of age were analyzed for relative gene expression of *CTLA4*, *IL10* and *CXCL8*. Relative gene expression was determined by the efficiency-calibrated ΔCt method (Pfaffl, 2001) and is expressed as fold change relative to the calibrator sample. Gene expression profiles were obtained for individual chickens, using individual-specific day 29 samples as calibrators and 28S as a reference gene. Data were aligned and averaged by age (days). The overall effect of time was determined using a mixed effects regression model setting time and individual bird as a fixed and random effect respectively. When a significant time effect was found, post-hoc multiple means comparisons were made against the 8 d samples using the Tukey-Kramer p-value adjustment. Differences were considered significant at $P < 0.05$ (*).Data are plotted as mean ± SEM; n = 5 chickens per time point.

a)

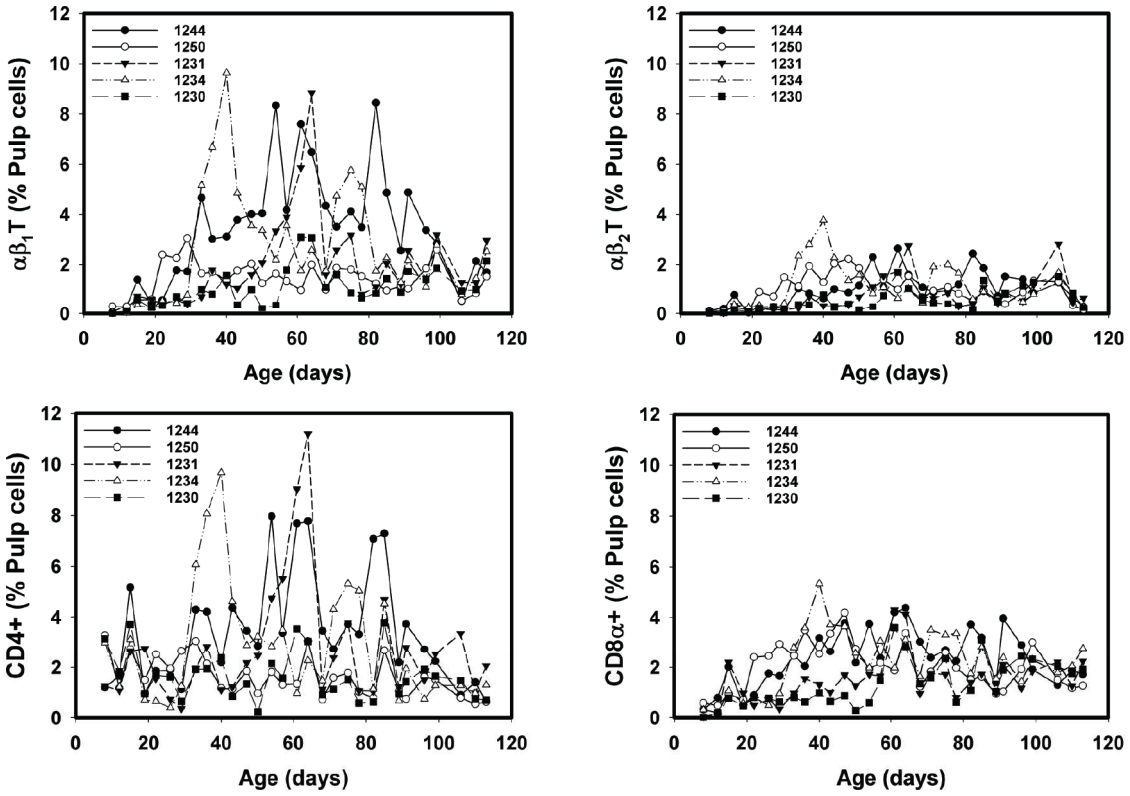
1244
1250
1231
1234
1230
αβ1T (% Pulp cells)
αβ2T (% Pulp cells)
CD4+ (% Pulp cells)
CD8α+ (% Pulp cells)
Age (days)

b)

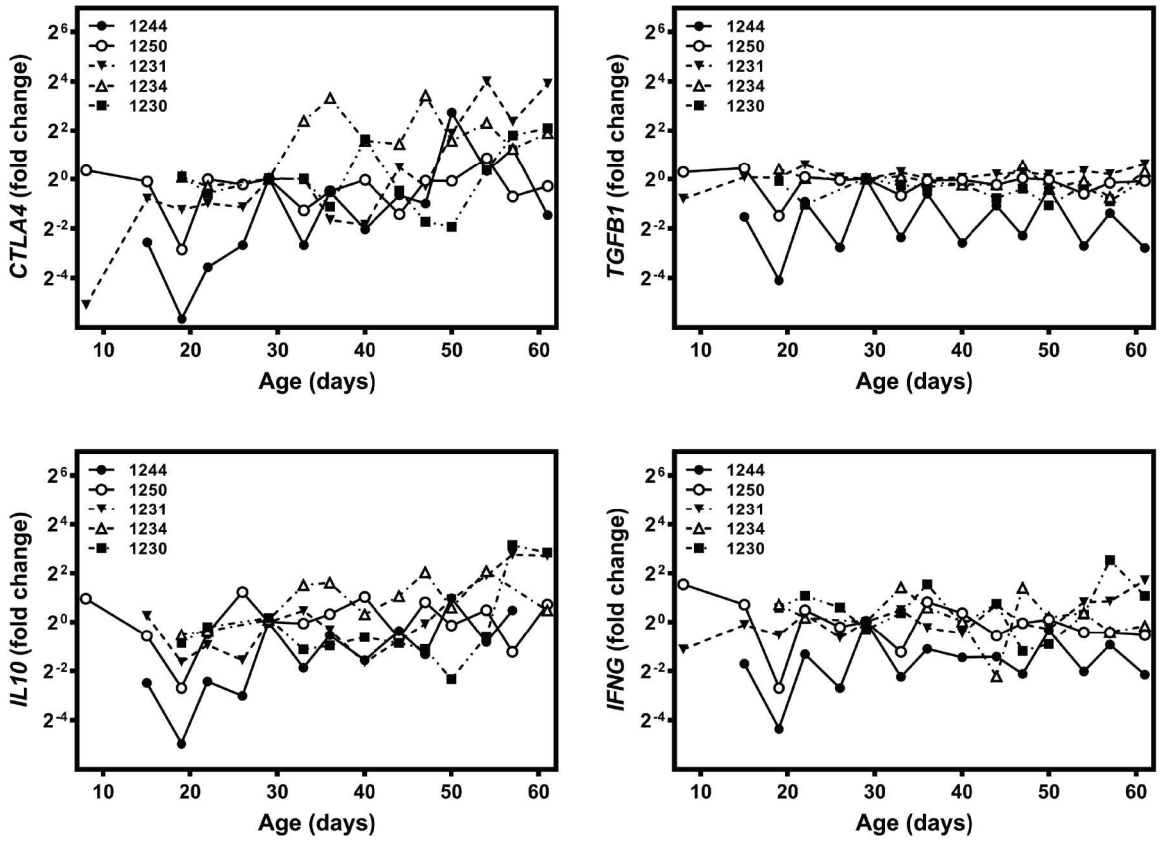
1244
1250
1231
1234
1230
CTLA4 (fold change)
TGFB1 (fold change)
IL10 (fold change)
IFNG (fold change)
Age (days)

Figure 10. **Individual-specific T cell subset infiltration, gene expression and T cell receptor perturbation profiles in growing feathers of non-expressing Brown line chickens.** Growing feathers were sampled from Brown line chickens (n=5) beginning at 1 day post-hatch and continued twice a week for 113 days. a) Single-cell suspensions were prepared from feather samples and immunofluorescently-stained for total leukocytes (CD45), B cells (Bu-1), γδ T cells (TCR1), $\alpha\beta_1$ T cells (TCR2), $\alpha\beta_2$ T cells (TCR3), CD4 and CD8α using chicken-specific antibodies. Population analysis was performed by flow cytometry. b) RNA and cDNA from day's 1 – 61 feather samples were prepared and used as templates for gene expression analysis with chicken-specific primers and probes. Relative gene expression was determined by the efficiency-calibrated ΔCt method (Pfaffl, 2001) and is expressed as fold change relative to the calibrator sample. Gene expression profiles were obtained for individual chickens, using individual-specific day 29 samples as calibrators and 28S as a reference gene.

Chapter II

Establishment of a method to assess and monitor melanocyte-specific autoimmune memory responses in the target tissue of completely de-pigmented vitiligo-prone Smyth chickens

Introduction

Immunological memory is a defining hallmark of the adaptive immune system. After initial exposure to an antigen, a relatively slow immune response is mounted resulting in the generation of highly-specific effector and memory cells. After resolution of the immune response, short-lived effector cells die by apoptosis while memory cells are maintained in the periphery as well as in the tissues. Upon re-encounter with antigen, memory cells are activated and a rapid and a relatively intensified immune response is mounted (Kaech and Wherry, 2007; Woodland and Kohlmeier, 2009). Autoimmunity results from the breakdown of immunological tolerance to self-antigen. As in the case of an immune response to a foreign antigen, an autoimmune response results in the generation of long-lived memory cells which prevent the natural replenishment of target cells and make difficult the possibility of organ or tissue-replacement via transplant (Devarajan and Chen, 2013; Ehlers and Rigby, 2015).

Vitiligo is an acquired de-pigmentation disorder characterized by the appearance of white patches in the skin resulting from the loss of epidermal pigment-producing cells (melanocytes). Disease onset is spontaneous and results from a complex interplay between environmental, genetic and immunological factors (Le Poole *et al.*, 1993; Ezzedine *et al.*, 2015). While identification of triggering mechanisms remain elusive, progression of vitiligo is strongly attributed to a melanocyte-specific autoimmune response. Furthermore, strong evidence of melanocyte-specific immunological memory in the T cell compartment is well documented in vitiligo patients (Mantovani *et al.*, 2003; Boniface *et al.*, 2018).

The vitiligo-prone Smyth chicken is a well-established model for autoimmune vitiligo. Similarly, to humans, melanocyte loss in Smyth chickens is spontaneous and results from the complex interplay between environmental, genetic and immunological factors. Despite the spontaneous nature of vitiligo in Smyth chickens, the identification of an environmental trigger (vaccination with herpes virus of turkey) has resulted in predictable disease incidence of vitiligo (80 – 95%) among hatch mates (Erf *et al.*, 2001). Similar to humans, melanocytes are localized to the epidermis in growing feathers (a skin-derivative). As in humans, evidence of humoral and cell-mediated immune activities are well documented in Smyth chickens, however studies on melanocyte-specific immunological memory in the target tissue are lacking.

In 2003, Wang and Erf revealed what appeared to be a melanocyte-specific, memory-like, cell-mediated immune response in the wattle of vitiliginous Smyth chickens injected with feather-derived melanocyte lysates. As would be expected in a memory response, maximum wattle swelling in vitiliginous Smyth chickens was significantly greater than controls and occurred within five days of injection (Wang and Erf, 2003).

In chickens the living portion (pulp) of growing feathers is encased in an outer sheath and consists of a column of dermis surrounded by epidermis. Thus, a growing feather represents an enclosed, sterile environment which can be used as a cutaneous test side to gain insights into tissue/cellular responses to test materials *in vivo*. Moreover, simultaneous injection of test materials into the pulp of several growing feathers on an individual followed by repeat sampling at different times allows for continuous monitoring of local immune responses over time (Erf and Ramachandran, 2016). The technique has since been applied to test the local response to such wide ranging materials as graphene nanomaterials, microbes and phytohemagglutinin in growing feathers (Erf and Ramachandran, 2016; Erf *et al.*, 2017; Sullivan and Erf, 2017).

The anatomical location of the target tissue (a growing feather) combined with the methodology of aforementioned feather-injection and sampling resents a unique opportunity to use growing feathers as a dermal test site for autoimmune memory responses in Smyth chickens *in vivo*. Therefore, for this study we sought to establish a method for assessing and monitoring the melanocyte-specific memory response in growing feathers of completely de-pigmented Smyth chickens. Histological analysis of growing feathers from completely de-pigmented Smyth chickens revealed a complete lack to pigment at the barb ridges (anatomical location of melanocytes) suggesting an absence of melanocytes (Boissy *et al.*, 1983). Furthermore, the close proximity of $CD8^+$ T cells with apoptotic ($TUNEL^+$) cells in growing feathers of Smyth chickens with active (progressing) vitiligo strongly suggests that melanocytes are eliminated during the primary response (Wang and Erf, 2004). Moreover, in Chapter 1 we have observed a gradual increase in B and T cell infiltration as well as rises in cell-mediated-related gene expression in growing feathers of Smyth chickens leading up to visual onset of vitiligo. As observed, post-onset, B cells and

$CD4^+CD8\alpha^-$ as well as gene expression activities return to basal levels while $CD4^-CD8\alpha^+$ and $CD4^+CD8\alpha^+$ cells remain elevated in the target tissue possibly as differentiated tissue-resident memory cells. In summary all evidence points to complete absence of melanocytes in the target tissue of de-pigmented Smyth chickens and thus a lack of melanocyte-specific immune activity.

To induce memory responses in de-pigmented Smyth chickens, feather-derived melanocytes were re-introduced back into the target tissue (a growing feather) via intradermal injection. To account for immune activity in response to the wound created by the injection itself, a separate group was injected with vehicle only (HBSS). Furthermore, growing feathers of fully pigmented (non-vitiliginous) MHC-matched Brown line chickens were also injected as above. As evidenced by their fully pigmented feathers, Brown line chickens, presumably, never mounted a primary melanocyte-specific autoimmune response and thus were not expected to demonstrate a memory response.

Injection of several feathers on a single individual allowed for the monitoring of the immune response over time. Lymphocyte infiltration profiles were obtained by direct immunofluorescent staining of single-cell suspensions derived from the pulp (dermis) of injected feathers following by flow cytometry. Gene expression profiles were also obtained using targeted gene expression assays and cDNA derived from the pulp of injected feathers. Lastly, changes in the overall diversity of the T cell receptor repertoire was also examined in injected feathers. Results from this study will provide valuable insights into the nature of the melanocyte-specific recall or memory response in completely de-pigmented Smyth chickens.

Materials and Methods

Animal care and rearing

This study was carried out in two trials using chickens from the Smyth and Brown line populations maintained by G. F. Erf at the Arkansas Experiment Station Poultry Farm in Fayetteville, AR. In Trial 1, three 15-week old completely de-pigmented Smyth and three age- and MHC-matched ($B^{101/101}$) fully pigmented, parental-control Brown line chicks (straight-run) were used. In Trial 2, five 18-week old chickens of each line and phenotype were used. All chickens were vaccinated against Marek's disease

with live herpesvirus of turkey (Fort Dodge Animal Health, Fort Dodge, IA) at 1-day post-hatch and kept on floor pens with wood shavings and free access to food and water at the Arkansas Agricultural Experiment Station Poultry Farm at the University of Arkansas, Division of Agriculture, Fayetteville, AR. All studies were conducted with the approval of the University of Arkansas Institutional Animal Care and Use Committee (IACUC) as outlined in protocol 15015.

Melanocyte culture

For both trials previously-established feather-derived melanocytes from Smyth chickens were used. Melanocyte cultures were established according to Bowers (1985) and stored in liquid nitrogen until use. All cells were maintained in a humidified incubator set at 40 °C, 5 % CO_2. Culture medium components were as follows: Ham's F12 medium supplemented with 10 % FBS, 2mM L-glutamine (Gibco, Carlsbad, CA), PSN solution (50 U/mL penicillin, 50 µg/mL streptomycin, 100 µg/mL neomycin), 40 ng/mL cholera toxin from *Vibrio cholera*, 10 ng/mLendothelin-3 (human, rat), 5 µg/mL insulin from bovine pancreas and 85 nM phorbol 12-myristate 13-acetate (PMA). All components with the exception of L-glutamine were purchased from Sigma-Aldrich (St. Louis, MO). Cells were harvested by incubation in Hanks' Balanced Salt Solution (calcium and magnesium-free; HBSS; Gibco, Carlsbad, CA) for 3-5 minutes at 40° C, 5 % CO_2. Detached cells were placed on ice, counted and promptly loaded into 0.3 mL syringes with 31 x 8 mm gauge needles (BD, Franklin Lakes, NJ). Control syringes were loaded with HBSS. All loaded syringes were kept on ice until used for injections.

Growing feather injection and sampling

Feather injections were performed according to Erf and Ramachandran (2016). To obtain growing feathers of uniform age, a row of mature feathers were plucked from the left and right breast tracts 18 days prior to initiation of the study. Prior to injection, an un-injected feather sample was taken as a control (0 d.p.i.). The barbs of regenerated feathers were trimmed such that column of pulp was left undisturbed and visible. For each chicken 10 feathers were injected with 10µL of test material through the epidermal cap and into the pulp. For Trail 1, 10 growing feathers of two chickens of each line were

injected with 10µL of a 7.4 x 10^6 melanocytes per mL suspension (74,000 cells per feather) and one was injected with 10µL Hank's Balanced Salt Solution (calcium and magnesium-free; HBSS; Gibco, Carlsbad, CA) as a vehicle-only control. For Trail 2, 10 growing feathers of three chickens of each line were injected with 10µL of a 5.5 x 10^6 melanocytes per mL suspension (55,000 cells per feather) and three were injected with 10µL Hank's Balanced Salt Solution (calcium and magnesium-free; HBSS; Gibco, Carlsbad, CA) as a vehicle-only control. Injected growing feather samples were taken at 6 hours post-injection and daily thereafter for 7 days post-injection. At each time point, two injected growing feathers were taken from each chicken with one being placed in D-PBS on ice, and the other being placed in Tissue-Tek® O.C.T. Compound (Sakura of America, Hayward, CA) and snap-frozen in liquid nitrogen. Samples stored in D-PBS were used for same-day population analysis of infiltrating leukocytes (see below). Samples snap-frozen in O.C.T. were stored at -80°C until use.

Population analysis of infiltrating lymphocytes

Single-cell suspensions were obtained from the feather pulp according to Erf and Ramachandran (2016). Briefly, a longitudinal slit was made along the feather sheath and the pulp was removed, placed in a D-PBS solution containing 0.1% collagenase (type IV, Life Technologies, Carlsbad, CA) and incubated for one hour at 40°C. Infiltrating cells were liberated from the digested pulp tissue by passage through a 60µm nylon mesh and washed in a D-PBS solution containing 1% bovine serum albumin (VWR, Randor, PA). Lymphocyte populations in prepared single-cell suspensions were immunofluorescently-stained using the following mouse monoclonal chicken-specific antibodies: Bu-1 (B cells), TCR1 (γδ T cells), TCR2-TCR3 cocktail (total αβ T cells), CD4 and CD8α (SouthernBiotech, Birmingham, AL). Interleukin-2 receptor alpha (CD25) was stained using a bivalent human recombinant Fab (lambda light chain) antibody (Bio-Rad, Hercules, CA). Stained samples were acquired (10,000 events) on a Becton Dickinson FACSort flow cytometer equipped with a 488nm laser and data analysis was performed using FlowJo software (FlowJo, LLC, Ashland, OR). Forward- versus side-scatter dot plots were used to filter out debris and data are expressed as the percentage of all acquired events (% pulp cells).

RNA isolation and cDNA synthesis

To ensure complete removal of O.C.T., frozen feather samples were thawed in 70% ethanol. Once thawed the pulp was removed as above and immediately placed in TRI Reagent® (Zymo Research, Irvine, CA). Extracted pulp tissue was homogenized in TRI Reagent using a Tissue-Tearor™ (BioSpec Products, Bartlesville, OK, model# 985370-395) and total RNA was isolated using the Direct-zol™ RNA Miniprep Plus kit (Zymo Research, Irvine, CA) with on-column DNase digestion according to the manufacturer's instructions. RNA was eluted in 30µL DEPC-treated molecular-grade water (VWR, Radnor, PA) and quantity and purity was assessed by absorbance at 260nm and 280nm on a BioTek Synergy HT (Winooski, VT). One microgram of RNA was reverse transcribed to cDNA in a 20µL sample volume (50ng/µL) using the High Capacity cDNA Reverse Transcription kit (Applied Biosystems, Foster City, CA) according to the manufacturer's instructions. Synthesized cDNA was diluted to 10ng/µL using DEPC-free molecular-grade water (VWR, Radnor, PA) and stored at -20°C until use.

Gene expression analysis

Quantitative real-time PCR was performed using the TaqMan™ system as previously described with modifications (Hamal *et al.*, 2010). Target primer and probe sequences are listed in Table 1. Reactions were carried out in a 12µL sample volume using 20ng of cDNA and were run on an Applied Biosystems® 7500 Real-Time PCR System using manufacturer-programmed cycling conditions. Relative gene expression was determined by the efficiency-calibrated ΔCt method (Pfaffl, 2001) and is expressed as fold change relative to the calibrator sample. To obtain gene expression profiles for individual chickens, results were calculated using individual-specific un-injected (0d) samples as calibrators and 28S as a reference gene.

Amplification of CDR3-containing regions of T cell receptor β-chains

Complementarity-determining 3-containing regions of the T cell receptor-β_1 (TCR-β_1) and –β_2 (TCR-β_2) gene were amplified from individual cDNA samples (prepared above) by end-point PCR. Using all available coding sequences in the NCBI database, fluorescently-labeled (forward) primers were

designed against conserved 5'-variable (V) gene segments of TCR-β_1 (TCR-$V_\beta 1$) and TCR-β_2 (TCR-$V_\beta 2$) genes. An unlabeled (reverse) primer was designed in a similar manner against a conserved 3'-constant (C) region shared by the two genes. Specificity of TCR-$V_\beta 1$ and TCR-$V_\beta 2$ forward primers was confirmed by testing against cDNA derived from TCR1 ($\gamma\delta$ T)-, TCR2 ($\alpha\beta_1$ T)- and TCR3 ($\alpha\beta_2$ T)-sorted PBMCs. Primer sequences and labels are listed in Table 2. Reactions were carried out in a 20µL sample volume using 20ng cDNA, 0.5µM primers and Phusion™ High-Fidelity PCR Master Mix (Thermo Scientific, Waltham, MA). Cycling conditions were as follows: 98°C for 20 seconds (initial denaturation), 98°C for 10 seconds (denaturation), 60°C for 30 seconds (annealing), 72°C for 30 seconds (extension), 72°C for 5 minutes (final extension) and hold at 4°C.

Quantification of changes in the T cell receptor repertoire

Fluorescently-labeled PCR products amplified from individual cDNA samples were sent to the DNA Analysis Facility on Science Hill at Yale University (New Haven, CT) for size-separation by capillary electrophoresis on a 3730xl DNA Analyzer (Applied Biosystems, Foster City, CA). Analysis of raw spectrographs (fluorescence signal versus size) for each sample was performed using GeneMapper® 4.0 (Applied Biosystems, Foster City, CA) with fluorescence height as the measure of quantity (Figure 4a, b). To discount non-specific fluctuations in the fluorescence signal, initial peak detection was performed using thresholds of 100 and 50 for TCR-$V_\beta 1$ and -$V_\beta 2$ samples, respectively. Alleles were defined based on an overlay of all spectrographs and were separated by approximately three base pairs (Figure 4c). Each individual CDR3 length profile was then converted to a frequency distribution by dividing the fluorescence height of a specific allele by the total fluorescence of all alleles in the sample (Figure 4d). To quantify overall changes in CDR3 frequency distributions over time the Hamming-distance (D-score) was calculated against a reference sample. Specifically, the absolute values of the difference in frequencies for every allele relative to samples taken at 1 day of age were summed and then divided by 2 (theoretical minimum and maximum: 0 % and 100 %, respectively; Gorochov *et al.*, 1998).

Statistical analysis

To increase the power of the study, data for Trail 1 and 2 were pooled (n=5 for melanocyte-injected per line, n=4 for HBSS-injected per line). Prior to pooling preliminary analysis (statistical and visual) was performed to ensure common trends between the two data sets.

Due to the exponential nature of relative gene expression (fold change) data, a $\log_2$ transformation was performed to convert the data to a linear scale appropriate for statistical modeling. Additionally, due to the procedure for calculating relative gene expression, data points of the calibrator sample (0 days post-injection; set to 1 fold change) were not included in the statistical analysis. Therefore relative gene expression can only be statistically tested in a post-injection context. No transformation was required for lymphocyte infiltration (% pulp cells) or T cell receptor diversity data (D-score).

The effects of test material (melanocytes and HBSS) and time as well as their interaction within each line of chicken was determined using a mixed-effects regression model. Time (days post-injection) and test material were defined as fixed effects and individual chickens were defined as a random effect. In the event of significant interaction between time and test material effects, multiple means comparisons were carried out using Student's t-test. In the absence of interaction and significant effect of time, multiple means comparisons were also carried out using Student's t-test. Differences were considered significant when $P \leq 0.05$. All statistical analysis was done using JMP Pro 13 (SAS Institute Inc., Cary, NC) software.

Results

Total lymphocyte infiltration into growing feathers of fully de-pigmented Smyth and pigmented Brown line chickens injected with feather-derived melanocytes

In fully de-pigmented growing feathers of Smyth chickens a significant interaction between time and test material effects on B cell infiltration was observed (Figure 1; $P = 0.0283$). Test material comparisons at each time point revealed differences in B cell levels between vehicle- and melanocyte-injected feathers at 2 days (3.7 ± 0.4 and 9.4 ± 2.3 % pulp cells, respectively; $P = 0.0277$) and 7 days (2.0 ± 0.3 and 7.0 ± 2.1 % pulp cells, respectively; $P = 0.0486$) post-injection.

In contrast, there was no significant interaction between time and test material effects in growing feathers from fully pigmented Brown line chickens (Figure 1). There was, however, an overall effect (i.e. independent of test material) of time on B cell infiltration ($P = 0.0153$). Specifically, overall B cell levels at 6 hours post-injection were lower than non-injected feathers ($P < 0.05$).

In Smyth chickens, there was also a significant interaction between time and test material effects on γδ T and αβ T cell infiltration (Figure 1; $P = 0.0214$ and 0.0086, respectively). Injection of feather-derived melanocytes resulted in infiltration of γδ T cells at 1 day (1.5 ± 0.2 % pulp cells) and 2 days (1.2 ± 0.2 % pulp cells) post-injection relative to vehicle-injected feathers (0.6 ± 0.2 and 0.4 ± 0.1 % pulp cells, respectively; $P < 0.05$). The dominant T cell population however were the αβ T cells which were elevated at 3 days (6.2 ± 0.9 % pulp cells), 4 days (6.0 ± 0.8 % pulp cells) and 6 days (7.3 ± 1.9 % pulp cells) post-injection relative to vehicle-injected feathers (3.3 ± 0.6, 3.2 ± 0.6 and 3.4 ± 1.1 % pulp cells, respectively; $P < 0.05$).

No significant effects of time, test material or their interaction on γδ T cell infiltration were observed in vehicle- or melanocyte-injected growing feathers of fully pigmented Brown line chickens (Figure 1). Furthermore, no significant interaction between time and test material effects were observed on αβ T cell infiltration, however a significant overall effect of time was observed on αβT cell infiltration independent of test material ($P = 0.0173$). In contrast to B cell infiltration, αβT cell levels did not differ significantly from non-injected feathers.

Infiltration of $CD4^+CD8\alpha^-$, $CD4^-CD8\alpha^+$ and $CD4^+CD8\alpha^+$ αβT cells into vehicle- and feather-derived melanocyte-injected growing feathers

A significant interaction between time and test material effects was observed on $CD4^+CD8\alpha^-$ and $CD4^+CD8\alpha^+$ αβT cell infiltration into injected feathers of Smyth chickens (Figure 2; $P = 0.0083$ and 0.0018, respectively). $CD4^+CD8\alpha^-$ αβT cells were elevated in melanocyte-injected feathers at 3 days (2.1 ± 0.5 % pulp cells), 4 days (2.2 ± 0.4 % pulp cells) and 6 days (2.2 ± 0.8 % pulp cells) post-injection relative to vehicle-injected feathers (0.7 ± 0.1, 0.7 ± 0.1 and 0.5 ± 0.2 % pulp cells, respectively; $P < 0.05$). Similarly, $CD4^+CD8\alpha^+$ αβT cells were elevated in melanocyte-injected feathers at 3 days (1.3 ± 0.3

% pulp cells), 4 days (1.4 ± 0.2 % pulp cells), 6 days (1.5 ± 0.4 % pulp cells) and 7 days (1.0 ± 0.2 % pulp cells) post-injection relative to vehicle-injected feathers (0.5 ± 0.2, 0.4 ± 0.1, 0.5 ± 0.2 and 0.2 ± 0.1 % pulp cells, respectively; $P < 0.05$). No significant effects of time, test material or their interaction on infiltration of $CD8\alpha^+$ αβT cells were observed (Figure 2).

No significant interaction between time and test material effects on $CD4^-CD8\alpha^+$ or $CD4^+CD8\alpha^+$ αβT cell infiltration were observed in fully pigmented feathers of Brown line chickens (Figure 2). However, an effect of time was observed on $CD4^-CD8\alpha^+$ and $CD4^+CD8\alpha^+$ αβT cells (Figure 2; $P = 0.0119$ and 0.0053, respectively). For $CD4^-CD8\alpha^+$ αβT cells no significant differences were observed relative to non-injected feathers, however $CD4^+CD8\alpha^+$ αβT cells were lower at 6 hours post-injection ($P < 0.05$). No significant effects of time, test material or their interaction on infiltration of $CD4^+CD8\alpha^-$ αβT cells were observed.

Infiltration of $CD4^+CD8\alpha^-CD25^+$, $CD4^-CD8\alpha^+CD25^+$ and $CD4^+CD8\alpha^+CD25^+$ cells into vehicle- and feather-derived melanocyte-injected growing feathers

A significant interaction between time and test material effects was observed on $CD4^+CD8\alpha^-CD25^+$ and $CD4^+CD8\alpha^+CD25^+$ cell infiltration in feathers of Smyth chickens (Figure 4; $P = 0.0190$ and 0.0.0465, respectively). $CD4^+CD8\alpha^-CD25^+$ cells were elevated in melanocyte-injected feathers at 1 day (0.7 ± 0.2 % pulp cells), 2 days (0.6 ± 0.1 % pulp cells) and 7 days (0.4 ± 0.1 % pulp cells) post-injection relative to vehicle-injected feathers (0.4 ± 0.1, 0.3 ± 0.1 and 0.3 ± 0.0 % pulp cells, respectively; $P < 0.05$). $CD4^+CD8\alpha^+$ αβT cells were elevated in melanocyte-injected feathers from days 1 through 5 post-injection (0.3 ± 0.2, 0.3 ± 0.1, 0.3 ± 0.1, 0.4 ± 0.1 and 0.3 ± 0.1 % pulp cells, respectively) relative to vehicle-injected feathers (0.0, 0.0, 0.0, 0.1 ± 0.0 and 0.0 % pulp cells, respectively; $P < 0.05$). An overall effect of time (i.e. independent of test material) on $CD4^-CD8\alpha^+CD25^+$ cell infiltration was also observed ($P = 0.0457$) with levels elevated at 1 and 2 days post-injection relative to non-injected feathers ($P < 0.05$).

No significant effects of time, test material or their interaction on infiltration of $CD4^{+}CD8\alpha^{-}CD25^{+}$, $CD4^{-}CD8\alpha^{+}CD25^{+}$ and $CD4^{+}CD8\alpha^{+}CD25^{+}$ cells were observed in fully pigmented feathers of Brown line chickens (Figure 3).

Alterations in the T cell repertoire in vehicle- and feather-derived melanocyte-injected growing feathers

No significant effects of time, test material or their interaction on the T cell repertoire were observed in melanocyte- or vehicle-injected growing feathers of completely de-pigmented Smyth or fully pigmented Brown line chickens (Figure 4).

Expression of recruitment and homing-related genes CCR7 and CCL19 in growing feathers of fully de-pigmented Smyth and pigmented Brown line chickens injected with feather-derived melanocytes

Post-injection, no significant interaction between time and test material effects on *CCR7* and *CCL19* expression was observed in growing feathers of fully de-pigmented Smyth chickens (Figure 5). However, injection of feather-derived melanocytes resulted in an overall increase in *CCR7* and *CCL19* expression compared to vehicle-injected feathers ($P = 0.0099$). Expression of *CCL19* at 6 hours post-injection relative to non-injected feathers was 3.3 ± 1.6 and 0.6 ± 0.1-fold for melanocyte- and vehicle-injected feathers, respectively. Expression of *CCR7* at 6 hours post-injection relative to non-injected feathers was 2.4 ± 1.7 and 0.9 ± 0.3-fold change for melanocyte- and vehicle-injected feathers, respectively. No significant effect of time on the expression of *CCL19* or *CCR7* was observed post-injection. Interestingly, expression of *CCR7* and *CCL19* actually fell below baseline in vehicle-injected feathers albeit not significantly.

Post-injection, no significant effects of time, treatment or their interaction on expression of *CCL19* or *CCR7* were observed in vehicle- or melanocyte-injected feathers from Brown line chickens (Figure 5).

Expression of IL2 and IL2R in vehicle- and feather-derived melanocyte-injected growing feathers

Post-injection, no significant interaction between time and test material effects on *IL2* or *IL2R* expression was observed in growing feathers of fully de-pigmented Smyth chickens (Figure 6). However, injection of feather-derived melanocytes resulted in an overall increase in *IL2* and *IL2R* expression

compared to vehicle-injected feathers (P = 0.0232 and 0.0106, respectively). Expression of *IL2* at 6 hours post-injection relative to non-injected feathers was 3.8 ± 2.0 and 0.9 ± 0.5-fold for melanocyte- and vehicle-injected feathers, respectively. Expression of *IL2R* at 6 hours post-injected relative to non-injected feathers was 2.3 ± 1.6 and 0.8 ± 0.2-fold for melanocyte- and vehicle-injected feathers, respectively. No significant effect of time was observed on expression of *IL2* or *IL2R* post-injection.

Post-injection, no significant effects of time, treatment or their interaction on expression of *IL2* or *IL2R* were observed in vehicle- or melanocyte-injected feathers from Brown line chickens (Figure 6).

Expression of IL21 and IL21R in vehicle- and feather-derived melanocyte-injected growing feathers

Post-injection, no significant interaction between time and test material effects on *IL2* or *IL2R* expression was observed in growing feathers of fully de-pigmented Smyth chickens (Figure 7) post-injection. However, injection of feather-derived melanocytes resulted in an overall increase in *IL21* and *IL21R* compared to vehicle-injected feathers (P = 0.0161 and 0.0179, respectively). Expression of *IL21* at 6 hours post-injection relative to non-injected feathers was 6.3 ± 3.5 and 0.8 ± 0.3-fold for melanocyte- and vehicle-injected feathers, respectively. Expression of *IL21R* at 6 hours post-injected relative to non-injected feathers was 1.6 ± 1.1 and 0.7 ± 0.1-fold for melanocyte- and vehicle-injected feathers, respectively. No significant effect of time was observed on expression of *IL21* or *IL21R* post-injection.

Post-injection, no significant interaction between time and test material effects on expression of *IL21* or *IL21R* was observed in growing feathers of fully pigmented Brown line chickens (Figure 7). However, an overall effect of time on the expression of *IL21R* was observed (P = 0.0294). Specifically, *IL21R* was upregulated on day 5 post-injection relative to day 1 post-injection samples (P = 0.0243). No significant effect of test material was observed for expression of *IL21R* post-injection. In addition, no significant effect of time or test material on expression of *IL21* was observed post-injection.

Expression cell-mediated immunity-related genes IFNG, FASLG and GZMA in vehicle- and feather-derived melanocyte-injected growing feathers

Post-injection, no significant interaction between time and test material effects on expression of *IFNG*, *FASLG* or *GZMA* was observed in growing feathers of fully de-pigmented Smyth chickens (Figure

8). Injection of feather-derived melanocytes resulted in an overall increase in *IFNG* expression compared to vehicle-injected feathers (P = 0.0333). Expression of *IFNG* at 6 hours post-injection relative to non-injected feathers was 6.3 ± 3.2 and 1.0 ± 0.3-fold for melanocyte- and vehicle-injected feathers, respectively. No significant effect of time on expression of *IFNG* was observed (P = 0.0632) post-injection. Expression of *FASLG* at 6 hours post-injection relative to non-injected feathers was 1.5 ± 0.7 and 0.8 ± 0.2-fold for melanocyte- and vehicle-injected feathers, respectively. Expression of *GZMA* at 6 hours post-injection relative to non-injected feathers was 1.8 ± 0.8 and 0.9 ± 0.2-fold for melanocyte- and vehicle-injected feathers, respectively. Post-injection, no significant effects of time or test material on the expression of *FASLG* or *GZMA*.

Post-injection, no significant interaction effect between time and test material was found on expression of *IFNG*, *FASLG* or *GZMA* in growing feathers of fully pigmented Brown line chickens (Figure 8). However, an overall effect of time on expression of *FASLG* independent of test material was observed (P = 0.0148). While expression never differed from non-injected feathers by more than 1.4-fold, significant rises of *FASLG* were seen at days 4 through 7 post-injection relative to day1 post-injection feathers (P < 0.05). No significant effects of time or test material on *GZMA* expression were observed in growing feathers of Brown line chickens post-injection.

Expression pro-inflammatory genes IL1B and IL18 in vehicle- and feather-derived melanocyte-injected growing feathers

Post-injection, no significant interaction effect between time and test material was found on expression of *IL1B* or *IL18* in growing feathers of fully de-pigmented Smyth chickens (Figure 9). However, overall effects of time and test material on expression of *IL1B* were observed (P = 0.0158 and <0.0001, respectively). Overall, melanocyte-injected feathers had significantly higher expression of *IL1B* relative to vehicle-injected feathers independent of time. Expression of IL1B at 6 hours post-injection relative to non-injected samples was 33.1 ± 29.6 and 5.3 ± 5.2-fold for melanocyte- and vehicle-injected feathers, respectively. Interestingly, *IL1B* was significantly lower overall (i.e. independent of test material) from days 3 through 7 post-injection relative to 6 hours post-injection feathers (P < 0.05).

Post-injection, no significant interaction effect between time and test material was found on expression of *IL1B* or *IL18* in growing feathers of fully pigmented Brown line chickens (Figure 9). However, an overall effect of time on the expression of *IL1B* was observed independent of test material. Similar to Smyth chickens, overall *IL1B* expression was down from days 2 to 7 post-injection relative to 6 hours post-injection samples ($P < 0.05$). No significant effects of time or test material on expression of *IL18* were observed post-injection.

Expression anti-inflammatory genes CTLA4, IL10 and TGFB1 in vehicle- and feather-derived melanocyte-injected growing feathers

Post-injection, no significant interaction between time and test material effects on expression of *CTLA4*, *IL10* or *TGFB1* were observed in growing feathers of fully de-pigmented Smyth chickens (Figure 10). Injection of feather-derived melanocytes resulted in an overall increase in *CTLA4* and *IL10* expression independent of time ($P = 0.0038$ and 0.0041, respectively). Relative to non-injected feathers, at 6 hours post-injection expression of *CTLA4* in melanocyte- and vehicle-injected feathers was 2.3 ± 1.4 and 0.4 ±0.5-fold, respectively. Additionally, at 6 hours post-injection expression of *IL10* in melanocyte- and vehicle-injected feathers was 10.5 ± 7.7 and 1.3 ±0.1-fold relative to non-injected feathers, respectively. No significant effects of time on expression of *CTLA4* or *IL10* were observed post-injection. Relative to non-injected feathers, at 6 hours post-injection expression of *TGFB1* in melanocyte- and vehicle-injected feathers was 1.4 ± 0.3 and 1.1 ±0.2-fold, respectively. No significant effects of time or test material on *TGFB1* expression were observed post-injection.

Post-injection, no significant interaction between time and test material effects on expression of *CTLA4*, *IL10* or *TGFB1* were observed in growing feathers of fully pigmented Brown line chickens (Figure 10). However, an overall effect of time on expression of *CTLA4* and *TGFB1* was observed ($P = 0.0082$ and 0.0312, respectively). Relative to 6 hours post-injection samples, overall *CTLA4* expression was elevated from days 2 through 7 post-injection ($P < 0.05$). In contrast, relative to 6 hours post-injection samples, overall expression of TGFB1 was decreased from days 1 through 7 post-injection ($P < 0.05$). No significant effects of time or test material on expression of *IL10* were observed post-injection.

Discussion

The Smyth chicken is a well-established model for autoimmune vitiligo. The unique benefit of an easily accessible target tissue (a growing feather) makes this an ideal model to continuously monitor the progression of the melanocyte-specific autoimmune response over time in a single individual. In addition, the growing feather can serve as a dermal test site to assess tissue and/or cellular responses to injected test materials over time (Erf and Ramachandran, 2016; Erf *et al.*, 2017; Sullivan and Erf, 2017). Current evidence suggests that growing feathers of vitiliginous Smyth chickens are completely devoid of melanocytes and thus of melanocyte-specific immune activity. However, given that vitiligo is thought to be driven by autoimmune targeting and elimination of melanocytes, it is reasonable to postulate that memory cells are generated during the primary response and thus re-exposure of de-pigmented Smyth chickens to melanocyte-specific antigen(s) will result in a rapid and intense memory response. In fact, Wang and Erf (2003) were the first to demonstrate a cell-mediated immunity, memory-like immune response to injected melanocyte lysates in the wattle of completely de-pigmented Smyth chickens.

Here, we have successfully applied the feather-injection system to develop a method to observe and characterize memory-like autoimmune responses in the target tissue of completely de-pigmented Smyth chickens. Melanocytes were re-introduced into the dermis of growing feathers (target tissue) of vitiliginous Smyth chickens via microinjection and responses were monitored over 7 days. Results obtained from melanocyte-injected feathers were compared to those obtained from vehicle-injected growing feathers which were used to account for the immune response generated from the injection itself. In addition, growing feathers of fully pigmented parental-control Brown line chickens, which presumably never experienced a primary melanocyte-specific autoimmune response, were injected in the same manner.

As described in Chapter 1, the primary melanocyte-specific response in growing feathers of Smyth chickens involves infiltration of both B and αβ T cells. In addition, evidence of melanocyte-specific cell-mediated and humoral immune responses are well documented in Smyth chickens (Lamont *et al.*, 1982; Austin *et al.*, 1992; Wang and Erf, 2003, 2004). Therefore a rapid rise in B and αβ T cells

would be expected in response to re-exposure to melanocyte-specific antigen(s) in vitiliginous Smyth chickens. In this study, we observed a sharp increase of B and total T cells (γδ and αβ) in melanocyte-injected growing feathers of vitiliginous Smyth chickens within 24 hours post-injection. Post-injection, levels of B and αβ T cells remained elevated while those of γδ T cells gradually returned to baseline. In contrast, with the exception of a transient rise in αβ T cells 5 days post-injection, levels of B and T cells remained unchanged in vehicle-injected feathers. Additionally, with the exception of a relatively small and transient increase of B cells in melanocyte-injected feathers 24 hours post-injection, levels of B and T cells remained unchanged in melanocyte- and vehicle-injected growing feathers of Brown line chickens.

The sharp rise in γδ T cells in response to melanocyte-injection in growing feathers of vitiliginous Smyth chickens was unexpected as they are not expected to play a role in vitiligo. In fact γδ T cell levels remain largely unchanged in growing feathers during vitiligo development (Erf *et al.*, 1995, Chapter 1). Here, rises in γδ T cells are likely a consequence of non-specific T cell recruitment into the tissue in response to melanocyte-injection in Smyth chickens. It is also worth noting that non-injected feathers from Smyth chickens had higher levels of B and αβ T cells than non-injected feathers from Brown line chickens – perhaps reflective of the presence of memory cells (both B and αβ T) generated during the primary melanocyte-specific immune response.

During the primary response, $CD4^{-}CD8\alpha^{+}$ and $CD4^{+}CD8\alpha^{+}$ cell levels in growing feathers of Smyth chickens gradually rise leading up to vitiligo onset and remain elevated post-onset. Levels of $CD4^{+}CD8\alpha^{-}$ cells were also elevated leading to visual onset, however, returned to baseline thereafter. In this study, levels of $CD4^{+}CD8\alpha^{-}$, $CD4^{-}CD8\alpha^{+}$ and $CD4^{+}CD8\alpha^{+}$ αβ T cells all demonstrated sharp rises 24 hours post-injection in melanocyte-injected growing feathers of vitiliginous Smyth chickens with levels remaining elevated for the duration of the study. Large fluctuations in baseline levels of $CD4^{-}CD8\alpha^{+}$ αβ T in vehicle-injected feathers of Smyth chickens likely cloud any statistically significant findings in melanocyte-injected feathers. However, when compared to responses in fully pigmented growing feathers of Brown line chickens (which were negligible) clear differences can be inferred. Furthermore, at 24 hours post-injection, a clear rise in $CD4^{-}CD8\alpha^{+}$ cells was observed in melanocyte-injected feathers of

Smyth chickens, in contrast to those in vehicle-injected feathers which fell relative to non-injected feathers. Lastly, while $CD4^+CD8\alpha^+$ αβ T cells accounted for a relatively minor proportion of lymphocytes in the primary response and while their function is unknown, their clear rise in response to melanocyte-injection in growing feathers of Smyth chickens clearly warrants further investigation.

For further insights into the make-up of the T cell infiltrate, we next examined the $CD4^-$ and $CD8\alpha^+$ compartments in the context of CD25 (IL2Rα) expression. Interleukin-2 receptor α is a component of the interleukin-2 high affinity receptor complex and is constitutively expressed on regulatory T cells and transiently expressed on recently-activated T cells. Additionally, although not expressed on resting memory cells, a re-encounter with antigen can induce the expression of CD25 (Kalia *et al.*, 2010; Khan *et al.*, 2015). Unlike total $CD4^+CD8\alpha^-$ and $CD4^-CD8\alpha^+$ αβ T cells levels which were elevated throughout the study, in melanocyte-injected growing feathers of Smyth chickens $CD4^+CD8\alpha^-$ $CD25^+$ and $CD4^-CD8\alpha^+$ $CD25^+$ cell levels reached a maximum 1 day post-injection and gradually declined thereafter – an indication of recent activation. It is worth noting that in contrast to total $CD4^-CD8\alpha^+$ αβ T cells there were no substantial fluctuations in vehicle-injected feathers of Smyth chickens and overall levels were well below those observed in melanocyte-injected feathers. Furthermore, virtually no changes were observed in $CD4^-CD8\alpha^+$ $CD25^+$ levels in melanocyte- or vehicle-injected growing feathers of Brown line chickens relative to non-injected feathers. Small variations were observed in $CD4^+CD8\alpha^-$ $CD25^+$ levels in Brown line chickens, however no obvious differences were observed between melanocyte- and vehicle-injected feathers. Curiously, CD25+ $CD4^+CD8\alpha^+$ cell levels in melanocyte-injected growing feathers of Smyth chickens closely mimicked the trend observed for total $CD4^+CD8\alpha^+$ αβ T cells further arguing for closer examination.

Collectively, results of lymphocyte infiltration studies suggest recent activation of T cells in melanocyte-injected growing feathers of completely de-pigmented Smyth chickens. Therefore, in order to gain insights into specific immunological activities taking place in response to melanocyte- or vehicle-injection, targeted gene expression analysis was performed on cDNA derived from growing feather samples. With the exception of *IL1B* and IL18, the same general trend of relative gene expression was

observed for all targets measured. In melanocyte-injected growing feathers of Smyth chickens, levels of *CCL19*, *CCR7*, *IL2*, *IL2R*, *IL21*, *IL21R*, *IFNG*, *FASLG*, *GZMA*, *IL18*, *CTLA4*, *IL10* and *TGFB1* were all elevated at 6 hours post-injection and remained as such throughout the study. In contrast, relative gene expression in vehicle-injected growing feathers of Smyth chickens remained largely stagnant. Additionally, gene expression profiles were nearly identical in melanocyte- and vehicle-injected growing feathers of Brown line chickens.

Increased expression of *IL1B* at 6 hours post-injection was observed in all treatment groups and is likely in response to the injection itself, which creates a wound in the tissue. However, levels in melanocyte-injected growing feathers of Smyth chickens were substantially higher relative to vehicle-injected feathers and melanocyte- and vehicle-injected feathers of Brown line chickens.

Collectively results of relative gene expression studies presented here represent strong evidence of active recruitment and homing (*CCL19* and *CCR7*), T cell activation (*IL2* and *IL2R*) and cell-mediated immune activity (*IFNG*, *FASLG* and *GZMA*) in melanocyte-injected feathers of completely de-pigmented Smyth chickens. Furthermore, while yet unexplained, elevated levels of *IL21*, *IL21R*, *CTLA4* and *IL10* mimic those seen in the primary response (Chapter 1). Taken together results of cell infiltration and gene expression studies suggest recent activation of melanocyte-specific, perhaps tissue-resident, T cells in melanocyte-injected growing feathers of completely de-pigmented Smyth chickens.

Here was have described, for the first time, the establishment of a method to assess and monitor melanocyte-specific autoimmune memory responses in the target tissue of completely de-pigmented Smyth chickens. Results from these studies not only provide a basis for characterization, but also a firm foundation for future studies examining the specificity of the response. For example, in the waddle, Wang and Erf observed a lack of a response to melanocyte lysates derived from melanocytes established from developing embryos. A repeat study utilizing embryo-derived melanocytes is warranted to confirm the specificity of the memory response to feather-derived melanocytes in the target tissue.

While Smyth and Brown line chickens carry the same MHC haplotype, thus allowing for the testing of immunological responses to biological material between lines, it is possible that Brown line

chickens are only responsive to Brown line-specific antigens. To test this hypothesis, a repeat study utilizing melanocytes established from Brown line chickens is necessary. Such an experiment would also test the ability of Smyth chickens to respond to a Brown-line specific antigen which would shed light on the nature of the autoantigen (i.e. common vs. unique).

Lastly, vitiligo patients often experience sporadic cycles of de- and re-pigmentation. Results presented here corroborate a recent report of tissue-resident memory T cells in the skin of vitiligo patients (Boniface *et al.*, 2018). Future studies should focus on confirmation of a memory T cell population in growing feathers of de-pigmented Smyth chickens – perhaps by looking at expression of interleukin-15 which has been demonstrated to be involved in memory T cell maintenance (Manjunath *et al.*, 2001; Weninger *et al.*, 2001). Moreover, an experiment where melanocytes were injected into Smyth chickens with "stable" vitiligo may shed light possible triggering mechanisms in partially de-pigmented individuals. Moreover, isolation of memory cells from melanocyte-injected feathers would provide an opportunity for deep characterization which may reveal possible therapeutic targets (Tsai *et al.*, 2010; Bhargava and Calabresi, 2015; Ehlers and Rigby, 2015).

References

Austin, L. M. *et al.* (1992) 'The detection of melanocyte autoantibodies in the Smyth chicken model for vitiligo.', *Clinical immunology and immunopathology*, 64(2), pp. 112–20. Available at: http://www.ncbi.nlm.nih.gov/pubmed/1643744.

Bhargava, P. and Calabresi, P. A. (2015) 'Novel therapies for memory cells in autoimmune diseases', *Clinical & Experimental Immunology*, 180(3), pp. 353–360. doi: 10.1111/cei.12602.

Boissy, R. E., Smyth, J. R. and Fite, K. V (1983) 'Progressive cytologic changes during the development of delayed feather amelanosis and associated choroidal defects in the DAM chicken line. A vitiligo model.', *The American journal of pathology*, 111(2), pp. 197–212. Available at: http://www.ncbi.nlm.nih.gov/pubmed/6846502.

Boniface, K. *et al.* (2018) 'Vitiligo Skin Is Imprinted with Resident Memory CD8 T Cells Expressing CXCR3.', *The Journal of investigative dermatology*, 138(2), pp. 355–364. doi: 10.1016/j.jid.2017.08.038.

Devarajan, P. and Chen, Z. (2013) 'Autoimmune effector memory T cells: the bad and the good', *Immunologic Research*, 57(1–3), pp. 12–22. doi: 10.1007/s12026-013-8448-1.

Ehlers, M. R. and Rigby, M. R. (2015) 'Targeting Memory T Cells in Type 1 Diabetes', *Current Diabetes Reports*. Springer US, 15(11), p. 84. doi: 10.1007/s11892-015-0659-5.

Erf, G. F. *et al.* (2001) 'Herpesvirus connection in the expression of autoimmune vitiligo in Smyth line chickens.', *Pigment cell research / sponsored by the European Society for Pigment Cell Research and the International Pigment Cell Society*, 14(1), pp. 40–46. doi: 10.1034/j.1600-0749.2001.140107.x.

Erf, G. F. *et al.* (2017) 'T lymphocytes dominate local leukocyte infiltration in response to intradermal injection of functionalized graphene-based nanomaterial', *Journal of Applied Toxicology*, 37(11), pp. 1317–1324. doi: 10.1002/jat.3492.

Erf, G. F. and Ramachandran, I. R. (2016) 'The growing feather as a dermal test site: Comparison of leukocyte profiles during the response to Mycobacterium butyricum in growing feathers, wattles, and wing webs', *Poultry Science*, 95(9), pp. 2011–2022. doi: 10.3382/ps/pew122.

Erf, G. F., Trejo-Skalli, A. V and Smyth, J. R. (1995) 'T cells in regenerating feathers of Smyth line chickens with vitiligo.', *Clinical immunology and immunopathology*, 76(2), pp. 120–6. Available at: http://www.ncbi.nlm.nih.gov/pubmed/7614730.

Ezzedine, K. *et al.* (2015) 'Vitiligo', *The Lancet*. Elsevier, 386(9988), pp. 74–84. doi: 10.1016/S0140-6736(14)60763-7.

Gorochov, G. *et al.* (1998) 'Perturbation of CD4+ and CD8+ T-cell repertoires during progression to AIDS and regulation of the CD4+ repertoire during antiviral therapy.', *Nature medicine*, 4(2), pp. 215–21. Available at: http://www.ncbi.nlm.nih.gov/pubmed/9461196 (Accessed: 31 May 2018).

Hamal, K. R. *et al.* (2010) 'Differential gene expression of proinflammatory chemokines and cytokines in lungs of ascites-resistant and -susceptible broiler chickens following intravenous cellulose microparticle injection.', *Veterinary immunology and immunopathology*, 133(2–4), pp. 250–5. doi: 10.1016/j.vetimm.2009.07.011.

Kaech, S. M. and Wherry, E. J. (2007) 'Heterogeneity and Cell-Fate Decisions in Effector and Memory CD8+ T Cell Differentiation during Viral Infection', *Immunity*. Cell Press, 27(3), pp. 393–405. doi: 10.1016/J.IMMUNI.2007.08.007.

Kaiser, P., Underwood, G. and Davison, F. (2003) 'Differential Cytokine Responses following Marek ' s Disease Virus Infection of Chickens Differing in Resistance to Marek ' s Disease', *Journal of virology*, 77(1), pp. 762–768. doi: 10.1128/JVI.77.1.762.

Kalia, V. *et al.* (2010) 'Prolonged Interleukin-2Rα Expression on Virus-Specific CD8+ T Cells Favors Terminal-Effector Differentiation In Vivo', *Immunity*, 32(1), pp. 91–103. doi: 10.1016/j.immuni.2009.11.010.

Khan, S. H. *et al.* (2015) 'The Timing of Stimulation and IL-2 Signaling Regulate Secondary CD8 T Cell Responses', *PLOS Pathogens*. Edited by C. A. Benedict, 11(10), p. e1005199. doi: 10.1371/journal.ppat.1005199.

Lamont, S. J., Boissy, R. E. and Smyth, J. R. J. (1982) 'Humoral immune response and expression of spontaneous postnatal amelanosis in DAM line chickens.', *Immunological communications*, 11(2), pp. 121–127.

Manjunath, N. *et al.* (2001) 'Effector differentiation is not prerequisite for generation of memory cytotoxic T lymphocytes.', *The Journal of clinical investigation*. American Society for Clinical Investigation, 108(6), pp. 871–8. doi: 10.1172/JCI13296.

Mantovani, S. *et al.* (2003) 'Molecular and functional bases of self-antigen recognition in long-term persistent melanocyte-specific CD8+T cells in one vitiligo patient', *Journal of Investigative Dermatology*. Elsevier Masson SAS, 121(2), pp. 308–314. doi: 10.1046/j.1523-1747.2003.12368.x.

Pfaffl, M. W. (2001) 'A new mathematical model for relative quantification in real-time RT-PCR', *Nucleic Acids Research*, 29(9), p. 45e–45. doi: 10.1093/nar/29.9.e45.

Le Poole, I. C. *et al.* (1993) 'Review of the etiopathomechanism of vitiligo: a convergence theory.', *Experimental dermatology*, 2(4), pp. 145–53. Available at: http://www.ncbi.nlm.nih.gov/pubmed/8162332.

Rothwell, L. *et al.* (2004) 'Cloning and Characterization of Chicken IL-10 and Its Role in the Immune Response to Eimeria maxima', *The Journal of Immunology*, 173(4), pp. 2675–2682. doi: 10.4049/jimmunol.173.4.2675.

Shi, F. and Erf, G. F. (2012) 'IFN-γ, IL-21, and IL-10 co-expression in evolving autoimmune vitiligo lesions of Smyth line chickens.', *The Journal of investigative dermatology*, 132(3 Pt 1), pp. 642–9. doi: 10.1038/jid.2011.377.

Sullivan, K. S. and Erf, G. F. (2017) 'CD4+ T cells dominate the leukocyte infiltration response initiated by intra-dermal injection of phytohemagglutinin into growing feathers in chickens', *Poultry Science*, 96(10), pp. 3574–3580. doi: 10.3382/ps/pex135.

Tsai, S. *et al.* (2010) 'Reversal of Autoimmunity by Boosting Memory-like Autoregulatory T Cells', *Immunity*, 32(4), pp. 568–580. doi: 10.1016/j.immuni.2010.03.015.

Wang, X. and Erf, G. F. (2003) 'Melanocyte-specific cell mediated immune response in vitiliginous Smyth line chickens', *Journal of Autoimmunity*, 21(2), pp. 149–160. doi: 10.1016/S0896-8411(03)00087-8.

Wang, X. and Erf, G. F. (2004) 'Apoptosis in feathers of Smyth line chickens with autoimmune vitiligo', *Journal of Autoimmunity*, 22(1), pp. 21–30. doi: 10.1016/j.jaut.2003.09.006.

Weninger, W. *et al.* (2001) 'Migratory properties of naive, effector, and memory CD8(+) T cells.', *The Journal of experimental medicine*. Rockefeller University Press, 194(7), pp. 953–66. doi: 10.1084/JEM.194.7.953.

Woodland, D. L. and Kohlmeier, J. E. (2009) 'Migration, maintenance and recall of memory T cells in peripheral tissues', *Nature Reviews Immunology*. Nature Publishing Group, 9(3), pp. 153–161. doi: 10.1038/nri2496.

Table 1. **Target gene primer[1] and probe[2] sequences**

Target	Accession NO.	Primer/Probe	Sequence (5'-3')
28S[3]	X59733	Forward	GGCGAAGCCAGAGGAAACT
		Reverse	GACGACCGATTTGCACGTC
		Probe	AGGACCGCTACGGACCTCCACCA
CCL19[6]	NM_001302168.1	Forward	GCTGCGCCTCCGAGAGA
		Reverse	ACACTTCTGCAGAGCCTAATTGC
		Probe	CAGCTCTGCCAGGAAGGTCCCAAATC
CCR7[6]	NM_001198752.1	Forward	ACCATGGACGGCGGTAAA
		Reverse	ATGGTGGTGTTGGCGTCATA
		Probe	TGTGCTGGGAACAACGTCACCGAC
CTLA4[6]	NM_001040091.1	Forward	GGGTCACCGTGAGCTTTCTC
		Reverse	GCCTGTTGGCCAGTACTATTGC
		Probe	CGCAGCCACCGCCACTGC
FASLG[6]	NM_001031559.1	Forward	CCAGTGAAAAAGGAAGCAAGGA
		Reverse	GAGACAGGTTCCCACTCCAATG
		Probe	CAGCACACTTAACAGGAAACCCCACACAG
GZMA[6]	NM_204457.1	Forward	CAGCTGCTCATTGCAATCTGA
		Reverse	GGACAGTAGTCTGGGTAGCGAATT
		Probe	CAGAGTTATTCTTGGAGCCCATTCACGGAC
IFNG[3]	NM_205149.1	Forward	GTGAAGAAGGTGAAAGATATCATGGA
		Reverse	GCTTTGCGCTGGATTCTCA
		Probe	TGGCCAAGCTCCCGATGAACGA
IL1B[3]	NM_204524.1	Forward	GCTCTACATGTCGTGTGTGATGAG
		Reverse	TGTCGATGTCCCGCATGA
		Probe	CCACACTGCAGCTGGAGGAAGCC
IL2[6]	NM_204153.1	Forward	TCATCTCGAGCTCTACACACCAA
		Reverse	AGTAACCACTTCTCCCAGGTAACACT
		Probe	TGAGACCCAGGAGTGCACCCAGC
IL2RA[6] (CD25)	NM_204596.1	Forward	GCCAGCAAGACAAACCCAAA
		Reverse	GGCATACCGCAAAAACTTGAA
		Probe	CCCAGCACCTCCGAAGCAAGCA
IL10[4]	NM_001004414.2	Forward	CATGCTGCTGGGCCTGAA
		Reverse	CGTCTCCTTGATCTGCTTGATG
		Probe	CGACGATGCGGCGCTGTCA
IL18[6]	NM_204608.1	Forward	GGCAGTGGAATGTACTTCGACAT
		Reverse	ACCTGGACGCTGAATGCAA
		Probe	ACTGTTACAAAACCACCGCGCCTTCA
IL21[5]	NM_001024835.1	Forward	GTGGTGAAAGATAAGGATGTCGAA
		Reverse	TGCCATTCTGGAAGCAGGTT
		Probe	TGCTGCATACACCAGAAAACCCTGGG
IL21R[6]	NM_001030640.1	Forward	CAGTACTCCACGTGTCACGAAAA
		Reverse	TGGCACCCAGGTCATTCCT
		Probe	ACTATGTGCAGACCCTGTCGTGCCTCC
TGFB1[6]	NM_001318456.1	Forward	GGTTATATGGCCAACTTCTGCAT
		Reverse	CCCCGGGTTGTGTTGGT
		Probe	AGCGCCGACACGCAGTACACCA

[1] All oligos were synthesized by Eurofins Genomics, Louisville, KY

[2] Probes were labeled with FAM and TAMARA on the 5'- and 3'-ends, respectively

[3, 4, 5] Sequences from (Kaiser *et al.*, 2003; Rothwell *et al.*, 2004; Shi and Erf, 2012), respectively

[6] Primers and probes were designed using Primer Express 3.0 (Applied Biosystems, Foster City, CA.)

Table 2. **Primers[1] used for T cell receptor spectratyping**

Gene segment	Accession NO.	Primers	Sequence (5'-3')
TCR Variable-β_1	EF554743.1	Forward[2]	GTGGGACTAAGGAGAAATCC
	EF554744.1		
	EF554745.1		
	EF554746.1		
	EF554747.1		
	EF554748.1		
	EF554749.1		
	EF554750.1		
	EF554751.1		
	EF554752.1		
	EF554753.1		
	EF554754.1		
	EF554755.1		
	EF554756.1		
	EF554757.1		
	M81147.1		
	M37802.1		
	M37803.1		
	M37804.1		
	M37805.1		
TCR Variable-β_2	EF554759.1	Forward[3]	GCGATATTCACACCGGATAC
	EF554760.1		
	EF554761.1		
	EF554763.1		
	EF554764.1		
	EF554765.1		
	EF554768.1		
	EF554769.1		
	EF554772.1		
	EF554773.1		
	EF554774.1		
	EF554775.1		
	EF554776.1		
	EF554777.1		
	EF554778.1		
	EF554779.1		
	EF554780.1		
	EF554782.1		
	M37806.1		
	M81149.1		
	M81148.1		
	M81150.1		
	M81151.1		
TCR Constant-β	EF554742.1	Reverse	GATCAGGGAAGAAACCAGAG

[1] Oligos were synthesized by Applied Biosystems, Foster City, CA

[2] Contains a 5'-VIC label

[3] Contains a 5'-FAM label

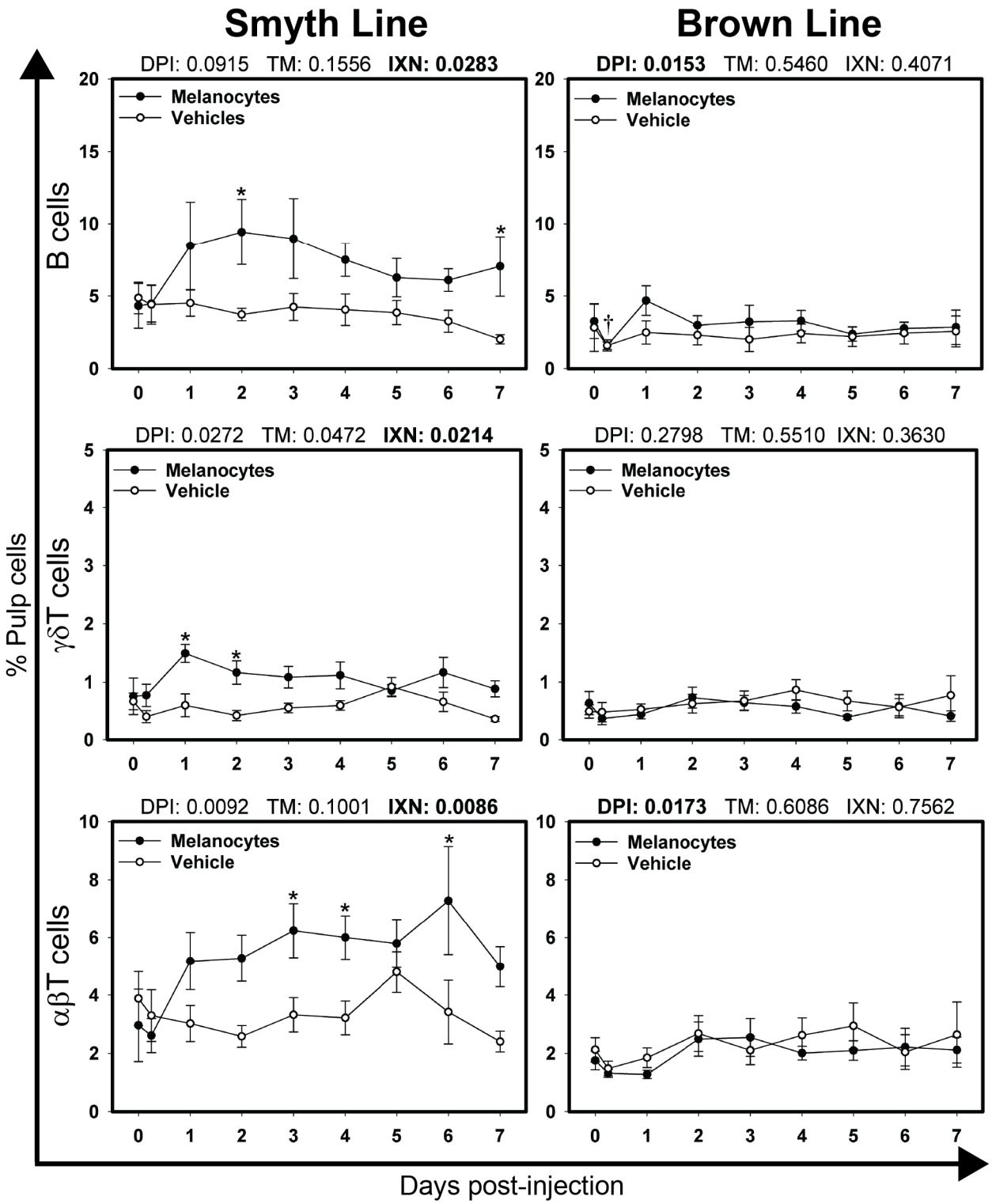
Smyth Line
Brown Line
DPI: 0.0915 TM: 0.1556 IXN: 0.0283
DPI: 0.0153 TM: 0.5460 IXN: 0.4071
DPI: 0.0272 TM: 0.0472 IXN: 0.0214
DPI: 0.2798 TM: 0.5510 IXN: 0.3630
DPI: 0.0092 TM: 0.1001 IXN: 0.0086
DPI: 0.0173 TM: 0.6086 IXN: 0.7562
Melanocytes
Vehicles
Vehicle
B cells
γδT cells
αβT cells
% Pulp cells
Days post-injection

Figure 1. **Lymphocyte infiltration profiles for feather-derived melanocyte- or vehicle-injected growing feathers from completely depigmented Smyth and fully pigmented parental-control Brown line chickens.** Eighteen day-old growing feathers on completely depigmented Smyth line and fully pigmented parental-control Brown line chickens were injected with either feather-derived melanocytes or vehicle (HBSS) (n=5 per treatment, per line). Non-injected feather samples were taken from each individual as a control (0 days post-injection). Injected feather samples were taken at 6 hours post-injection and daily thereafter for 7 days. Single-cell suspensions were prepared from feather samples and immunofluorescently-stained for B cells (Bu-1), γδT cells (TCR1) and αβT cells (TCR2 and TCR3 cocktail) using mouse monoclonal chicken-specific antibodies. Population analysis was performed by flow cytometry. A mixed effects regression model was used to determine the effects of time (days post-injection) and test material as well as their interaction on cell infiltration. Individual bird was defined as a random effect. When a significant time by test material interaction was found, post-hoc multiple means comparisons between vehicle- and melanocyte-injected samples were made at each time point using Student's t-test. In the absence of significant interactions, Student's t-test was used to test for differences between time points and test material. Differences were considered significant at $P < 0.05$ (*, † and ‡ for IXN, DPI and TM, respectively). Data are plotted as mean ± SEM; n = 5 chickens per time point.

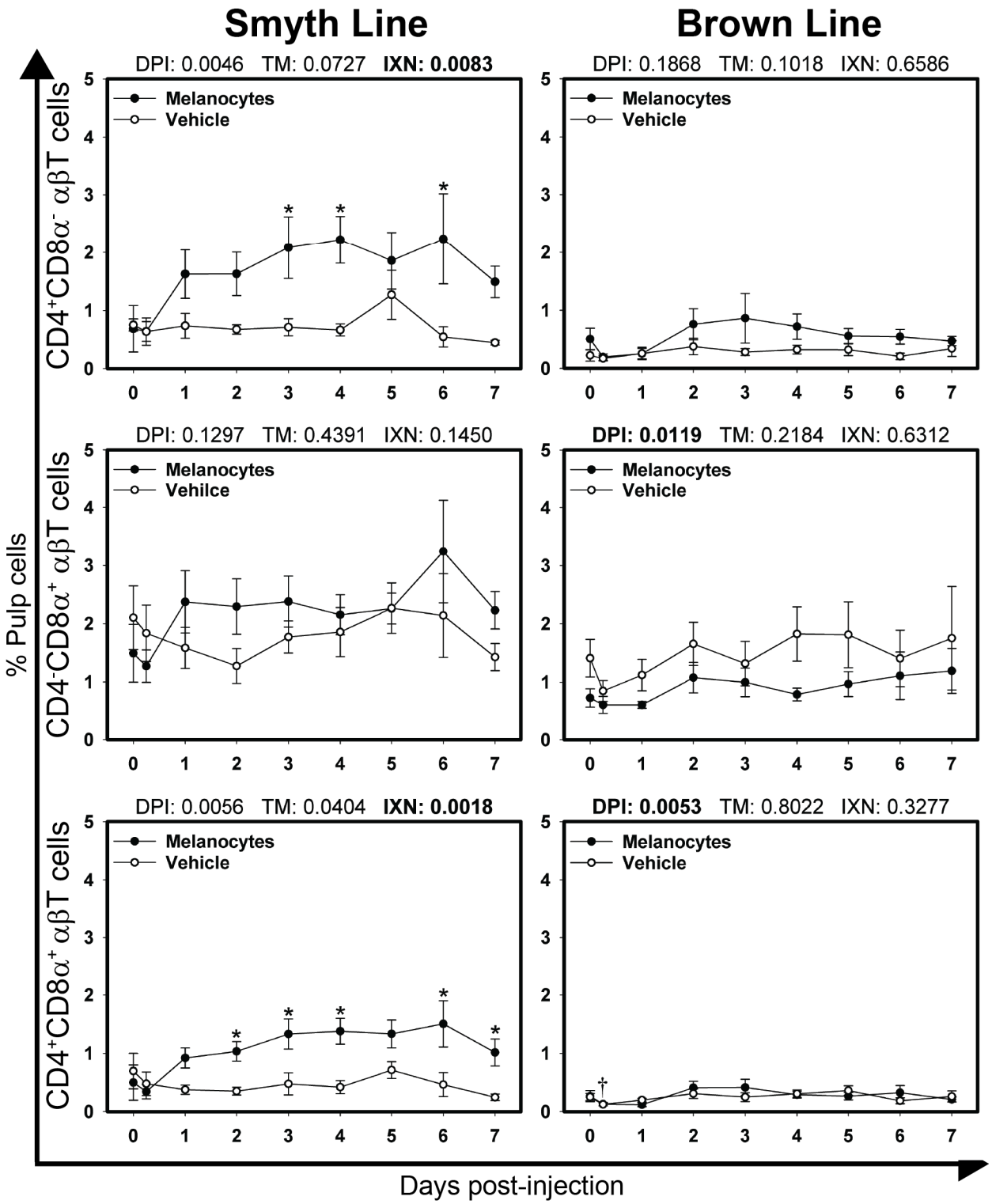
Smyth Line
Brown Line
DPI: 0.0046 TM: 0.0727 IXN: 0.0083
DPI: 0.1868 TM: 0.1018 IXN: 0.6586
DPI: 0.1297 TM: 0.4391 IXN: 0.1450
DPI: 0.0119 TM: 0.2184 IXN: 0.6312
DPI: 0.0056 TM: 0.0404 IXN: 0.0018
DPI: 0.0053 TM: 0.8022 IXN: 0.3277
Melanocytes
Vehicle
Vehilce
CD4+CD8α- αβT cells
CD4-CD8α+ αβT cells
CD4+CD8α+ αβT cells
% Pulp cells
Days post-injection

Figure 2. αβ**T cell subset infiltration profiles for feather-derived melanocyte- or vehicle-injected growing feathers from completely depigmented Smyth and fully pigmented parental-control Brown line chickens.** Eighteen day-old growing feathers on completely depigmented Smyth line and fully pigmented parental-control Brown line chickens were injected with either feather-derived melanocytes or vehicle (HBSS) (n=5 per treatment, per line). Non-injected feather samples were taken from each individual as a control (0 days post-injection). Injected feather samples were taken at 6 hours post-injection and daily thereafter for 7 days. Single-cell suspensions were prepared from feather samples and immunofluorescently-stained for total αβT cells (TCR2 and TCR3 cocktail), CD4 and CD8α using mouse monoclonal chicken-specific antibodies. Population analysis was performed by flow cytometry. A mixed effects regression model was used to determine the effects of time (days post-injection) and test material as well as their interaction on cell infiltration. Individual bird was defined as a random effect. When a significant time by test material interaction was found, post-hoc multiple means comparisons between vehicle- and melanocyte-injected samples were made at each time point using Student's t-test. In the absence of significant interactions, Student's t-test was used to test for differences between time points and test material. Differences were considered significant at $P < 0.05$ (*, † and ‡ for IXN, DPI and TM, respectively). Data are plotted as mean ± SEM; n = 5 chickens per time point.

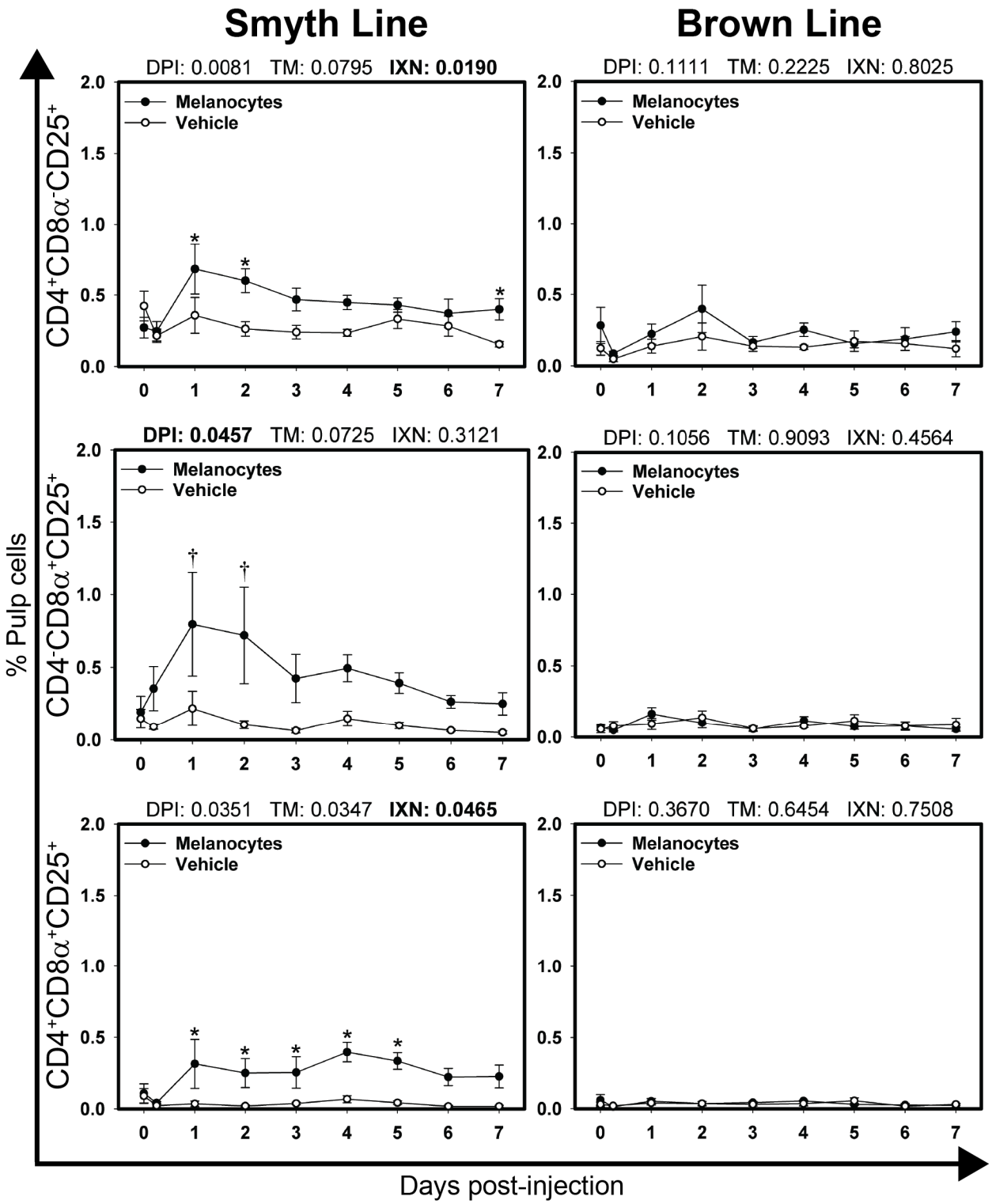
Smyth Line
Brown Line
DPI: 0.0081 TM: 0.0795 IXN: 0.0190
DPI: 0.1111 TM: 0.2225 IXN: 0.8025
DPI: 0.0457 TM: 0.0725 IXN: 0.3121
DPI: 0.1056 TM: 0.9093 IXN: 0.4564
DPI: 0.0351 TM: 0.0347 IXN: 0.0465
DPI: 0.3670 TM: 0.6454 IXN: 0.7508
Melanocytes
Vehicle
CD4+CD8α-CD25+
CD4-CD8α+CD25+
CD4+CD8α+CD25+
% Pulp cells
Days post-injection

Figure 3. **CD25+ T cell subset infiltration profiles for feather-derived melanocyte- or vehicle-injected growing feathers from completely depigmented Smyth and fully pigmented parental-control Brown line chickens.** Eighteen day-old growing feathers on completely depigmented Smyth line and fully pigmented parental-control Brown line chickens were injected with either feather-derived melanocytes or vehicle (HBSS)(n=5 per treatment, per line). Non-injected feather samples were taken from each individual as a control (0 days post-injection). Injected feather samples were taken at 6 hours post-injection and daily thereafter for 7 days. Single-cell suspensions were prepared from feather samples and immunofluorescently-stained for CD25, CD4 and CD8α using chicken-specific antibodies. Population analysis was performed by flow cytometry. A mixed effects regression model was used to determine the effects of time (days post-injection) and test material as well as their interaction on cell infiltration. Individual bird was defined as a random effect. When a significant time by test material interaction was found, post-hoc multiple means comparisons between vehicle- and melanocyte-injected samples were made at each time point using Student's t-test. In the absence of significant interactions, Student's t-test was used to test for differences between time points and test material. Differences were considered significant at $P < 0.05$ (*, † and ‡ for IXN, DPI and TM, respectively). Data are plotted as mean ± SEM; n = 5 chickens per time point.

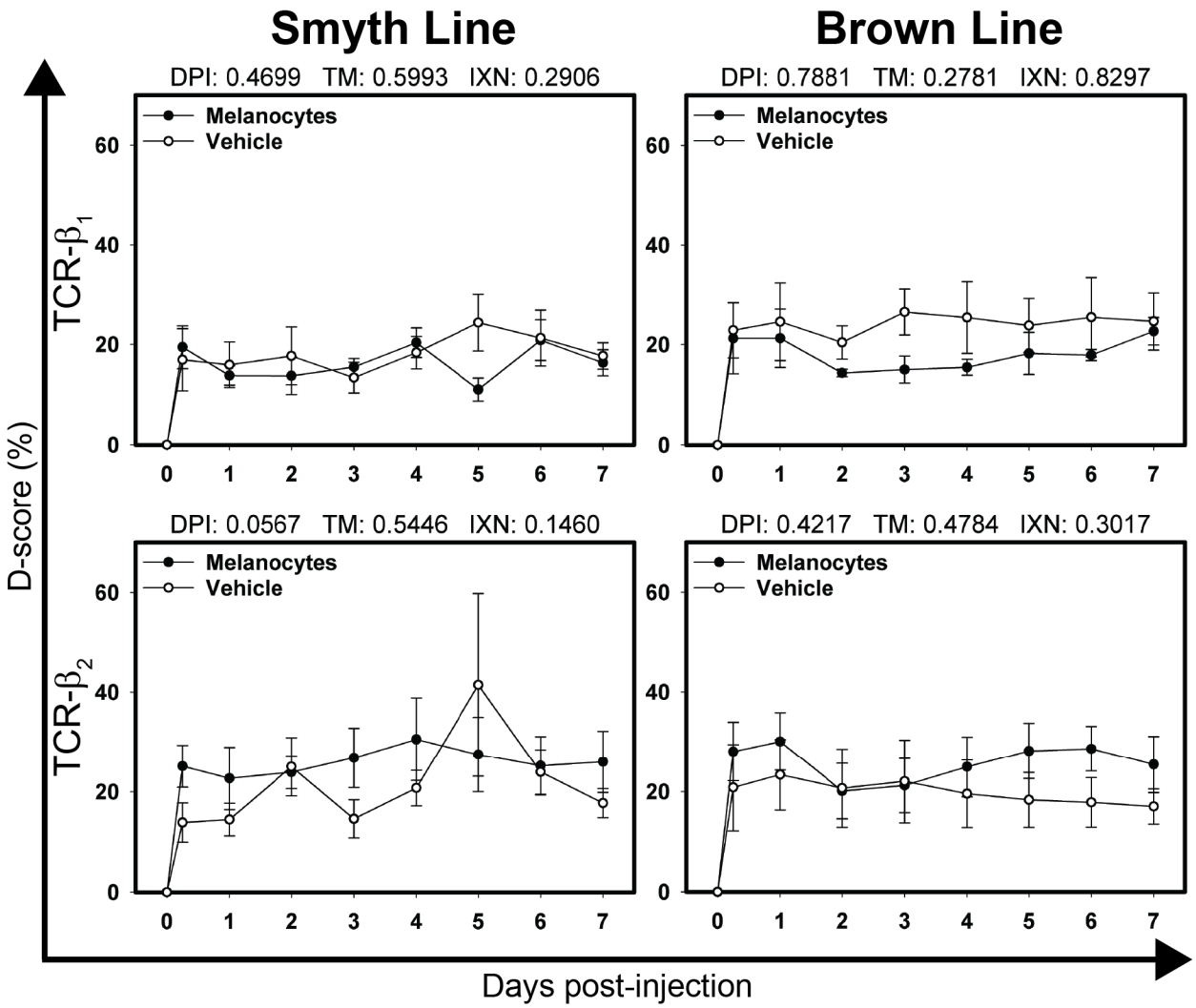
Smyth Line
Brown Line
DPI: 0.4699 TM: 0.5993 IXN: 0.2906
DPI: 0.7881 TM: 0.2781 IXN: 0.8297
DPI: 0.0567 TM: 0.5446 IXN: 0.1460
DPI: 0.4217 TM: 0.4784 IXN: 0.3017
Melanocytes
Vehicle
TCR-β1
TCR-β2
D-score (%)
Days post-injection
0
20
40
60
0 1 2 3 4 5 6 7

Figure 4. **Alterations in the T cell receptor repertoire in growing feathers from completely depigmented Smyth and fully pigmented parental-control Brown line chickens injected with either feather-derived melanocytes or vehicle.** Eighteen day-old growing feathers on completely depigmented Smyth line and fully pigmented parental-control Brown line chickens were injected with either feather-derived melanocytes or vehicle (HBSS). Non-injected feather samples were taken from each individual as a control (0 days post-injection). Injected feather samples were taken at 6 hours post-injection and daily thereafter for 7 days. Complementarity-determining 3-containing regions of the T cell receptor-variable β_1 (TCR-β_1) and -variable β_2 (TCR-β_2) genes were amplified from cDNA derived from growing feather samples by end-point PCR using fluorescently-labeled forward primers specific to conserved 5' regions of variable (V) gene segments and an unlabeled reverse primer specific to conserved 3' constant regions shared by the two genes. The resulting fluorescently-labeled products were size-separated by capillary electrophoresis and the quantities of each group of alleles estimated based on fluorescence intensity. Quantification profiles for each sample was converted to a frequency distribution and the Hamming-distance (D-score) was calculated by summing the absolute difference of each allele group relative to a reference sample and then dividing by 2. A mixed effects regression model was used to determine the effects of time (days post-injection) and test material as well as their interaction on D-scores. Individual bird was defined as a random effect. When a significant time by test material interaction was found, post-hoc multiple means comparisons between vehicle- and melanocyte-injected samples were made at each time point using Student's t-test. In the absence of significant interactions, Student's t-test was used to test for differences between time points and test material. Differences were considered significant at $P < 0.05$ (*, † and ‡ for IXN, DPI and TM, respectively). Data are plotted as mean ± SEM; n = 5 chickens per time point.

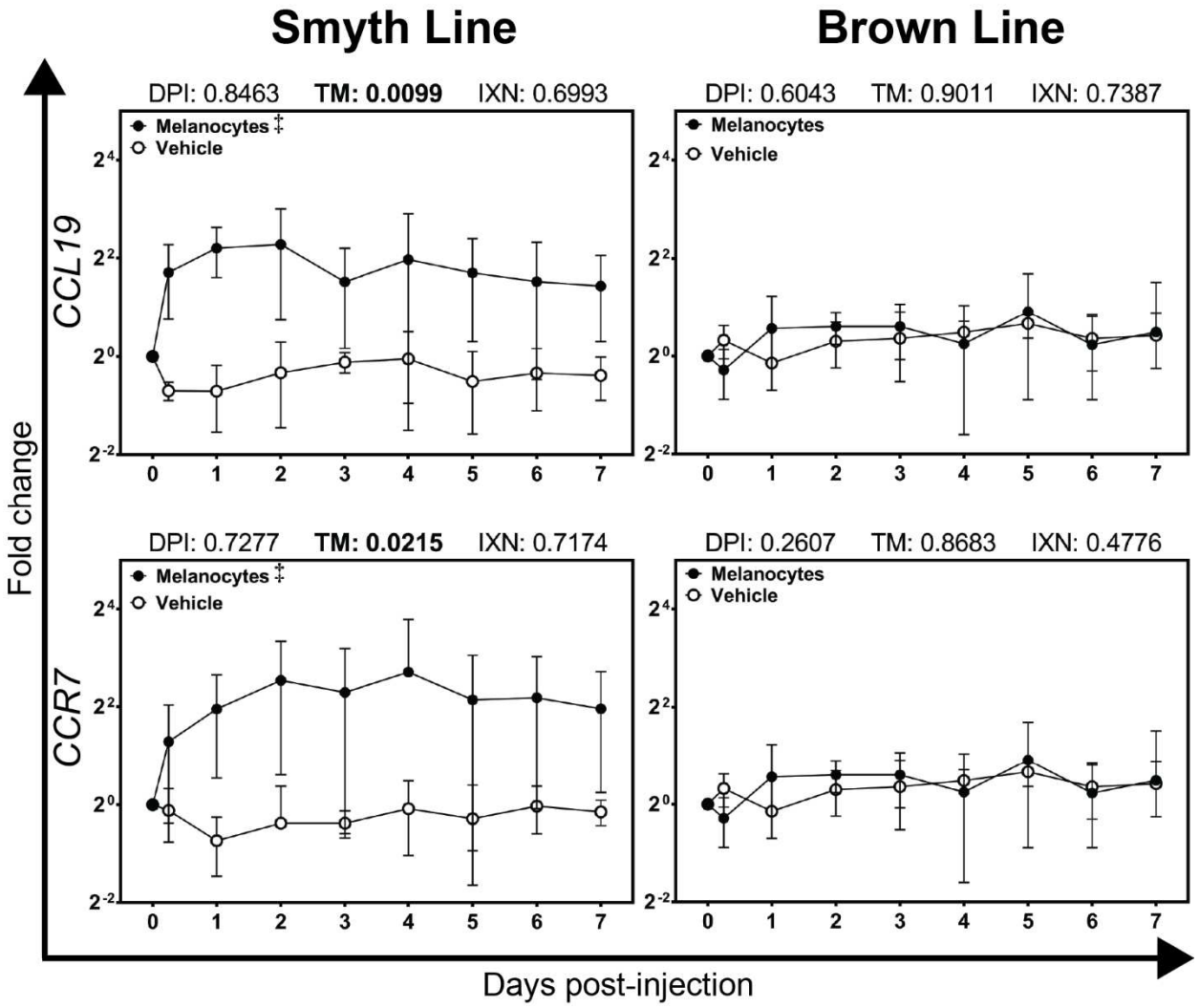
Smyth Line
Brown Line
DPI: 0.8463
TM: 0.0099
IXN: 0.6993
DPI: 0.6043
TM: 0.9011
IXN: 0.7387
DPI: 0.7277
TM: 0.0215
IXN: 0.7174
DPI: 0.2607
TM: 0.8683
IXN: 0.4776
Melanocytes ‡
Melanocytes
Vehicle
CCL19
CCR7
Fold change
Days post-injection

Figure 5. **Gene expression profiles of *CCL19* and *CCR7* in growing feathers of completely depigmented Smyth and fully pigmented Brown line chickens injected with either feather-derived melanocytes or vehicle.** Eighteen day-old growing feathers on completely depigmented Smyth line and fully pigmented parental-control Brown line chickens were injected with either feather-derived melanocytes or vehicle (HBSS). Non-injected feather samples were taken from each individual as a control (0 days post-injection). Injected feathers were sampled at 6 hours post-injection and daily thereafter for 7 days. RNA and cDNA from feather samples were analyzed for relative gene expression of *CCL19* and *CCR7*. Relative gene expression was determined by the efficiency-calibrated ΔCt method (Pfaffl, 2001) and is expressed as fold change relative to non-injected feathers. Gene expression profiles were first obtained for individual chickens, using individual-specific non-injected samples as calibrators and 28S as a reference gene. The overall effects of time and test material as well as their interaction was determined using a mixed effects regression model setting time and test material as fixed effects and individual bird as a random effect. When significant interaction between time and test material effects were observed, comparisons between melanocyte- and vehicle-injected samples were made at each individual time point using Student's t-test. When a significant overall effect of time was observed (i.e. independent of test material), individual time points were compared using Student's t-test. When a significant overall effect of test material was observed (i.e. independent of time), comparisons were made using Student's t-test. Differences were considered significant at $P < 0.05$ (*, † and ‡ for IXN, DPI and TM, respectively). Data are plotted as mean ± SEM; n = 5 chickens per time point.

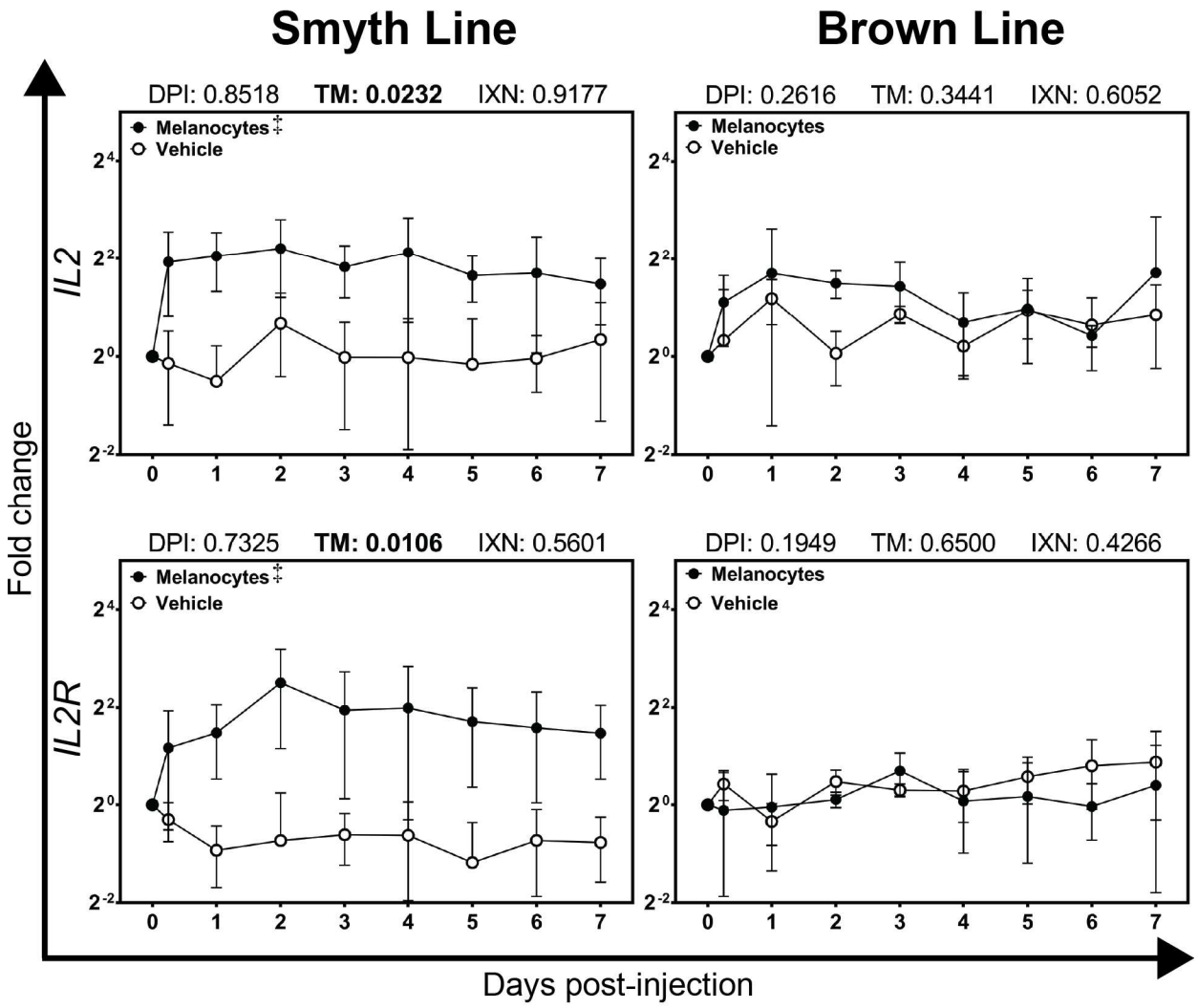
Smyth Line
Brown Line
DPI: 0.8518
TM: 0.0232
IXN: 0.9177
DPI: 0.2616
TM: 0.3441
IXN: 0.6052
DPI: 0.7325
TM: 0.0106
IXN: 0.5601
DPI: 0.1949
TM: 0.6500
IXN: 0.4266
Melanocytes ‡
Melanocytes
Vehicle
IL2
IL2R
Fold change
Days post-injection

Figure 6. **Gene expression profiles of *IL2* and *IL2R* in growing feathers of completely depigmented Smyth and fully pigmented Brown line chickens injected with either feather-derived melanocytes or vehicle.** Eighteen day-old growing feathers on completely depigmented Smyth line and fully pigmented parental-control Brown line chickens were injected with either feather-derived melanocytes or vehicle (HBSS). Non-injected feather samples were taken from each individual as a control (0 days post-injection). Injected feathers were sampled at 6 hours post-injection and daily thereafter for 7 days. RNA and cDNA from feather samples were analyzed for relative gene expression of *IL2* and *IL2R*. Relative gene expression was determined by the efficiency-calibrated ΔCt method (Pfaffl, 2001) and is expressed as fold change relative to non-injected feathers. Gene expression profiles were first obtained for individual chickens, using individual-specific non-injected samples as calibrators and 28S as a reference gene. The overall effects of time and test material as well as their interaction was determined using a mixed effects regression model setting time and test material as fixed effects and individual bird as a random effect. When significant interaction between time and test material effects were observed, comparisons between melanocyte- and vehicle-injected samples were made at each individual time point using Student's t-test. When a significant overall effect of time was observed (i.e. independent of test material), individual time points were compared using Student's t-test. When a significant overall effect of test material was observed (i.e. independent of time), comparisons were made using Student's t-test. Differences were considered significant at $P < 0.05$ (*, † and ‡ for IXN, DPI and TM, respectively). Data are plotted as mean ± SEM; n = 5 chickens per time point.

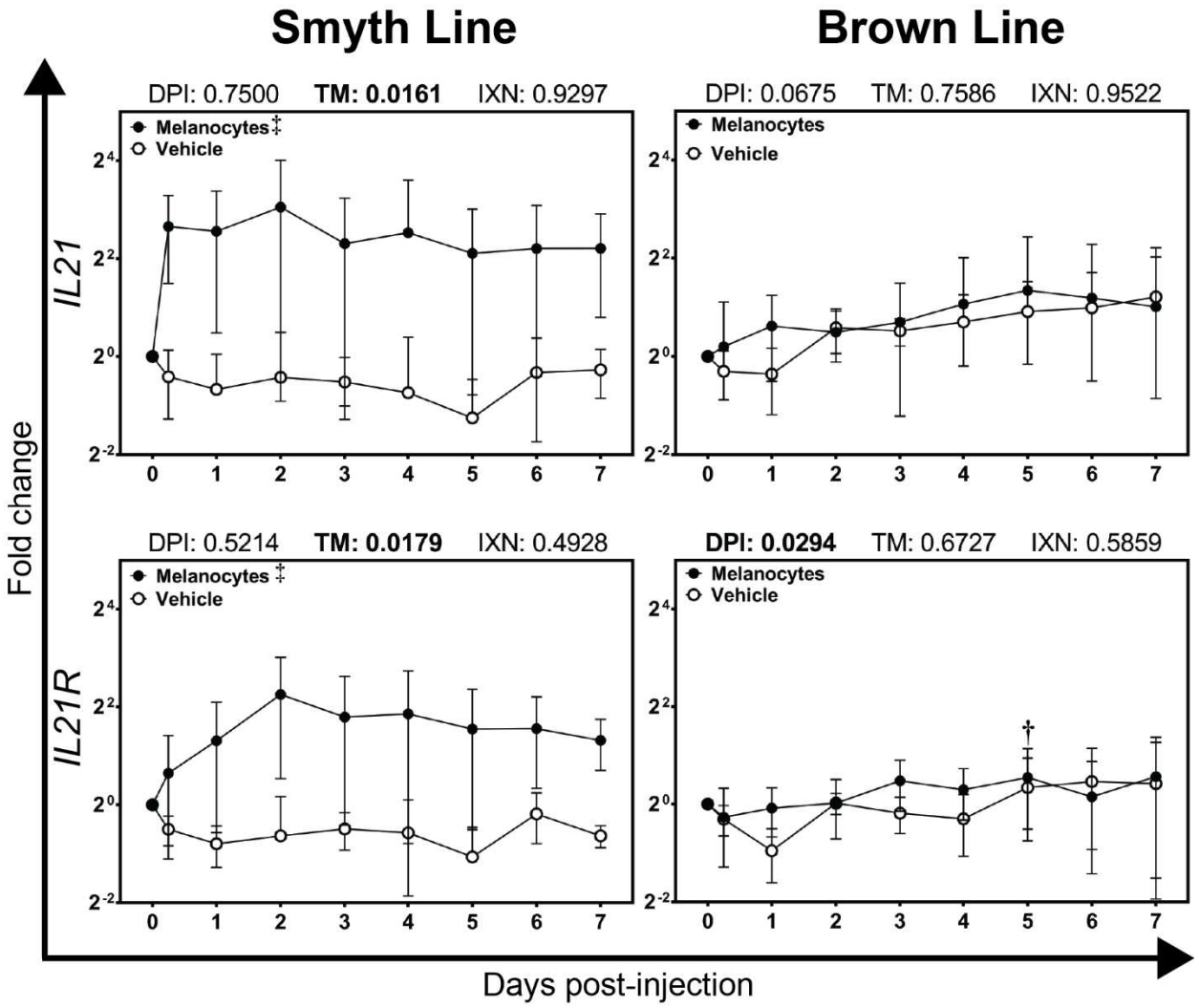
Smyth Line
Brown Line
DPI: 0.7500 TM: 0.0161 IXN: 0.9297
DPI: 0.0675 TM: 0.7586 IXN: 0.9522
DPI: 0.5214 TM: 0.0179 IXN: 0.4928
DPI: 0.0294 TM: 0.6727 IXN: 0.5859
Melanocytes
Vehicle
IL21
IL21R
Fold change
Days post-injection

Figure 7. **Gene expression profiles of *IL21* and *IL21R* in growing feathers of completely depigmented Smyth and fully pigmented Brown line chickens injected with either feather-derived melanocytes or vehicle.** Eighteen day-old growing feathers on completely depigmented Smyth line and fully pigmented parental-control Brown line chickens were injected with either feather-derived melanocytes or vehicle (HBSS). Non-injected feather samples were taken from each individual as a control (0 days post-injection). Injected feathers were sampled at 6 hours post-injection and daily thereafter for 7 days. RNA and cDNA from feather samples were analyzed for relative gene expression of *IL21* and *IL21R*. Relative gene expression was determined by the efficiency-calibrated ΔCt method (Pfaffl, 2001) and is expressed as fold change relative to non-injected feathers. Gene expression profiles were first obtained for individual chickens, using individual-specific non-injected samples as calibrators and 28S as a reference gene. The overall effects of time and test material as well as their interaction was determined using a mixed effects regression model setting time and test material as fixed effects and individual bird as a random effect. When significant interaction between time and test material effects were observed, comparisons between melanocyte- and vehicle-injected samples were made at each individual time point using Student's t-test. When a significant overall effect of time was observed (i.e. independent of test material), individual time points were compared using Student's t-test. When a significant overall effect of test material was observed (i.e. independent of time), comparisons were made using Student's t-test. Differences were considered significant at $P < 0.05$ (*, † and ‡ for IXN, DPI and TM, respectively). Data are plotted as mean ± SEM; n = 5 chickens per time point.

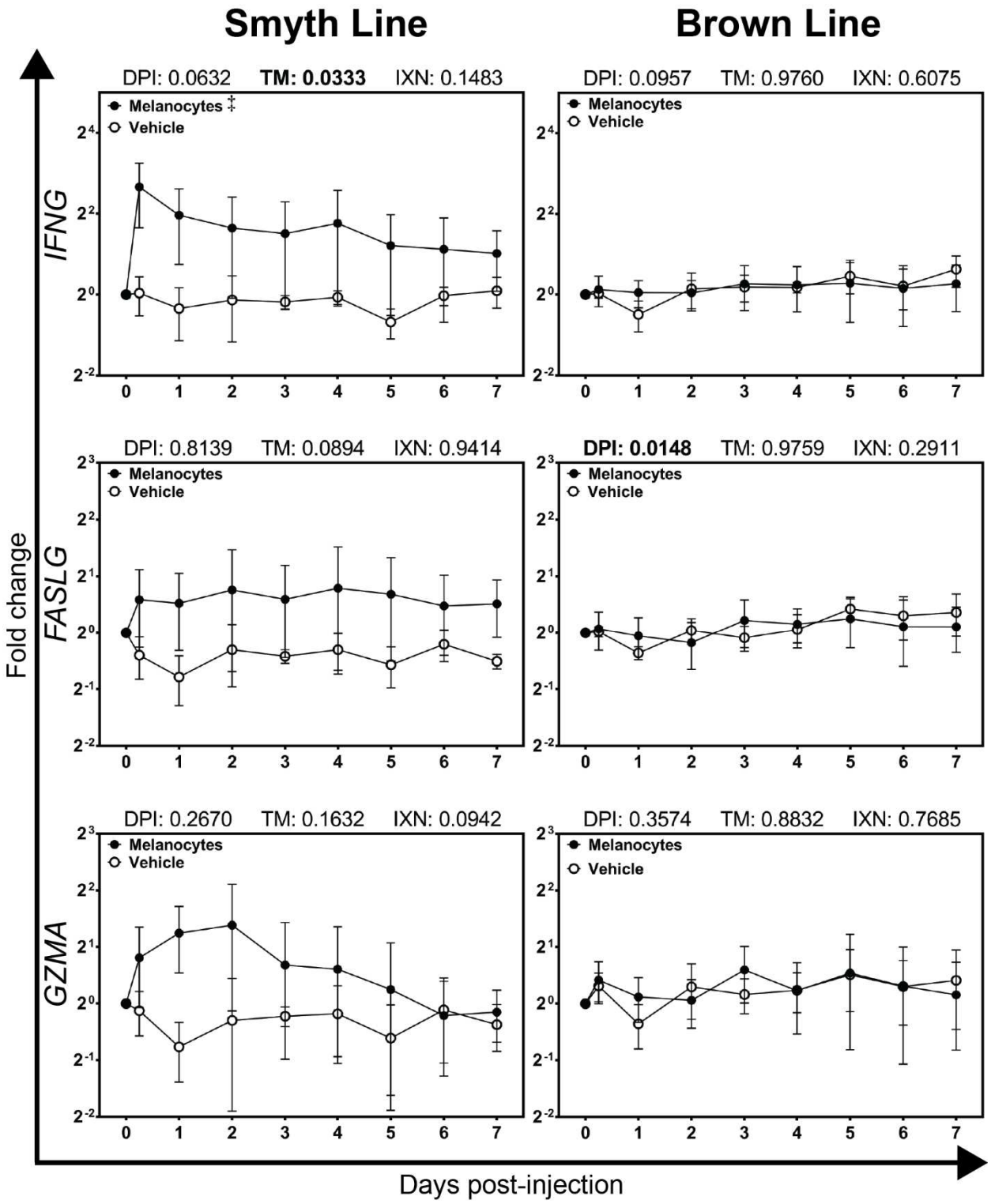
Smyth Line
Brown Line
DPI: 0.0632
TM: 0.0333
IXN: 0.1483
DPI: 0.0957
TM: 0.9760
IXN: 0.6075
DPI: 0.8139
TM: 0.0894
IXN: 0.9414
DPI: 0.0148
TM: 0.9759
IXN: 0.2911
DPI: 0.2670
TM: 0.1632
IXN: 0.0942
DPI: 0.3574
TM: 0.8832
IXN: 0.7685
Melanocytes
Vehicle
IFNG
FASLG
GZMA
Fold change
Days post-injection

Figure 8. **Gene expression profiles of *IFNG*, *FASLG* and *GZMA* in growing feathers of completely depigmented Smyth and fully pigmented Brown line chickens injected with either feather-derived melanocytes or vehicle.** Eighteen day-old growing feathers on completely depigmented Smyth line and fully pigmented parental-control Brown line chickens were injected with either feather-derived melanocytes or vehicle (HBSS). Non-injected feather samples were taken from each individual as a control (0 days post-injection). Injected feathers were sampled at 6 hours post-injection and daily thereafter for 7 days. RNA and cDNA from feather samples were analyzed for relative gene expression of *IFNG*, *FASLG* and *GZMA*. Relative gene expression was determined by the efficiency-calibrated ΔCt method (Pfaffl, 2001) and is expressed as fold change relative to non-injected feathers. Gene expression profiles were first obtained for individual chickens, using individual-specific non-injected samples as calibrators and 28S as a reference gene. The overall effects of time and test material as well as their interaction was determined using a mixed effects regression model setting time and test material as fixed effects and individual bird as a random effect. When significant interaction between time and test material effects were observed, comparisons between melanocyte- and vehicle-injected samples were made at each individual time point using Student's t-test. When a significant overall effect of time was observed (i.e. independent of test material), individual time points were compared using Student's t-test. When a significant overall effect of test material was observed (i.e. independent of time), comparisons were made using Student's t-test. Differences were considered significant at $P < 0.05$ (*, † and ‡ for IXN, DPI and TM, respectively). Data are plotted as mean ± SEM; n = 5 chickens per time point.

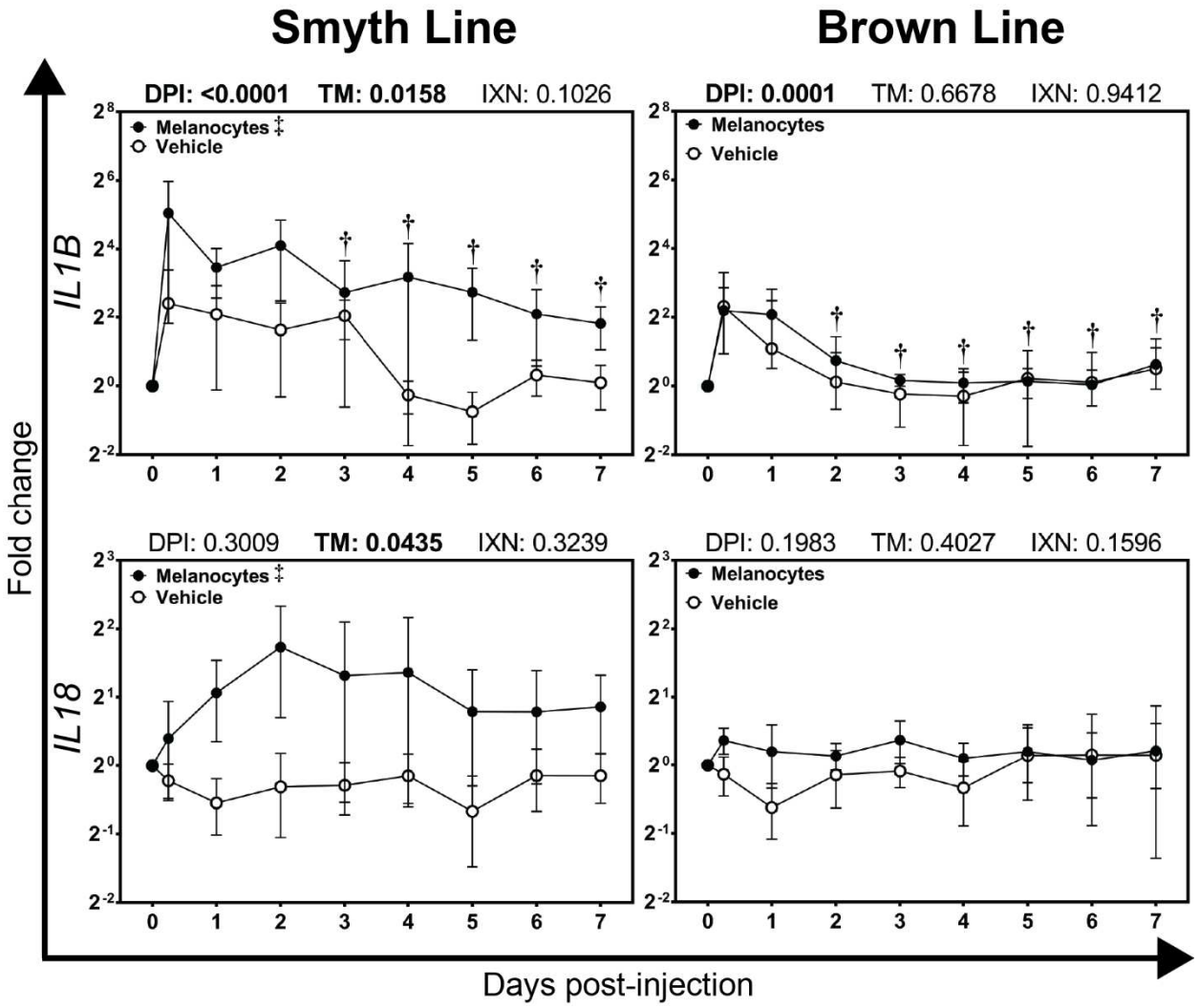
Smyth Line
Brown Line
DPI: <0.0001 TM: 0.0158 IXN: 0.1026
DPI: 0.0001 TM: 0.6678 IXN: 0.9412
DPI: 0.3009 TM: 0.0435 IXN: 0.3239
DPI: 0.1983 TM: 0.4027 IXN: 0.1596
Melanocytes ‡
Melanocytes
Vehicle
IL1B
IL18
Fold change
Days post-injection

Figure 9. **Gene expression profiles of *IL1B* and *IL18* in growing feathers of completely depigmented Smyth and fully pigmented Brown line chickens injected with either feather-derived melanocytes or vehicle.** Eighteen day-old growing feathers on completely depigmented Smyth line and fully pigmented parental-control Brown line chickens were injected with either feather-derived melanocytes or vehicle (HBSS). Non-injected feather samples were taken from each individual as a control (0 days post-injection). Injected feathers were sampled at 6 hours post-injection and daily thereafter for 7 days. RNA and cDNA from feather samples were analyzed for relative gene expression of *IL1B* and *IL18*. Relative gene expression was determined by the efficiency-calibrated ΔCt method (Pfaffl, 2001) and is expressed as fold change relative to non-injected feathers. Gene expression profiles were first obtained for individual chickens, using individual-specific non-injected samples as calibrators and 28S as a reference gene. The overall effects of time and test material as well as their interaction was determined using a mixed effects regression model setting time and test material as fixed effects and individual bird as a random effect. When significant interaction between time and test material effects were observed, comparisons between melanocyte- and vehicle-injected samples were made at each individual time point using Student's t-test. When a significant overall effect of time was observed (i.e. independent of test material), individual time points were compared using Student's t-test. When a significant overall effect of test material was observed (i.e. independent of time), comparisons were made using Student's t-test. Differences were considered significant at $P < 0.05$ (*, † and ‡ for IXN, DPI and TM, respectively). Data are plotted as mean ± SEM; n = 5 chickens per time point.

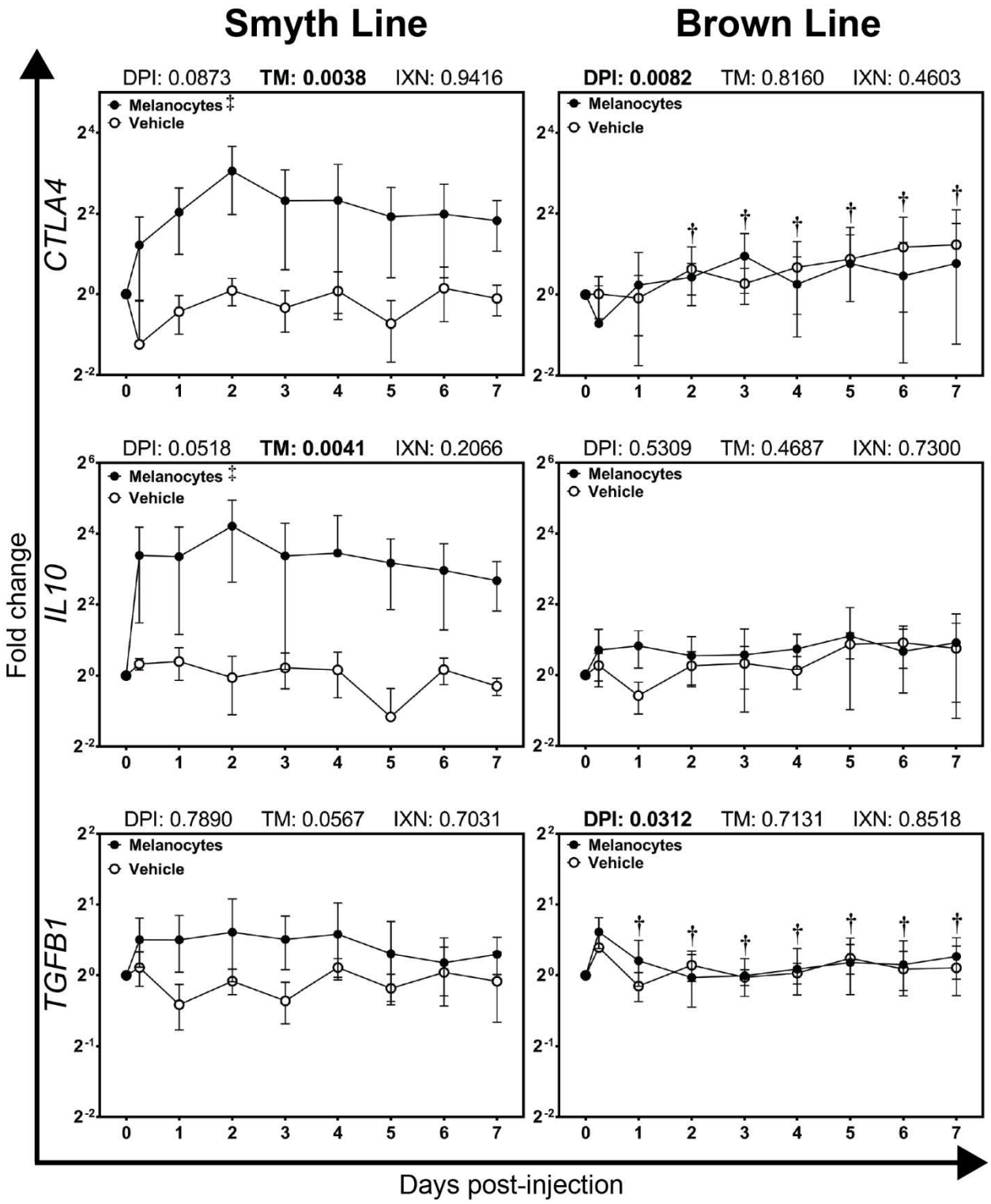
Smyth Line
Brown Line
DPI: 0.0873 TM: 0.0038 IXN: 0.9416
DPI: 0.0082 TM: 0.8160 IXN: 0.4603
DPI: 0.0518 TM: 0.0041 IXN: 0.2066
DPI: 0.5309 TM: 0.4687 IXN: 0.7300
DPI: 0.7890 TM: 0.0567 IXN: 0.7031
DPI: 0.0312 TM: 0.7131 IXN: 0.8518
Melanocytes
Vehicle
CTLA4
IL10
TGFB1
Fold change
Days post-injection

Figure 10. **Gene expression profiles of *CTLA4*, *IL10* and *TGFB1* in growing feathers of completely depigmented Smyth and fully pigmented Brown line chickens injected with either feather-derived melanocytes or vehicle.** Eighteen day-old growing feathers on completely depigmented Smyth line and fully pigmented parental-control Brown line chickens were injected with either feather-derived melanocytes or vehicle (HBSS). Non-injected feather samples were taken from each individual as a control (0 days post-injection). Injected feathers were sampled at 6 hours post-injection and daily thereafter for 7 days. RNA and cDNA from feather samples were analyzed for relative gene expression of *CTLA4*, *IL10* and *TGFB1*. Relative gene expression was determined by the efficiency-calibrated ΔCt method (Pfaffl, 2001) and is expressed as fold change relative to non-injected feathers. Gene expression profiles were first obtained for individual chickens, using individual-specific non-injected samples as calibrators and 28S as a reference gene. The overall effects of time and test material as well as their interaction was determined using a mixed effects regression model setting time and test material as fixed effects and individual bird as a random effect. When significant interaction between time and test material effects were observed, comparisons between melanocyte- and vehicle-injected samples were made at each individual time point using Student's t-test. When a significant overall effect of time was observed (i.e. independent of test material), individual time points were compared using Student's t-test. When a significant overall effect of test material was observed (i.e. independent of time), comparisons were made using Student's t-test. Differences were considered significant at $P < 0.05$ (*, † and ‡ for IXN, DPI and TM, respectively). Data are plotted as mean ± SEM; n = 5 chickens per time point.

Chapter III

Assessment of immunological activities of primary feather-derived melanocytes in response to acute oxidative stress

Introduction

Vitiligo is an acquired de-pigmentation disorder characterized by the loss of epidermal pigment-producing cells (melanocytes) in the skin resulting in the appearance of white patches. Onset of vitiligo is currently thought to involve a complex interaction of genetic, environmental and immunological factors (Le Poole, *et al.*, 1993; Ezzedine *et al.*, 2015). While a melanocyte-specific autoimmune pathology is a well-established factor in disease progression, triggering mechanisms remain a mystery.

Oxidative stress is considered a key component in triggering vitiligo (Laddha *et al.*, 2013). Accumulation of epidermal H_2O_2 in the millimolar range has been reported in the skin of patients with active vitiligo (Schallreuter *et al.*, 1999, 2001). Membrane lipoperoxidation of melanocytes from vitiligo patients has also been observed in conjunction with elevated production of reactive oxygen species (ROS) relative to normal controls (Dell'Anna *et al.*, 2007). Furthermore, melanocytes from vitiligo patients have a demonstrated diminished capacity to cope with oxidative stress (Maresca *et al.*, 1997; Manga *et al.*, 2006).

The Nrf2-ARE (nuclear factor E2-related factor 2; Nrf2-antioxidant response element) pathway has emerged as a major player in protecting melanocytes against damage induced by oxidative stress (Jian *et al.*, 2011; Arowojolu *et al.*, 2017; Jung *et al.*, 2017). Recent evidence of impaired activation of the Nrf2-ARE pathway in melanocytes from perilesional skin of vitiligo patients supports the notion of a diminished capacity to cope with oxidative stress in susceptible individuals. In humans, a functional immune system is required for progression of vitiligo (i.e. melanocyte dysfunction is not sufficient for disease expression). An immune-driven pathology in vitiligo is evidenced by use of immunosuppressive drugs is often prescribed either as a mono- or combination therapy in an attempt to halt progression of the disease and re-stimulate

pigmentation (Bae *et al.*, 2017; Kim *et al.*, 2018; Nguyen *et al.*, 2018). Unfortunately, the link between impaired anti-oxidant responses in vitiligo melanocytes and melanocyte-specific autoimmune targeting is a mystery. The expression of the inducible form of heat shock protein 70 (HSP70) in stressed melanocytes is suspected to play a role in initiating the immune response in vitiligo (Denman *et al.*, 2008; Mosenson *et al.*, 2012, 2013, 2014). Evidence of elevated HSP70 expression in perilesional vitiligo skin compared to normal skin has also been reported (Abdou *et al.*, 2013). Furthermore, while the expression of immunologically-relevant proteins (e.g. IL-6, CXCL8, MHC-II, CD40) has been observed in stressed melanocytes (Le Poole *et al.*, 1993; Lu *et al.*, 2002; Toosi *et al*., 2012; Yao *et al.*, 2012), their role in provoking the autoimmune response in vitiligo is unknown.

The vitiligo-prone Smyth chicken is an excellent model for vitiligo as it mimics all the characteristics of the human condition including a multifactorial etiology involving the complex interaction of genetic, environmental and immunological components. In addition, melanocyte cultures from growing feathers (a skin derivative and anatomical location of melanocytes in chickens) can be established prior to development of vitiligo. As in humans, melanocyte abnormalities have been observed in growing feathers of Smyth chickens including enlarged melanosomes and retracted dendrites (Boissy *et al.*, 1983; Boissy *et al.*, 1984). Furthermore, as in humans, the progression of vitiligo in Smyth chickens requires a functional immune system. This was demonstrated by the administration of corticosterone (an immunosuppressive steroid) which resulted in a significant reduction in vitiligo incidence compared to untreated controls (Boyle *et al.*, 1987).

The full Smyth Line model is composed of three lines of chicken: the vitiligo-prone Smyth chicken (incidence 80-95%), the vitiligo-susceptible, parental Brown line (incidence 0-

2%) and the vitiligo-resistant, distantly related Light Brown Leghorn line (incidence 0%). The inherent genetic susceptibility to autoimmune vitiligo was revealed by intra-abdominal injection with the DNA methylation inhibitor 5-azacytidine. When treated in this manner, the incidence of vitiligo in Brown line chickens was over 70% compared to 0% in vehicle-injected chickens. In contrast there was no change in the incidence (0%) of vitiligo in Light Brown Leghorn chickens (Sreekumar *et al*., 1996).

The purpose of the following study was to compare the response of primary melanocytes of age-matched vitiligo-prone Smyth-, vitiligo-susceptible Brown- and vitiligo-resistant Light Brown Leghorn-line chickens to oxidative stress induced by treatment with H_2O_2. Primary melanocyte cultures were established from growing feathers before the onset of vitiligo. Specifically, the effect of *in vitro* H_2O_2 exposure of melanocytes from each line on viability as well as the, surface expression of MHC-I and –II and the relative expression of genes involved in the antioxidant response, co-stimulation of T cell signaling and inflammation. Results from these studies will shed light on the immunological response of melanocytes in response to acute oxidative stress.

Materials and Methods

Experimental animals

All chickens used in this study were from the MHC-matched ($B^{101/101}$) Smyth-, Brown- and Light Brown Leghorn-line populations maintained by G. F. Erf at the Arkansas Experiment Station Poultry Farm in Fayetteville, AR. All chickens were vaccinated against Marek's disease with live herpesvirus of turkey (Fort Dodge Animal Health, Fort Dodge, IA) at 1-day post-hatch and kept on floor pens with wood shavings and free access to food and water at the Arkansas Agricultural Experiment Station Poultry Farm at the University of Arkansas, Division of

Agriculture, Fayetteville, AR. All studies were conducted with the approval of the University of Arkansas Institutional Animal Care and Use Committee (IACUC) as outlined in protocol 15015.

Melanocyte culture

Melanocyte cultures were established from growing feathers of 4-week old fully pigmented Smyth, Brown line and Light Brown Leghorn chickens according to Bowers *et al.* (1985) with modifications. Growing feathers from ten chickens (straight run) from each line were used. Growing feathers on the breast track were first saturated with 70% ethanol then trimmed leaving the column of pulp intact. Plucked feathers were promptly placed in Hank's Balanced Salt Solution (calcium and magnesium-free; HBSS; Gibco, Carlsbad, CA) supplemented with PSN solution (50U/mL penicillin, 50µg/mL streptomycin, 100 µg/mL neomycin; Sigma-Alrich, St. Louis, MO) and kept on ice until further processing. Under aseptic conditions, a longitudinal slit was made into the feather sheath and the pulp was removed from the sheath by holding the distal end with forceps and pulling the column of tissue towards the proximal end (the newest growth). The pulp tissue was then discarded. This procedure removes all of the pulp dermis and epidermis, except the newest growth of the epidermis, which is modified into barb ridges containing melanocytes and columns of keratinocytes (barbule cells). The remaining tissue containing the sheath and the epidermal barb ridges including the barb ridges (location of melanocytes) was trimmed down to the newest 3mm and placed sheath-up in 60mm x 15mm culture dishes (Corning, Corning, NY) with 3mL of culture medium. Culture medium components were as follows: Ham's F10 medium supplemented with 10% FBS, 2mM L-glutamine (Gibco, Carlsbad, CA), PSN solution, 40ng/mL cholera toxin from *Vibrio cholera*, 10ng/mLendothelin-3 (human, rat), 5µg/mL insulin from bovine pancreas and 85nM phorbol 12-myristate 13-acetate (PMA). All components with the exception of L-glutamine were purchased

from Sigma-Aldrich. Feather tissues from the same chicken were placed in the same dish to a maximum of three. Culture medium was replenished every other day and tissue sections were removed at the first sign of melanocyte growth. Passaging was carried out by incubation in HBSS for 3-5 minutes at 40°C, 5% CO_2 followed by washing and seeding in fresh culture medium. Cells were used between passages 2 – 4.

Cell viability assay

Melanocytes were seeded into flat-bottom 96-well plates at 10,000 cells and 100µL per well and incubated overnight at 40°C, 5% CO_2. Dilutions of H_2O_2 were prepared in endotoxin-free D-PBS (Sigma-Alrich). Cells were treated in triplicate with 10µL of H_2O_2 at various concentrations (1 mM – 0 mM) for 4 hours. Treatments were also added to a set of medium-only wells at the same concentration. After incubation the culture medium was removed, the cells were washed with 200µL HBSS and 100µL of PMA-free culture medium was added along with 10µL of MTT solution (5mg/mL 3-(4,5-Dimethyl-2-thiazolyl)-2,5-diphenyl-2H-tetrazolium bromide in endotoxin-free D-PBS). After a 1-3 hour incubation at 40°C, 5% CO_2, 85µL of the culture medium was removed and 50µL dimethyl sulfoxide (Sigma-Aldrich, St. Louis, MO) was added with gentle mixing. The mixture was placed at 40°C, 5% CO_2 for 10 minutes and then read at 540nm using a BioTek Synergy HT (Winooski, VT) plate reader. Background readings were calculated as the average OD of medium-only (including H_2O_2 treatments) and subtracted from treated cultures. Cell viability was determined by dividing the background-corrected OD by the average background-corrected OD of the non-treated wells (100%). Data are expressed as percent viability.

Flow cytometry analysis

Melanocytes were seeded into 24-well plates at 125,000 cells and 1.25mL per well and incubated overnight at 40°C, 5% CO_2. Dilutions of H_2O_2 were prepared in endotoxin-free D-PBS. Cells were treated with H_2O_2 at various concentrations for 4 hours. After incubation the culture medium was removed and cells were washed twice with 1 mL Hanks' Balanced Salt Solution (calcium and magnesium-free; HBSS; Gibco, Carlsbad, CA). Cells were harvested by incubation in HBSS for 3-5 minutes at 40° C, 5 % CO2. Detached cells were washed in D-PBS/1% BSA and seeded into wells of a round-bottom 96-well plate. Melanocytes were immunofluorescently stained using mouse monoclonal chicken-specific β_2-microglobulin (MHC-I) and MHC-II antibodies (SouthernBiotech, Birmingham AL). To control for non-specific binding and identify negative populations for gating, a pool of all samples was prepared and incubated with a cocktail of mouse IgG1 isotype-control antibodies (FITC and rPE). Pooled samples were also single-stained with anti-MHC-I-FITC and MHC-II-rPE in order to set compensation. Stained samples were acquired (10,000 events) on a BD Accuri™ C6 flow cytometer equipped with a 488nm laser. Data analysis was performed using FlowJo software (FlowJo, LLC, Ashland, OR). Forward- versus side-scatter dot plots were used to filter out debris and data were expressed as the percentage of all acquired events.

Relative gene expression analysis

Melanocytes were seeded into 24-well plates at 125,000 cells and 1.25mL per well and incubated overnight at 40°C, 5% CO_2. Dilutions of H_2O_2 were prepared in endotoxin-free D-PBS (). Cells were treated with H_2O_2 at various concentrations for 4 hours. After incubation the culture medium was removed and cells were washed with twice with 1 mL D-PBS. Cells were harvested in 300 µL TRI Reagent® (Zymo Research, Irvine, CA and total RNA was isolated

using the Direct-zol™ RNA Microprep kit (Zymo Research) with on-column DNase digestion according to the manufacturer's instructions. RNA was eluted in 10µL DEPC-treated molecular-grade water (VWR, Radnor, PA) and quantity and purity was assessed by absorbance at 260nm and 280nm on a BioTek Synergy HT (Winooski, VT). Five-hundred nanograms of RNA was reverse transcribed to cDNA in a 20µL sample volume (50ng/µL) using the High Capacity cDNA Reverse Transcription kit (Applied Biosystems, Foster City, CA) according to the manufacturer's instructions. Synthesized cDNA was diluted to 10ng/µL using DEPC-free molecular-grade water (VWR, Radnor, PA) and stored at -20°C until use.

Quantitative real-time PCR was performed as previously described using the TaqMan™ system with modifications (Hamal *et al.*, 2010). Target primer and probe sequences are listed in Table 1. All targeted gene expression assays were performed on a single plate in a 12µL sample volume using 20ng of cDNA and were run on an Applied Biosystems® 7500 Real-Time PCR System using manufacturer-programmed cycling conditions. Relative gene expression was determined by the efficiency-calibrated ΔCt method (Pfaffl, 2001) and is expressed as fold change relative to the calibrator sample. To obtain gene expression profiles for individual cultures, results were calculated using culture-specific non-treated samples as calibrators and 28S as a reference gene. To determine variation among non-treated samples relative gene expression was calculated using the average C_T of all non-treated LBL cDNA as a calibrator.

Statistical analysis

Due to the exponential nature of relative gene expression (fold change) and flow cytometry (geometric mean of fluorescence) data, a $\log_2$ transformation was performed to convert the data to a linear scale appropriate for statistical modeling. The effects of line and H_2O_2 treatment as well as their interaction was determined using a mixed-effects regression

model. Line and treatments were defined as fixed effects and individual cultures were defined as a random effect. In the event of significant interaction between line and treatment effects, multiple means comparisons were carried out using Student's t-test. In the absence of interaction multiple means comparisons were also carried out using Student's t-test. Differences were considered significant when $P \leq 0.05$. All statistical analysis was done using JMP Pro 13 (SAS Institute Inc., Cary, NC) software.

Results

Establishment of feather-derived melanocyte cultures

Of the 30 cultures established from growing feathers of fully pigmented Smyth, Brown line and Light Brown Leghorn line chickens: 6 Smyth, 5 Light Brown Leghorn and 4 Brown line cultures grew to sufficient quantity for experimentation.

H_2O_2-mediated cytotoxicity

No significant interaction between line or treatment effects on cell viability was observed in H_2O_2-treated feather-derived melanocyte cultures (Figure 1). In addition, no significant effect of line was observed. There was, however, an overall effect of H_2O_2-treatment on melanocyte viability ($P < 0.0001$). When treated with 125 μM H_2O_2, overall cell viability dropped to 90.7 ± 2.6% ($P < 0.05$). A doubling of H_2O_2 resulted in a further drop to 56.8 ± 4.1% ($P < 0.05$). Viability continued to decrease with each doubling of H_2O_2 reaching its lowest point at 1mM (1.0 ± 0.8%; $P < 0.05$).

Melanocyte expression of MHC-I and MHC-II in response to H_2O_2 treatment

No significant interaction between line or treatment effects on MHC-I expression was observed in H_2O_2-treated feather-derived melanocyte cultures (Figure 2, top). In addition, no significant effects of line or treatment were detected.

No significant interaction between line or treatment effects on MHC-II expression was observed in H_2O_2-treated feather-derived melanocyte cultures (Figure 2, bottom). In addition, no significant effect of line was observed. There was, however, an overall effect of H_2O_2-treatment on MHC-II expression (P = 0.0030). Overall the geometric mean of MHC-II staining increased from 470.5 ± 9.0 in non-treated controls to 544.5 ± 16.5 (P = 0.0084) and 574.6 ± 10.8 (P = 0.0013) in 100 μM and 200 μM H_2O_2-treated cells, respectively.

Relative expression of CAT, HMOX1 and HSP70 in H_2O_2-treated feather-derived melanocytes

A significant interaction between line and treatment effects on the relative expression of *CAT*, *HMOX1* and *HSP70* was observed in H_2O_2 treated feather-derived melanocytes (Figure 3; P = 0.0119, < 0.0001 and = 0.0008, respectively).

Levels of *CAT* in non-treated melanocytes established from feathers of Smyth, Brown line and Light Brown Leghorn line did not significantly differ (1.0 ± 0.1-, 1.4 ± 0.6- and 1.0 ± 0.1-fold, respectively). Minimal, yet statistically significant differential expression of *CAT* was observed Brown line melanocytes in response to 100 μM and 200 μM H_2O_2 (1.0 ± 0.3- and 1.2 ± 0.4-fold, respectively; P = 0.0005 and = 0.0281, respectively). No significant differences in *CAT* expression were observed in response to H_2O_2 in melanocytes from Smyth or Light Brown Leghorn feathers.

In melanocytes established from growing feathers of Smyth chickens, levels of *HMOX1* increased from 2.1 ± 0.5-fold in non-treated controls to 5.3 ± 0.2-fold and 8.3 ± 0.7-fold in 100 μM and 200 μM H_2O_2-treated cells respectively (P < 0.0001 and = 0.0037, respectively). In melanocytes from Brown line chickens, levels of *HMOX1* increased from 7.3 ± 2.6-fold in non-treated controls to 13.9 ± 3.3-fold and then decreased to 5.8 ± 2.9-fold in 100 μM and 200 μM H_2O_2-treated cells respectively (P = 0.0017 and < 0.0001, respectively). In melanocytes from

Light Brown Leghorn line chickens, levels of *HMOX1* increased from 1.0 ± 0.3-fold in non-treated controls to 4.3 ± 0.5-fold and 5.4 ± 0.3-fold in 100 μM and 200 μM H_2O_2-treated cells respectively ($P < 0.0001$ and non-significant, respectively). Lastly, levels of *HMOX1* in non-treated melanocytes from Brown line feathers were higher than those in Smyth feathers which were higher than those in Light Brown Leghorn feathers ($P < 0.0001$ and $= 0.0009$, respectively)

Levels of *HSP70* in non-treated melanocytes established from feathers of Smyth, Brown line and Light Brown Leghorn line did not significantly differ (0.6 ± 0.2-, 1.0 ± 0.3- and 1.0 ± 0.1-fold, respectively). In response to 100 μM H_2O_2, *HSP70* expression increased to 0.9 ± 0.1-fold in Smyth melanocytes ($P = 0.0135$) whereas levels in Brown line melanocytes did not significantly differ from non-treated controls. However, when treated with 200 μM H_2O_2, *HSP70* expression increased to 2.8 ± 0.8-fold in Brown line melanocytes ($P = 0.0002$) whereas levels in Smyth line melanocytes did not significantly differ from 100 μM H_2O_2-treated cells. No differences in *HSP70* expression in response to H_2O_2-treatment were observed in melanocytes from Light Brown Leghorn chickens.

Relative expression of B7-1, CD40 and FAS in H_2O_2-treated feather-derived melanocytes

A significant interaction between line and treatment effects on the relative expression of *B7-1 and CD40* was observed in H_2O_2 treated feather-derived melanocytes (Figure 4, top and middle; $P = 0.0009$ and < 0.0001, respectively).

Levels of *B7-1* in non-treated melanocytes established from feathers of Smyth, Brown line and Light Brown Leghorn line did not significantly differ (0.8 ± 0.3-, 1.0 ± 0.5- and 3.6 ± 3.3-fold, respectively). In melanocytes established from growing feathers of Smyth chickens, levels of *B7-1* increased to 3.3 ± 0.7- and 99.0 ± 24.6-fold in response to 100 μM and 200 μM H_2O_2-treatment, respectively ($P < 0.0001$ and < 0.0001, respectively). In melanocytes from

Brown line chickens, levels of *B7-1* increased to 35.5 ± 34.1- and 280.8 ± 192.5-fold in 100 μM and 200 μM H_2O_2-treated cells respectively ($P < 0.0001$ and < 0.0001, respectively). In melanocytes from Light Brown Leghorn line chickens, levels of *B7-1* increased to 3.1 ± 1.6- and 55.2 ± 27.9-fold in 100 μM and 200 μM H_2O_2-treated cells respectively ($P = 0.0009$ and < 0.0001, respectively). When treated with 100 μM H_2O_2, levels of *B7-1* in Brown line melanocytes were higher than those in Smyth and Light Brown Leghorn cells ($P = 0.0003$ and $P = 0.0002$, respectively). Levels between Smyth and Light Brown Leghorn melanocytes did not significantly differ when treated with 100 μM H_2O_2. When treated with 200 μM H_2O_2, only *B7-1* levels between Brown line and Light Brown Leghorn melanocytes were significantly different ($P = 0.0064$).

Levels of *CD40* expression in non-treated cells were minimally but significantly elevated in Brown line melanocytes relative to Light Brown Leghorn cells (1.3 ± 0.3- and 1.0 ± 0.1-fold, respectively; $P = 0.0275$). In addition, CD40 expression in Light Brown Leghorn melanocytes was higher than Smyth melanocytes ($P < 0.0001$). In melanocytes established from growing feathers of Smyth chickens, levels of *CD40* increased to 1.1 ± 0.1- and 1.6 ± 0.1-fold in response to 100 μM and 200 μM H_2O_2-treatment, respectively ($P < 0.0001$ and < 0.0001, respectively). In melanocytes from Brown line chickens, levels of *CD40* increased to 1.6 ± 0.3-fold in 100 μM H_2O_2-treated cells ($P = 0.0095$) and did not significantly increase in response to 200 μM H_2O_2 treatment. In melanocytes from Light Brown Leghorn line chickens, levels of *CD40* increased to 1.2 ± 0.0- and 1.4 ± 0.1-fold in 100 μM and 200 μM H_2O_2-treated cells respectively ($P = 0.0054$ and $= 0.0060$, respectively). When treated with 100 μM H_2O_2, levels of *CD40* in Brown line melanocytes were higher than those in Smyth and Light Brown Leghorn cells ($P = 0.0018$ and $P = 0.0057$, respectively). Levels between Smyth and Light Brown Leghorn melanocytes did not

significantly differ when treated with 100 μM H_2O_2. When treated with 200 μM H_2O_2, only *CD40* levels between Brown line and Light Brown Leghorn melanocytes were significantly different (P = 0.0059).

No significant interaction between line and treatment effects on *FAS* expression were observed in melanocytes established from growing feathers (Figure 4, bottom). In addition no effect of line on *FAS* expression was detected. An overall effect of H_2O_2-treatment on *FAS* expression was observed (P = 0.0023). Overall, relative gene expression of *FAS* was increased in 100 μM (1.5 ± 0.2, P = 0.0475) and 200 μM (1.9 ± 0.3, P = 0.0006) H_2O_2-treated cells relative to non-treated cells.

Relative expression of IL6 and CXCL8 in H_2O_2-treated feather-derived melanocytes

There was no significant effect of line and treatment or their interaction on *IL6* expression in melanocytes established from growing feathers (Figure 5, top).

A significant interaction between line and treatment effects on the relative expression of *CXCL8* was observed in H_2O_2 treated feather-derived melanocytes (Figure 5, bottom; P = 0.0290). Levels of *CXCL8* expression in non-treated cells were elevated in Brown line melanocytes relative to Smyth and Light Brown Leghorn cells (11.3 ± 7.0-, 1.3 ± 0.8- and 1.0 ± 0.4-fold, respectively; P = 0.0005 and = 0.0013, respectively). In melanocytes established from growing feathers of Smyth chickens, no significant differences in *CXCL8* expression were observed in response to 100 μM H_2O_2-treatment (1.3 ± 0.4), however, when treated with 200 μM H_2O_2, levels increased to 25.5 ± 20.4 (P < 0.0001). Similarly, in melanocytes established from growing feathers of Light Brown Leghorn chickens, no significant differences in *CXCL8* expression were observed in response to 100 μM H_2O_2-treatment (1.2 ± 0.2), however, when treated with 200 μM H_2O_2, levels increased to 10.0 ± 3.4 (P < 0.0001). In melanocytes from

Brown line chickens, levels of *CXCL8* increased to 45.9 ± 40.6- and 657.0 ± 496.3-fold in 100 μM and 200 μM H_2O_2-treated cells respectively ($P < 0.0001$ and < 0.0001, respectively). When treated with 100 μM H_2O_2, levels of *CXCL8* in Brown line melanocytes were higher than those in Smyth and Light Brown Leghorn cells ($P < 0.0001$ and < 0.0001, respectively). Levels between Smyth and Light Brown Leghorn melanocytes did not significantly differ when treated with 100 μM H_2O_2. Similarly, when treated with 200 μM H_2O_2, levels of *CXCL8* in Brown line melanocytes were higher than those in Smyth and Light Brown Leghorn cells ($P < 0.0001$ and < 0.0001, respectively).

Relative expression of IL1B and IL18 in H_2O_2-treated feather-derived melanocytes

A significant interaction between line and treatment effects on the relative expression of *IL1B* and *IL18* were observed in H_2O_2 treated feather-derived melanocytes (Figure 6; $P = 0.0279$ and $= 0.0486$, respectively). Levels of *IL1B* in non-treated melanocytes established from feathers of Smyth, Brown line and Light Brown Leghorn line did not significantly differ (1.6 ± 0.7-, 3.6 ± 3.3- and 1.0 ± 0.5-fold, respectively). No significant differences in *IL1B* expression in response to H_2O_2-treatment were observed in melanocytes from Light Brown Leghorn chickens. In response to 100 μM H_2O_2, levels of *IL1B* in melanocytes from Smyth and Brown line chickens remained unchanged (1.3 ± 0.4 and 2.5 ± 3.0, respectively). However, treatment with 200 μM H_2O_2 resulted in significant rises in expression relative to 100 μM H_2O_2-treated cells (2.4 ± 1.8, $P = 0.0337$; 18.8 ± 23.1, $P < 0.0001$). When treated with 200 μM H_2O_2, levels of *IL1B* in Brown line melanocytes were higher than those in Smyth and Light Brown Leghorn cells ($P = 0.0066$ and $= 0.0039$, respectively).

Levels of *IL18* in non-treated melanocytes established from feathers of Smyth, Brown line and Light Brown Leghorn line did not significantly differ (0.9 ± 0.2-, 1.5 ± 0.8- and 1.0 ±

0.1-fold, respectively). No significant differences in *IL18* expression in response to H_2O_2-treatment were observed in melanocytes from Smyth or Light Brown Leghorn chickens. In response to 100 μM H_2O_2, levels of *IL18* in melanocytes from Brown line chickens remained unchanged (0.9 ± 1.2). However, treatment with 200 μM H_2O_2 resulted in significant decreases in expression relative to 100 μM H_2O_2-treated cells (0.9 ± 0.7, $P < 0.0001$).

Discussion

In this study we investigated the response of primary melanocytes established from the feathers of vitiligo-prone Smyth-, vitiligo-susceptible Brown- and vitiligo-resistant Light Brown Leghorn-line chickens to oxidative stress induced by treatment with H_2O_2. Cell viability, surface expression of MHC-I and –II as well as relative expression of genes involved in the antioxidant response, co-stimulation of T cell signaling and inflammation.

In 2006, Manga *et al.* demonstrated an impaired ability of melanocytes from vitiligo patients to cope with oxidative stress induced by exposure to 4-*tert*-butylphenol (4-TPB; an alternative substrate for tyrosinase – a key enzyme in melanogenesis) compared to normal controls. Therefore we first examined the ability of melanocytes derived from growing feathers of Smyth, Brown line and Light Brown Leghorn line chickens to cope with various doses of H_2O_2. As seen in Figure 1, we observed no difference between lines in cell viability curves in response to treatment. Melanocyte viability across lines began to decline in response to H_2O_2 treatment at 125μM. Viability continued to decline with each doubling of H_2O_2 and reach a minimum at the maximum dose tested (1mM). Collectively, results demonstrate an equal susceptibility of melanocytes derived from growing feathers of Smyth-, Brown- and Light Brown Leghorn-line chickens to challenge with H_2O_2.

Le Poole *et al*. were the first to demonstrate the capability of melanocytes to express antigen in the context of MHC-II (1993). In addition, abnormal expression of MHC-II in perilesional melanocytes has been reported in vitiligo (Al Badri *et al.*, 1993). We therefore examined the surface expression of MHC-II in melanocytes established from growing feathers of Smyth, Brown line and Light Brown Leghorn chickens challenged with H_2O_2. Concentrations of 100 μM and 200 μM of H_2O_2 were selected based on results from cell viability studies (i.e. first signs of an effect to ~50% viability, respectively). We also tested the ability of H_2O_2 treatment to increase surface expression of MHC-I. We observed no effect of H_2O_2 treatment on MHC-I expression. This was not unexpected as all nucleated cells, including melanocytes, express MHC-I as a means to present endogenous viral antigens to T cells. It is worth noting that, while not statistically significant, levels of MHC-I staining in Smyth and Light Brown Leghorn melanocytes trended upward in response to H_2O_2 treatment (Figure 2). MHC-I levels of melanocytes from Brown line chickens were virtually unchanged across treatments. In contrast, a strong effect of H_2O_2 treatment on the expression of MHC-II was observed. While independent of line, the effect was most pronounced in melanocytes from Light Brown Leghorn chickens. Collectively, these results demonstrate that H_2O_2 treatment of melanocytes induces an increase in surface expression of MHC-II.

Next, we examined the relative expression of anti-oxidant genes *HMOX1* and *CAT* as well as the molecular chaperone gene *HSP70* in melanocytes established from growing feathers of Smyth, Brown line and Light Brown Leghorn chickens challenged with H_2O_2. Differential expression of *HSP70* in immortalized human melanocytes from vitiligo (PIG3) and normal skin (PIG1) in response to 4-TBP treatment has been demonstrated and is suspected to play a role in triggering vitiligo (Kroll *et al.*, 2005; Denman *et al.*, 2008; Mosenson *et al.*, 2012, 2013, 2014).

Also, recent evidence strongly supports a role for transcription of *HMOX1* (gene for heme oxygenase-1) through Nrf2-signaling in the protection of melanocytes against oxidative stress (Jian *et al.*, 2011, 2016). Treatment of normal human melanocytes with afzelin, an activator of Nrf2, alleviated H_2O_2-mediated cytotoxicity through increased transcription of *HMOX1* and *CAT* (Jung *et al.*, 2017). Moreover, impaired activation of the Nrf2-ARE pathway in perilesional skin of vitiligo patients compared to normal skin was reported by Jian *et al.*, 2014.

Incremental increases in *HMOX1* expression were seen in melanocytes from Smyth chickens in response to H_2O_2-treatment while levels in 100 μM and 200 μM H_2O_2-treated melanocytes from Light Brown Leghorn chickens were equally elevated relative to non-treated controls. Curiously, melanocytes from Brown line chickens demonstrated an increase when treated with 100 μM H_2O_2 while *HMOX1* expression in cells treated with 200 μM H_2O_2 did not differ from non-treated controls. Also worth noting is the over 7-fold and 2-fold difference in baseline expression of *HMOX1* in Brown line and Smyth melanocytes, respectively relative to Light Brown Leghorn melanocytes. Similarly, in melanocytes from Brown line chickens, baseline *CAT* expression was also elevated. Curiously, the expression pattern of *CAT* in response to H_2O_2 treatment was opposite that of *HMOX1* suggesting an inverse role of these two genes in alleviating oxidative stress. Also notable was the lack of *CAT* expression in melanocytes from Smyth and Light Brown Leghorn chickens. Lastly, expression of *HSP70* was only observed in melanocytes from Brown line chickens treated with 200 μM H_2O_2. Collectively, these results suggest an elevated baseline state of oxidative stress in melanocytes from Smyth and Brown line chickens and deficient expression of *CAT* and *HSP70* in response to H_2O_2-mediated stress in Smyth melanocytes.

We next examined the ability of H_2O_2-treatment to induce expression of genes involved in co-stimulation of T cells (*B7-1* and *CD40*) as well as *FAS* which may mediate melanocyte death through Fas-FasL signaling. Expression of *B7-1* and *CD40* has been demonstrated in melanocytes, however their relevance to vitiligo is unknown (Denfeld *et al.*, 1995; Lu *et al.*, 2002). Additionally, functional polymorphisms of *FAS* were associated with vitiligo-risk in a case-controlled study in Chinese populations (Li *et al.*, 2008). Fas-FasL interactions were also, at least, partially responsible for melanocyte-specific autoimmunity in a transgenic mouse model (Lambe *et al.*, 2006). Despite differential expression of oxidative stress-response genes in Brown line and Smyth melanocytes, no differences in baseline *B7-1* levels were observed. However, melanocytes from all three lines demonstrated incremental increases in *B7-1* expression in response to increased H_2O_2 treatment. Interestingly, levels of *B7-1* in H_2O_2-treated melanocytes from Smyth and Light Brown Leghorn lines were similar while those of Brown line melanocytes were higher than both (Figure 3). Similar expression patterns were observed for *CD40*, however in this case baseline levels in melanocytes from Smyth chickens were 0.5-fold lower relative to those in Light Brown Leghorn melanocytes. Lastly, while not statistically significant, clear incremental increases in *FAS* expression can be inferred in H_2O_2-treated melanocytes from Smyth and Light Brown Leghorn chickens while those from Brown line melanocytes were virtually unchanged.

Contrary to reports of increased expression of *IL6* in response to 4-TBP-induced oxidative stress in melanocytes, in this study we observed no change in response to H_2O_2-treatment (Toosi *et al*., 2012; Yao *et al.*, 2012). We did, however, observe a steep rise in *CXCL8* expression in melanocytes from all three lines in response to 200 μM H_2O_2. Incremental rises in *CXCL8* expression in response to increased exposure to H_2O_2 were only observed in melanocytes

from Brown line chickens. In a similar pattern, levels of *CXCL8* in melanocytes from Brown line chickens were higher in all three treatment groups compared to Smyth and Light Brown Leghorn melanocytes, which did not differ from each other.

No obvious changes in *IL1B* and *IL18* expression were observed in response to H_2O_2 treatment in melanocytes from Smyth and Light Brown Leghorn chickens. While statistical analysis indicates a significant interaction of line and treatment effects, large culture-to-culture variation in melanocytes from Brown line chickens makes interpretation of *IL1B* and *IL18* expression patterns difficult.

Here we have surveyed the antioxidant and immunological responses of feather-derived melanocytes from vitiligo-prone Smyth- (80-95% incidence), vitiligo-susceptible but low-expressing (0-2% incidence) Brown- and vitiligo-resistant Light Brown Leghorn line chickens in response to H_2O_2-mediated oxidative stress. Taken together, it appears that Brown line melanocytes are under an elevated state of oxidative stress as evidenced by increased baseline levels of *HMOX1*, *CAT* and *CXCL8* relative to Light Brown Leghorn melanocytes. Melanocytes from Smyth chickens also had elevated levels of *HMOX1* relative to Light Brown Leghorn melanocytes, albeit to a lesser extent. Interestingly, the overall responses of Brown line melanocytes appeared to be heightened, while those of Smyth chickens were similar, relative to Light Brown Leghorn melanocytes. In a recent report on the response of primary melanocytes from vitiligo patients to 4-TBP treatment, the authors noted a deficient response of *CAT* and *HMOX1* expression compared to normal melanocytes treated in the same manner. In addition, the authors observed elevated levels of ROS in non-treated melanocytes from vitiligo patients compared to normal controls (Bellei *et al.*, 2013). It is possible that in melanocytes from vitiligo-prone Smyth chickens there is a heightened, baseline, level of oxidative stress as well as an

impaired ability to cope. In melanocytes from Brown line chickens (which are vitiligo-susceptible), there is also a heightened baseline level of oxidative stress, however, the protective response is normal or even heightened. This is further evidenced in the diminished response of *HSP70* in melanocytes from Smyth chickens compared to those from Brown line chickens.

Future studies should examine ROS levels in treated and non-treated melanocytes as well as the upstream events of the Nrf2-ARE pathway. Additionally, the roles of pigment level and melanogenic activities in susceptibility to oxidative stress should also be examined due to the generation of H_2O_2 by oxidation of eumelanin precursors (Nappi and Vass, 1996).

References

Abdou, A. G., Maraee, A. H. and Reyad, W. (2013) 'Immunohistochemical expression of heat shock protein 70 in vitiligo', *Annals of Diagnostic Pathology*. Elsevier Inc., 17(3), pp. 245–249. doi: 10.1016/j.anndiagpath.2012.11.005.

Arowojolu, O. A. *et al.* (2017) 'The nuclear factor (erythroid-derived 2)-like 2 (NRF2) antioxidant response promotes melanocyte viability and reduces toxicity of the vitiligo-inducing phenol monobenzone', *Experimental Dermatology*, 26(7), pp. 637–644. doi: 10.1111/exd.13350.

Al Badri, A. M. T. *et al.* (1993) 'Abnormal expression of MHC class II and ICAM-1 by melanocytes in vitiligo.', *The Journal of pathology*. Wiley-Blackwell, 169(2), pp. 203–6. doi: 10.1002/path.1711690205.

Bae, J. M. *et al.* (2017) 'Phototherapy for Vitiligo', *JAMA Dermatology*. American Medical Association, 153(7), p. 666. doi: 10.1001/jamadermatol.2017.0002.

Bellei, B. *et al.* (2013) 'Vitiligo: A Possible Model of Degenerative Diseases', *PLoS ONE*. Edited by T. G. Hofmann. Public Library of Science, 8(3), p. e59782. doi: 10.1371/journal.pone.0059782.

Boissy, R. E., Lamont, S. J. and Smyth, J. R. (1984) 'Persistence of abnormal melanocytes in immunosuppressed chickens of the autoimmune "DAM" line.', *Cell and tissue research*, 235(3), pp. 663–8. Available at: http://www.ncbi.nlm.nih.gov/pubmed/6713493.

Boissy, R. E., Smyth, J. R. and Fite, K. V (1983) 'Progressive cytologic changes during the development of delayed feather amelanosis and associated choroidal defects in the DAM chicken line. A vitiligo model.', *The American journal of pathology*, 111(2), pp. 197–212. Available at: http://www.ncbi.nlm.nih.gov/pubmed/6846502.

Bowers, R. R. and Gatlin, J. E. (1985) 'A simple method for the establishment of tissue culture melanocytes from regenerating fowl feathers', *In Vitro Cellular & Developmental Biology*, 21(1), pp. 39–44. doi: 10.1007/BF02620912.

Boyle, M. L., Pardue, S. L. and Smyth, J. R. (1987) 'Effect of corticosterone on the incidence of amelanosis in Smyth delayed amelanotic line chickens.', *Poultry science*, 66(2), pp. 363–7. Available at: http://www.ncbi.nlm.nih.gov/pubmed/3588505.

Dell'Anna, M. L. *et al.* (2007) 'Membrane Lipid Alterations as a Possible Basis for Melanocyte Degeneration in Vitiligo', *Journal of Investigative Dermatology*. Elsevier, 127(5), pp. 1226–1233. doi: 10.1038/SJ.JID.5700700.

Denfeld, R. W. *et al.* (1995) 'In situ expression of B7 and CD28 receptor families in human malignant melanoma: relevance for T-cell-mediated anti-tumor immunity.', *International journal of cancer*, 62(3), pp. 259–65. Available at: http://www.ncbi.nlm.nih.gov/pubmed/7543078 (Accessed: 10 July 2018).

Denman, C. J. *et al.* (2008) 'HSP70i accelerates depigmentation in a mouse model of autoimmune vitiligo', *Journal of Investigative Dermatology*, 128(8), pp. 2041–2048. doi: 10.1038/jid.2008.45.

Ezzedine, K. *et al.* (2015) 'Vitiligo', *The Lancet*. Elsevier, 386(9988), pp. 74–84. doi: 10.1016/S0140-6736(14)60763-7.

Hamal, K. R. *et al.* (2010) 'Differential gene expression of proinflammatory chemokines and cytokines in lungs of ascites-resistant and -susceptible broiler chickens following intravenous cellulose microparticle injection.', *Veterinary immunology and immunopathology*, 133(2–4), pp. 250–5. doi: 10.1016/j.vetimm.2009.07.011.

Jian, Z. *et al.* (2011) 'Heme Oxygenase-1 Protects Human Melanocytes from H2O2-Induced Oxidative Stress via the Nrf2-ARE Pathway', *Journal of Investigative Dermatology*. Nature Publishing Group, 131(7), pp. 1420–1427. doi: 10.1038/jid.2011.56.

Jian, Z. *et al.* (2014) 'Impaired activation of the Nrf2-ARE signaling pathway undermines H 2 O 2-induced oxidative stress response: A possible mechanism for melanocyte degeneration in vitiligo', *Journal of Investigative Dermatology*. Nature Publishing Group, 134(8), pp. 2221–2230. doi: 10.1038/jid.2014.152.

Jian, Z. *et al.* (2016) 'Aspirin induces Nrf2-mediated transcriptional activation of haem oxygenase-1 in protection of human melanocytes from H2O2-induced oxidative stress', *Journal of Cellular and Molecular Medicine*, 20(7), pp. 1307–1318. doi: 10.1111/jcmm.12812.

Jung, E. *et al.* (2017) 'Melanocyte-protective effect of afzelin is mediated by the Nrf2-ARE signalling pathway via GSK-3β inactivation', *Experimental Dermatology*, 26(9), pp. 764–770. doi: 10.1111/exd.13277.

Kaiser, P., Underwood, G. and Davison, F. (2003) 'Differential Cytokine Responses following Marek ' s Disease Virus Infection of Chickens Differing in Resistance to Marek ' s Disease', *Journal of virology*, 77(1), pp. 762–768. doi: 10.1128/JVI.77.1.762.

Kim, S. R. *et al.* (2018) 'Rapid Repigmentation of Vitiligo Using Tofacitinib Plus Low-Dose, Narrowband UV-B Phototherapy', *JAMA Dermatology*. American Medical Association, 154(3), p. 370. doi: 10.1001/jamadermatol.2017.5778.

Kogut, M. H. *et al.* (2005) 'Expression and function of Toll-like receptors in chicken heterophils', *Developmental and Comparative Immunology*, 29(9), pp. 791–807. doi: 10.1016/j.dci.2005.02.002.

Kroll, T. M. *et al.* (2005) '4-Tertiary butyl phenol exposure sensitizes human melanocytes to dendritic cell-mediated killing: Relevance to vitiligo', *Journal of Investigative Dermatology*, 124(4), pp. 798–806. doi: 10.1111/j.0022-202X.2005.23653.x.

Laddha, N. C. *et al.* (2013) 'Vitiligo: interplay between oxidative stress and immune system.', *Experimental dermatology*, 22(4), pp. 245–50. doi: 10.1111/exd.12103.

Lambe, T. *et al.* (2006) 'CD4 T cell-dependent autoimmunity against a melanocyte neoantigen induces spontaneous vitiligo and depends upon Fas-Fas ligand interactions.', *Journal of immunology (Baltimore, Md. : 1950)*. American Association of Immunologists, 177(5), pp. 3055–62. doi: 10.4049/JIMMUNOL.177.5.3055.

Li, M. *et al.* (2008) 'Functional Polymorphisms of the FAS Gene Associated with Risk of Vitiligo in Chinese Populations: A Case–Control Analysis', *Journal of Investigative Dermatology*. Elsevier, 128(12), pp. 2820–2824. doi: 10.1038/JID.2008.161.

Lu, Y. *et al.* (2002) 'Melanocytes are potential immunocompetent cells: evidence from recognition of immunological characteristics of cultured human melanocytes.', *Pigment cell research*, 15(6), pp. 454–60. Available at: http://www.ncbi.nlm.nih.gov/pubmed/12453188 (Accessed: 10 July 2018).

Manga, P. *et al.* (2006) 'A role for tyrosinase-related protein 1 in 4-tert-butylphenol-induced toxicity in melanocytes: Implications for vitiligo', *American Journal of Pathology*, 169(5), pp. 1652–1662. doi: 10.2353/ajpath.2006.050769.

Maresca, V. *et al.* (1997) 'Increased sensitivity to peroxidative agents as a possible pathogenic factor of melanocyte damage in vitiligo.', *The Journal of investigative dermatology*, 109(3), pp. 310–3. Available at: http://www.ncbi.nlm.nih.gov/pubmed/9284096 (Accessed: 10 July 2018).

Mosenson, J. A. *et al.* (2012) 'HSP70i is a critical component of the immune response leading to vitiligo', *Pigment Cell and Melanoma Research*, 25(1), pp. 88–98. doi: 10.1111/j.1755-148X.2011.00916.x.

Mosenson, J. A. *et al.* (2013) 'Mutant HSP70 reverses autoimmune depigmentation in vitiligo', *Science Translational Medicine*, 5(174). doi: 10.1126/scitranslmed.3005127.

Mosenson, J. A. *et al.* (2014) 'Preferential secretion of inducible HSP70 by vitiligo melanocytes under stress', *Pigment Cell and Melanoma Research*, 27(2), pp. 209–220. doi: 10.1111/pcmr.12208.

Nappi, A. J. and Vass, E. (1996) 'Hydrogen peroxide generation associated with the oxidations of the eumelanin precursors 5,6-dihydroxyindole and 5,6-dihydroxyindole-2-carboxylic acid', *Melanoma Research*, 6(5), pp. 341–349. doi: 10.1097/00008390-199610000-00001.

Nguyen, S. *et al.* (2018) 'Atorvastatin in Combination With Narrowband UV-B in Adult Patients With Active Vitiligo', *JAMA Dermatology*. American Medical Association, 154(6), p. 725. doi: 10.1001/jamadermatol.2017.6401.

Pfaffl, M. W. (2001) 'A new mathematical model for relative quantification in real-time RT-PCR', *Nucleic Acids Research*, 29(9), p. 45e–45. doi: 10.1093/nar/29.9.e45.

Le Poole, I. C., Mutis, T., *et al.* (1993) 'A novel, antigen-presenting function of melanocytes and its possible relationship to hypopigmentary disorders.', *Journal of immunology (Baltimore, Md. : 1950)*, 151(12), pp. 7284–92. Available at: http://www.ncbi.nlm.nih.gov/pubmed/8258725.

Le Poole, I. C., Das, P. K., *et al.* (1993) 'Review of the etiopathomechanism of vitiligo: a convergence theory.', *Experimental dermatology*, 2(4), pp. 145–53. Available at: http://www.ncbi.nlm.nih.gov/pubmed/8162332.

Schallreuter, K. U. *et al.* (1999) 'In vivo and in vitro evidence for hydrogen peroxide (H2O2) accumulation in the epidermis of patients with vitiligo and its successful removal by a UVB-activated pseudocatalase.', *The journal of investigative dermatology. Symposium proceedings*, 4(1), pp. 91–6. Available at: http://www.ncbi.nlm.nih.gov/pubmed/10537016.

Schallreuter, K. U. *et al.* (2001) 'Epidermal H(2)O(2) accumulation alters tetrahydrobiopterin (6BH4) recycling in vitiligo: identification of a general mechanism in regulation of all 6BH4-dependent processes?', *The Journal of investigative dermatology*, 116(1), pp. 167–74. doi: 10.1046/j.1523-1747.2001.00220.x.

Shi, F. (2011) *Gene expression analysis of immune and melanocyte related proteins in Smyth line of chickens - The avian model for human autoimmune vitiligo*. University of Arkansas, Fayetteville.

Sreekumar, G. P., Erf, G. F. and Smyth, Jr., J. R. (1996) '5-Azacytidine Treatment Induces Autoimmune Vitiligo in Parental Control Strains of the Smyth Line Chicken Model for Autoimmune Vitiligo', *Clinical Immunology and Immunopathology*, 81(2), pp. 136–144. doi: 10.1006/clin.1996.0169.

Toosi, S., Orlow, S. J. and Manga, P. (2012) 'Vitiligo-inducing phenols activate the unfolded protein response in melanocytes resulting in upregulation of IL6 and IL8', *Journal of Investigative Dermatology*, 132(11), pp. 2601–2609. doi: 10.1038/jid.2012.181.

Yao, L. *et al.* (2012) 'Subtoxic levels hydrogen peroxide-induced expression of interleukin-6 by epidermal melanocytes.', *Archives of dermatological research*, 304(10), pp. 831–8. doi: 10.1007/s00403-012-1277-6.

Table 1. **Target gene primer[1] and probe[2] sequences**

Target	Accession NO.	Primer/Probe	Sequence (5'-3')
28S[3]	X59733	Forward	GGCGAAGCCAGAGGAAACT
		Reverse	GACGACCGATTTGCACGTC
		Probe	AGGACCGCTACGGACCTCCACCA
B7-1[6] (CD80)	NM_001079739.1	Forward	GCTGTCACCCTAGCAGTAAAGTACCT
		Reverse	TTCACGTCGTCTTCTGCTGAA
		Probe	AGGCACGCCTGTTCCCACTGTTCTAAGA
CAT	NM_001031215.2	Forward	CCCTGCGCGTGCTTCT
		Reverse	GCTTTGCCACCGCTTCA
		Probe	TCGCTCTGCAGCGCTCTTCCTG
CD40[6]	NM_204665.2	Forward	TCATCGCTGTCAGTGCTGATC
		Reverse	CGGCCTCAGCCTGCTTT
		Probe	CCATCACAGCTGCAGTTGTCACCTGC
FAS[6]	NM_001199487.1	Forward	GAATGCAAGTCAAGAGAAAAGTGAATA
		Reverse	GGGTCAGGTCAACATCTATATGTATGA
		Probe	CCCAAGGTAACACAGCTGCAGCAGACA
HMOX1[6]	NM_205344.1	Forward	CGGAGAACACACCCTTCATGA
		Reverse	CCTTGTTACGTTCGATCTCTTCCT
		Probe	TCCCTCCACGAGTTCAAGCTGGTCAC
HSPA2[4] (HSP70)	NM_001006685.1	Forward	GACTGCTCTCATCAAGCGTAACA
		Reverse	TCATACACCTGGACGAGGACACT
		Probe	CACCATTCCCACCAAACAAACACAGACC
IL1B[3]	NM_204524.1	Forward	GCTCTACATGTCGTGTGTGATGAG
		Reverse	TGTCGATGTCCCGCATGA
		Probe	CCACACTGCAGCTGGAGGAAGCC
IL6[5]	NM_204628.1	Forward	GCTCGCCGGCTTCGA
		Reverse	GGTAGGTCTGAAAGGCGAACAG
		Probe	AGGAGAAATGCCTGACGAAGCTCTCCA
IL8L2[5] (IL8, CXCL8)	NM_205498.1	Forward	GCCCTCCTCCTGGTTTCA
		Reverse	TGGCACCGCAGCTCATT
		Probe	TCTTTACCAGCGTCCTACCTTGCGACA
IL18[6]	NM_204608.1	Forward	GGCAGTGGAATGTACTTCGACAT
		Reverse	ACCTGGACGCTGAATGCAA
		Probe	ACTGTTACAAAACCACCGCGCCTTCA

[1] All oligos were synthesized by Eurofins Genomics, Louisville, KY

[2] Probes were labeled with FAM and TAMARA on the 5'- and 3'-ends respectively

[3, 4, 5] Sequences from (Kaiser *et al*., 2003; Kogut *et al.*, 2005; Shi, 2011)

[7] Primers and probes were designed using Primer Express 3.0 (Applied Biosystems, Foster City, CA.)

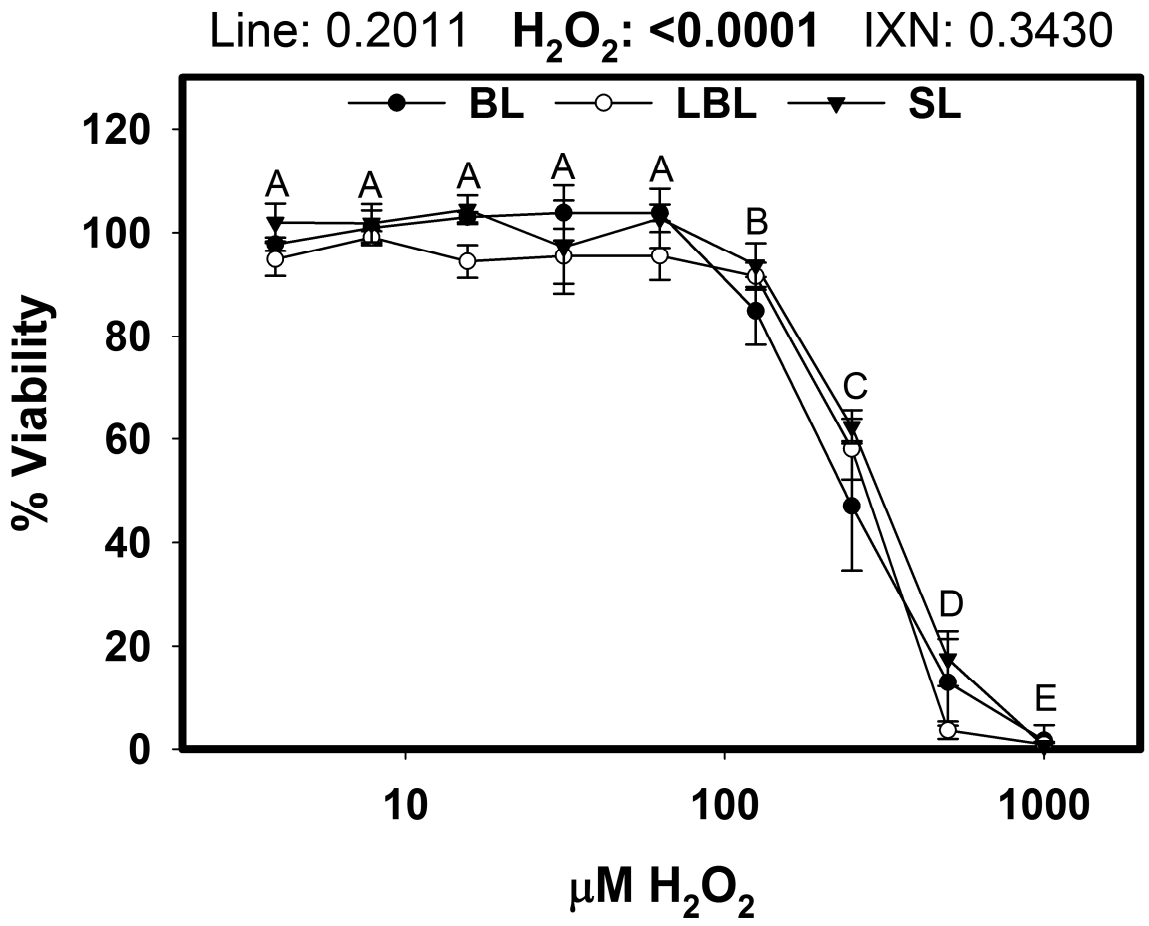

Figure 1. **Viability of primary melanocytes established from growing feathers of vitiligo-prone Smyth line (SL), vitiligo-susceptible parental-control Brown line (BL) and vitiligo-resistant distantly-related Light Brown Leghorn (LBL) chickens in the presence of varying concentrations of hydrogen peroxide.** Primary melanocytes established from growing feathers were seeded into 96-well flat bottom plates (10,000 cells per well) and treated with varying concentrations of H_2O_2 for 4 hours. Cell viability was determined by MTT assay using TPA-free culture medium. Percent viability was calculated relative to un-treated controls (100%). A mixed effects regression model was used to determine the effects of line and H_2O_2 on cell viability. Individual cultures were defined as a random effect. When a significant interaction of line and H_2O_2 effects was found, post-hoc multiple means comparisons between lines were made at each dose of H_2O_2 using Student's t-test. In the absence of significant interactions, Student's t-test was used to test for differences between lines and concentrations of H_2O_2. Differences were considered significant at $P < 0.05$. Data are plotted as mean ± SEM; n = 4 – 6 chickens per time point. Means without a common letter are significantly different.

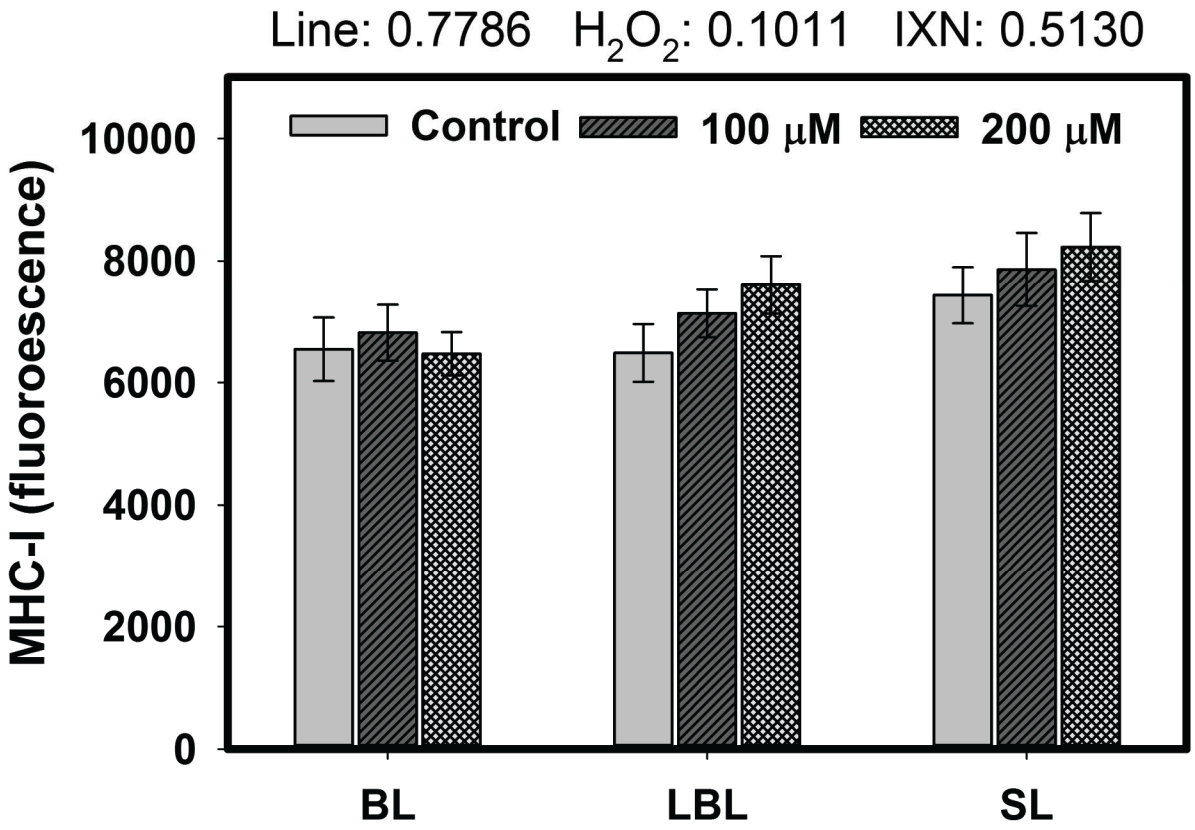
Line: 0.7786 H2O2: 0.1011 IXN: 0.5130
Control
100 μM
200 μM
MHC-I (fluoroescence)
10000
8000
6000
4000
2000
0
BL
LBL
SL

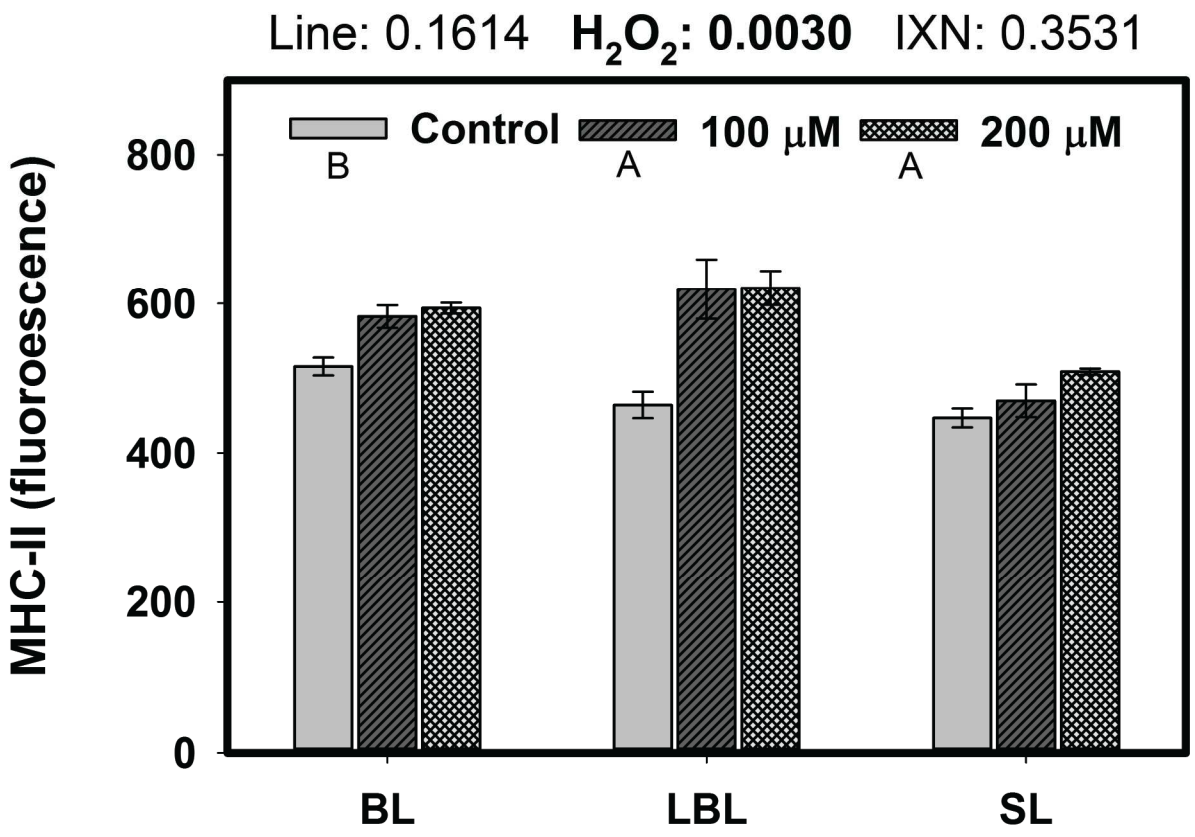
Line: 0.1614 H2O2: 0.0030 IXN: 0.3531
Control
100 μM
200 μM
B
A
A
MHC-II (fluoroescence)
800
600
400
200
0
BL
LBL
SL

Figure 2. **Expression of MHC-I and MHC-II in primary melanocytes established from growing feathers of vitiligo-prone Smyth line (SL), vitiligo-susceptible parental-control Brown line (BL) and vitiligo-resistant distantly-related Light Brown Leghorn (LBL) chickens in the presence of varying concentrations of hydrogen peroxide.** Primary melanocytes established from growing feathers were seeded into 24-well plates (125,000 cells per well) and treated with varying concentrations of H_2O_2 for 4 hours. Expression of MHC-I and MHC-II was determined by flow cytometry. A mixed effects regression model was used to determine the effects of line and H_2O_2 on expression of MHC-I and MHC-II. Individual cultures were defined as a random effect. When a significant interaction of line and H_2O_2 effects was found, post-hoc multiple means comparisons were made using Student's t-test. In the absence of significant interactions, Student's t-test was used to test for differences between lines and concentrations of H_2O_2. Differences were considered significant at $P < 0.05$. Data are plotted as geometric mean ± GSEM; n = 3 – 5 chickens per time point. Main effect treatment means (H_2O_2) without a common letter are significantly different.

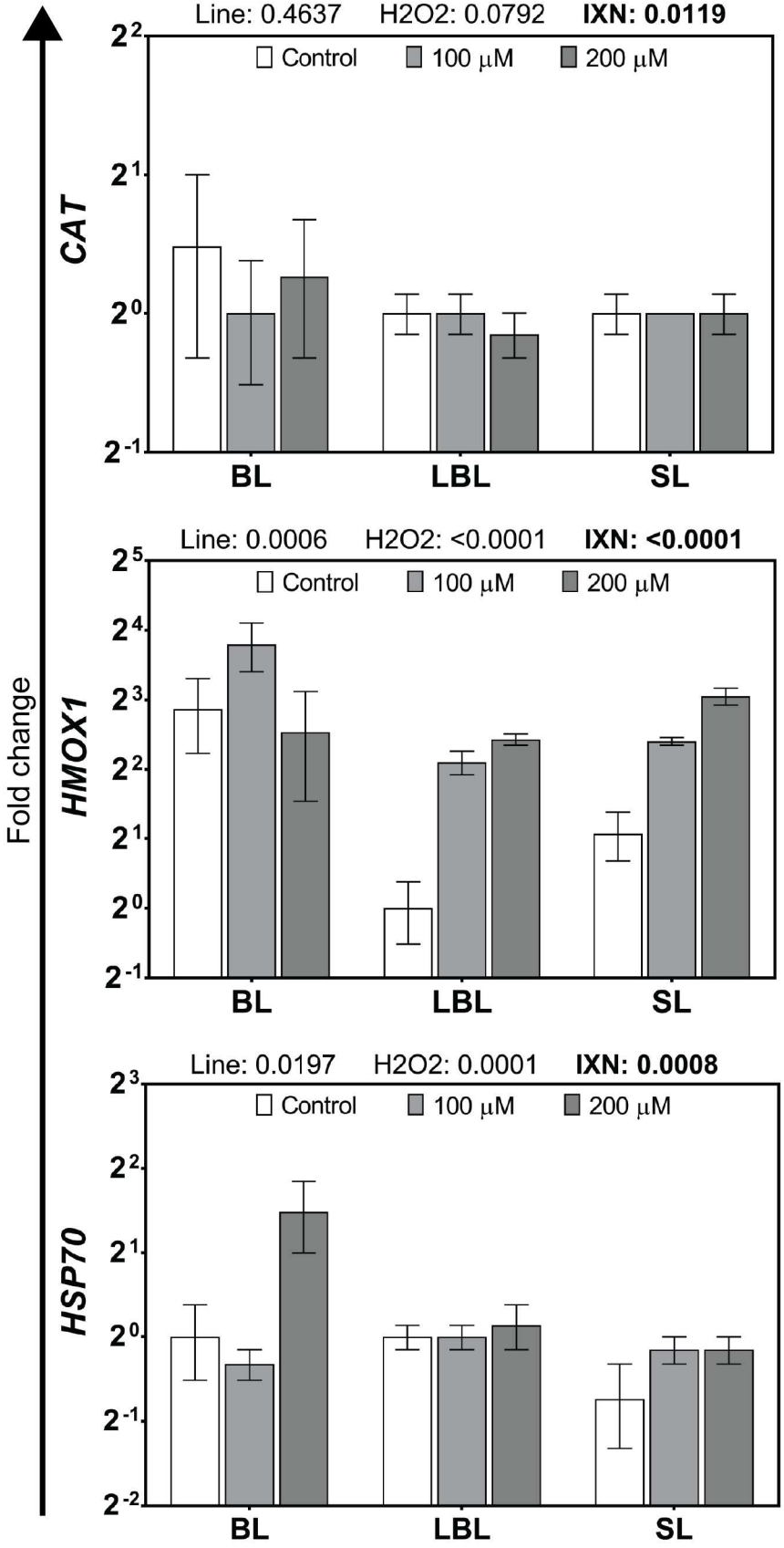
Line: 0.4637 H2O2: 0.0792 IXN: 0.0119
Control
100 μM
200 μM
CAT
BL
LBL
SL
Line: 0.0006 H2O2: <0.0001 IXN: <0.0001
HMOX1
Line: 0.0197 H2O2: 0.0001 IXN: 0.0008
HSP70
Fold change

Figure 3. **Relative expression of *CAT*, *HMOX1* and *HSP70* in primary melanocytes established from growing feathers of vitiligo-prone Smyth line (SL), vitiligo-susceptible parental-control Brown line (BL) and vitiligo-resistant distantly-related Light Brown Leghorn (LBL) chickens in the presence of varying concentrations of hydrogen peroxide.** Primary melanocytes established from growing feathers were seeded into 24-well plates (125,000 cells per well) and treated with varying concentrations of H_2O_2 for 4 hours. Relative expression of *CAT*, *HMOX1* and *HSP70* was determined by the efficiency-calibrated ΔCt method (Pfaffl, 2001) and is expressed as fold change relative to non-treated controls. Gene expression profiles were first obtained for individual cultures using non-treated controls as calibrators and 28S as a reference gene. The overall effects of line and H_2O_2 as well as their interaction was determined using a mixed effects regression model setting line and treatment as fixed effects and individual culture as a random effect. When a significant interaction of line and H_2O_2 effects was found, post-hoc multiple means comparisons were made using Student's t-test. In the absence of significant interactions, Student's t-test was used to test for differences between lines and concentrations of H_2O_2. Differences were considered significant at $P < 0.05$. Data are plotted as geometric mean ± GSEM; n = 2 – 5 chickens per time point.

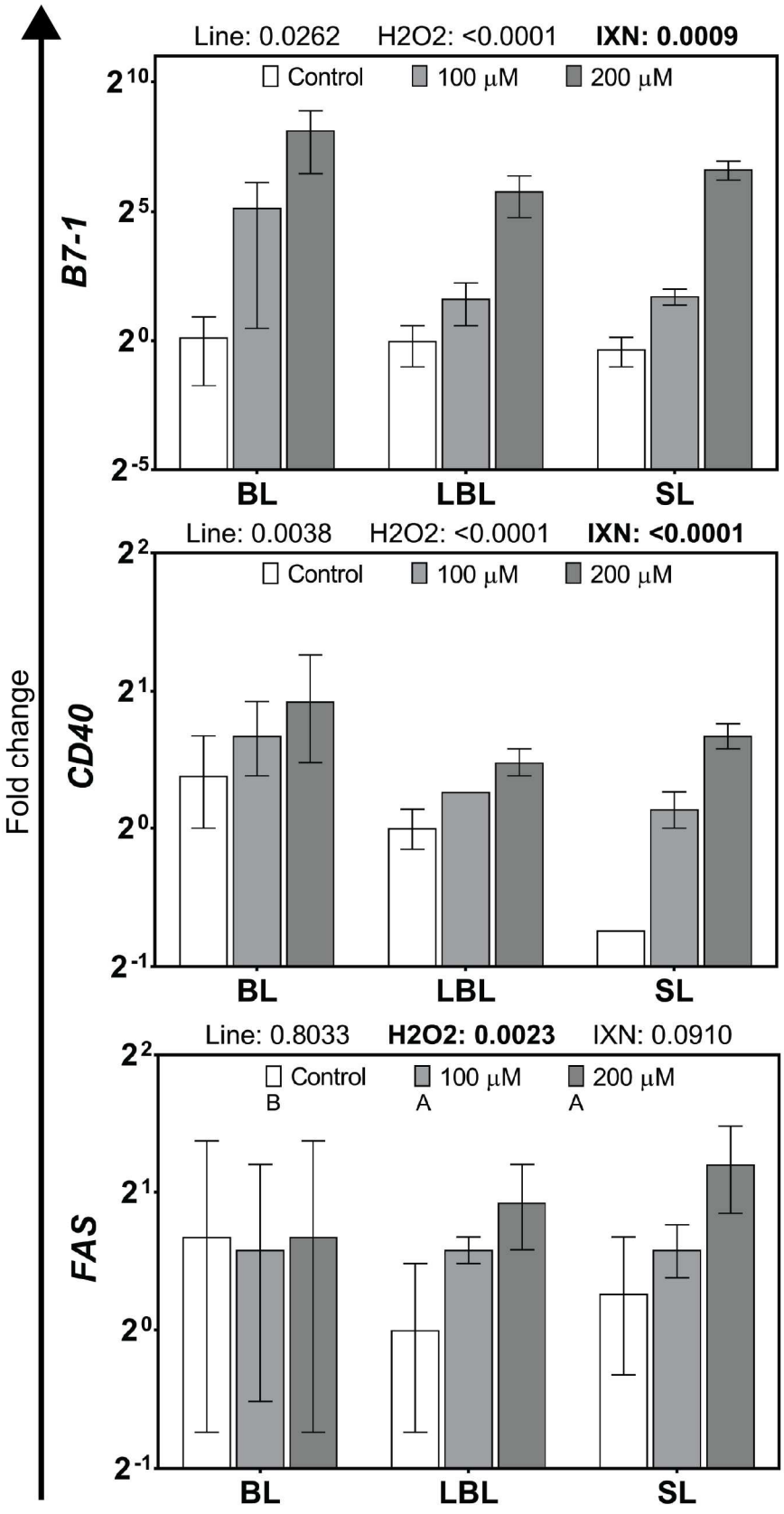
Fold change
B7-1
Line: 0.0262
H2O2: <0.0001
IXN: 0.0009
Control
100 μM
200 μM
2^10
2^5
2^0
2^-5
BL
LBL
SL
CD40
Line: 0.0038
H2O2: <0.0001
IXN: <0.0001
2^2
2^1
2^0
2^-1
FAS
Line: 0.8033
H2O2: 0.0023
IXN: 0.0910
B
A
A

Figure 4. **Relative expression of *B7-1*, *CD40* and *FAS* in primary melanocytes established from growing feathers of vitiligo-prone Smyth line (SL), vitiligo-susceptible parental-control Brown line (BL) and vitiligo-resistant distantly-related Light Brown Leghorn (LBL) chickens in the presence of varying concentrations of hydrogen peroxide.** Primary melanocytes established from growing feathers were seeded into 24-well plates (125,000 cells per well) and treated with varying concentrations of H_2O_2 for 4 hours. Relative expression of *B7-1*, *CD40* and *FAS* was determined by the efficiency-calibrated ΔCt method (Pfaffl, 2001) and is expressed as fold change relative to non-treated controls. Gene expression profiles were first obtained for individual cultures using non-treated controls as calibrators and 28S as a reference gene. The overall effects of line and H_2O_2 as well as their interaction was determined using a mixed effects regression model setting line and treatment as fixed effects and individual culture as a random effect. When a significant interaction of line and H_2O_2 effects was found, post-hoc multiple means comparisons were made using Student's t-test. In the absence of significant interactions, Student's t-test was used to test for differences between lines and concentrations of H_2O_2. Differences were considered significant at $P < 0.05$. Data are plotted as geometric mean ± GSEM; n = 2 – 5 chickens per time point. Main effect treatment means (H_2O_2) without a common letter are significantly different.

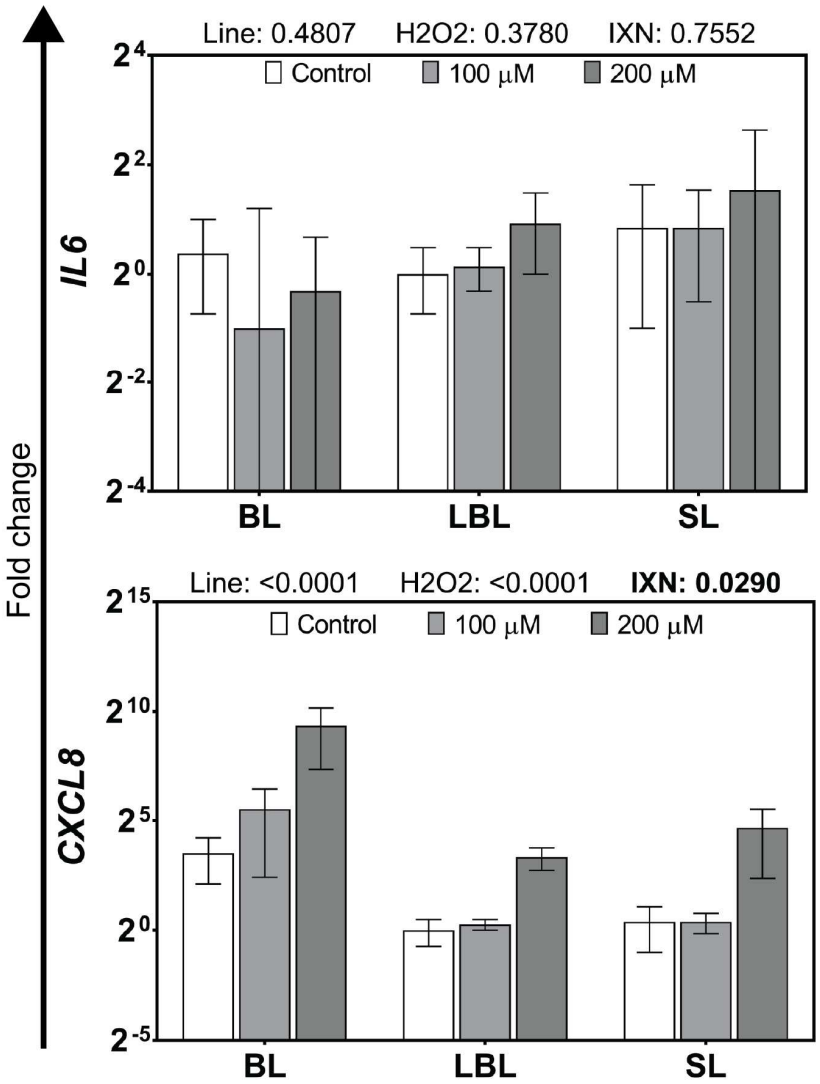

Figure 5. **Relative expression of *IL6* and *CXCL8* in primary melanocytes established from growing feathers of vitiligo-prone Smyth line (SL), vitiligo-susceptible parental-control Brown line (BL) and vitiligo-resistant distantly-related Light Brown Leghorn (LBL) chickens in the presence of varying concentrations of hydrogen peroxide.** Primary melanocytes established from growing feathers were seeded into 24-well plates (125,000 cells per well) and treated with varying concentrations of H_2O_2 for 4 hours. Relative expression of *IL6* and *CXCL8* was determined by the efficiency-calibrated ΔCt method (Pfaffl, 2001) and is expressed as fold change relative to non-treated controls. Gene expression profiles were first obtained for individual cultures using non-treated controls as calibrators and 28S as a reference gene. The overall effects of line and H_2O_2 as well as their interaction was determined using a mixed effects regression model setting line and treatment as fixed effects and individual culture as a random effect. When a significant interaction of line and H_2O_2 effects was found, post-hoc multiple means comparisons were made using Student's t-test. In the absence of significant interactions, Student's t-test was used to test for differences between lines and concentrations of H_2O_2. Differences were considered significant at $P < 0.05$. Data are plotted as geometric mean ± GSEM; n = 2 – 5 chickens per time point.

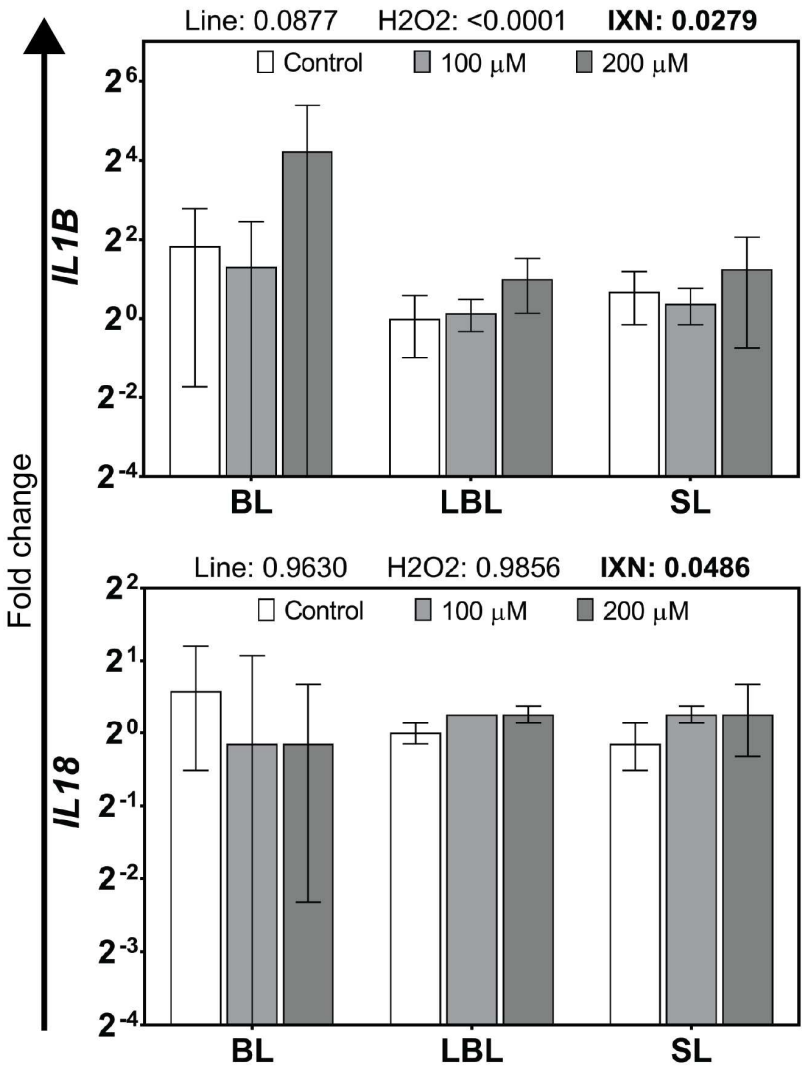

Figure 6. **Relative expression of *IL1B* and *IL18* in primary melanocytes established from growing feathers of vitiligo-prone Smyth line (SL), vitiligo-susceptible parental-control Brown line (BL) and vitiligo-resistant distantly-related Light Brown Leghorn (LBL) chickens in the presence of varying concentrations of hydrogen peroxide.** Primary melanocytes established from growing feathers were seeded into 24-well plates (125,000 cells per well) and treated with varying concentrations of H_2O_2 for 4 hours. Relative expression of *IL1B* and *IL18* was determined by the efficiency-calibrated ΔCt method (Pfaffl, 2001) and is expressed as fold change relative to non-treated controls. Gene expression profiles were first obtained for individual cultures using non-treated controls as calibrators and 28S as a reference gene. The overall effects of line and H_2O_2 as well as their interaction was determined using a mixed effects regression model setting line and treatment as fixed effects and individual culture as a random effect. When a significant interaction of line and H_2O_2 effects was found, post-hoc multiple means comparisons were made using Student's t-test. In the absence of significant interactions, Student's t-test was used to test for differences between lines and concentrations of H_2O_2. Differences were considered significant at $P < 0.05$. Data are plotted as geometric mean ± GSEM; n = 2 – 5 chickens per time point.

Conclusion

The Smyth chicken model for autoimmune vitiligo represents a unique opportunity to study the temporal events leading up to and throughout the development of an auto-immune response. The application of the feather-injection system to study spontaneously-occurring and naturally-generated memory responses adds further value to the model. The evaluation of spontaneous immunological activities in the target tissue of vitiligo-prone Smyth chickens in Chapter 1 provides further support for a T cell-initiated and -driven melanocyte-specific autoimmune response. Indeed evidence of a potent melanocyte-specific memory-like response was observed in growing feathers of vitiliginous Smyth chickens injected with feather-derived melanocytes (Chapter 2). Furthermore, we have uncovered evidence of a novel anti-inflammatory response in vitiligo-susceptible Brown line chickens which may represent the establishment of peripheral tolerance to, possibly defective, melanocytes (Chapter 1). The anergic response observed in growing feathers of Brown line chickens injected with feather-derived melanocytes certainly supports this hypothesis (Chapter 2). In Chapter 3, we revealed what appears to be evidence of an elevated level of basal oxidative pressure in melanocytes from Smyth line and Brown line chickens compared to Light Brown Leghorn line chickens. In addition, we found evidence of a diminished antioxidant response in melanocytes from Smyth line chickens compared to those from Brown line and Light Brown Leghorn line chickens. Finally, we report, for the first time, a novel finding on the induction of expression of the co-stimulatory receptors B7-1 and CD40 in melanocytes in response to oxidative stress challenge. Collectively, the data presented here have opened new avenues of study in the breaking of immunological tolerance in vitiligo-prone Smyth chickens and the possible establishment of

peripheral tolerance to functional but inherently defective melanocytes in vitiligo-susceptible Brown line chickens.

UNIVERSITY OF ARKANSAS

Office of Research Compliance

MEMORANDUM

TO: Dr. Gisela Erf

FROM: Craig N. Coon, Chairman
Institutional Animal Care and Use Committee (IACUC)

DATE: November 7, 2014

SUBJECT: IACUC APPROVAL
Expiration date: November 7, 2017

The Institutional Animal Care and Use Committee (IACUC) has APPROVED your to protocol 15015 GENETIC BASES FOR RESISTANCE AND IMMUNITY TO AVIAN DISEASES: SMYTH LINE AUTOIMMUNE VITILIGO

In granting its approval, the IACUC has approved only the information provided. Should there be any further changes to the protocol during the research, please notify the IACUC in writing(via the Modification form) prior to initiating the changes. If the study period is expected to extend beyond November 7, 2017, you must submit a modification or new protocol prior to that date to avoid any interruption. By policy the IACUC cannot approve a study for more than 3 years at a time.

The IACUC appreciates your cooperation in complying with University and Federal guidelines involving animal subjects.

CNC/aem

cc: Animal Welfare Veterinarian

Administration Building 210 • 1 University of Arkansas • Fayetteville, AR 72701-1201 • 479-575-4572
Fax: 479-575-3846 • http://vpred.uark.edu/199

UNIVERSITY OF ARKANSAS

Office of Research Compliance

To: Gisela Erf
Fr: Craig Coon
Date: November 6th, 2017
Subject: IACUC Approval
Expiration Date: November 2nd, 2020

The Institutional Animal Care and Use Committee (IACUC) has APPROVED your protocol # 18049: GENETIC BASES FOR RESIST ANCE AND IMMUNITY T O AVIAN DISEASES: SMYTH LINE AUT OIMMUNE VITILIGO .

In granting its approval, the IACUC has approved onlythe information provided. Should there be any further changes to the protocol during the research, please notify the IACUC in writing (via the Modification form) prior to initiating the changes. If the study period is expected to extend beyond November 2nd, 202you must submit a newly drafted protocol prior to that date to avoid any interruption. By policy the IACUC cannot approve a study for more than 3 years at a time.

The following individuals are approved to work on this study: Gisela Erf, Howard Lester, Daniel Falcon, Chelsea Ellington, Chris L yle, Guillermo T ellez JR, and Marites Sales. Please submit personnel additions to this protocol via the modification form prior to their start of work.

The IACUC appreciates your cooperation in complying with University and Federal guidelines involving animal subjects.

CNC/tmp

18049